

TRIESKOVÉ A BEZTRIESKOVÉ OBRÁBANIE DREVA 2020

CHIP AND CHIPLESS WOODWORKING PROCESSES 2020

Vedecký časopis // Scientific journal



TECHNICKÁ UNIVERZITA VO ZVOLENE // TECHNICAL UNIVERSITY IN ZVOLEN
DREVÁRSKA FAKULTA // FACULTY OF WOOD SCIENCES AND TECHNOLOGY
KATEDRA OBRÁBANIA DREVA // DEPARTMENT OF WOODWORKING

Technická univerzita vo Zvolene // **Technical University in Zvolen**
Drevárska fakulta // **Faculty of Wood Sciences and Technology**
Katedra obrábania dreva // **Department of Woodworking**



**TRIESKOVÉ A BEZTRIESKOVÉ
OBRÁBANIE DREVA 2020**

**CHIP AND CHIPLESS
WOODWORKING PROCESSES 2020**

Vedecký časopis // **Scientific journal**

Trieskové a beztrieskové obrábanie dreva (ISSN 2453-904X (print), ISSN 1339-8350 (online)) je vedecký časopis uverejňujúci recenzované pôvodné vedecké práce, z oblasti technického a technologického výskumu trieskového delenie a obrábanie dreva, procesu tvorby triesky, kvality vytváraného povrchu a fyzikálno-mechanických vlastnostiach triesky. Súčasťou zamerania časopisu je i problematika termickej a hydrotermickej úpravy drevnej hmoty teplom a realizácie týchto procesov. Časopis vychádza s dvojročnou periodicitou v elektronickej a printovej forme.

Chip and chipless woodworking processes (ISSN 2453-904X (print), ISSN 1339-8350 (online)) is a scientific journal publishing the reviewed original scientific works focusing on the technical and technological research of chip separation and wood processing, the process of making chips, the quality of created surface as well as the physico-mechanical chips characteristics. The journal focuses also on the issue of thermal and hydrothermal modification of the wood pulp by heat and how these processes are realized. The journal is published in a two-year periodicity in an electronic and a print form.

Redakčná rada/Editorial Board

Predseda redakčnej rady/Editorial Board Chief

Ladislav DZURENDA

Členovia edičnej rady/Editorial Board Members

Vladimír GOGLIA, Zhivko GOCHEV, Mikuláš SIKLIENKA, Kazimierz A. ORLOWSKI, Grzegorz KOWALUK, Alena OČKAJOVA, Zdeněk KOPECKY

Zodpovední vedeckí redaktori/Responsible scientific editors

Ladislav DZURENDA

Adrián BANSKI

Technický redaktor/Technical Editor

Silvia NEMCOVA

Redakcia/Editorial office

Technická univerzita vo Zvolene/ Technical university in Zvolen

Drevárska fakulta/ Faculty of Wood Sciences and Technology

Katedra obrábania dreva/ Department of Woodworking

T. G. Masaryka 24

960 01 Zvolen

Vydavateľ/Publisher

Technická univerzita vo Zvolene/Technical university in Zvolen,

T. G. Masaryka 24

960 01 Zvolen, IČO 00397440, 2020

Náklad (Circulation) 80 výtlačkov, rozsah (Pages) 117 strán

Tlač (Printed by) Vydavateľstvo Technickej univerzity vo Zvolene.

Vydanie I. – september

Periodikum s periodicitou raz za dva roky.

Za vedeckú úroveň tejto publikácie zodpovedajú autori.

Všetky práva vyhradené. Nijaká časť textu ani ilustrácie nemôžu byť použité na ďalšie šírenie akoukoľvek formou bez predchádzajúceho súhlasu autorov alebo vydavateľa.

© Technická univerzita vo Zvolene

ISSN 2453-904X (print), ISSN 1339-8350 (online)

OBSAH / CONTENTS

Andrejko Michal – Kúdela Jozef – Mišíková Olga – Kminiak Richard: Štúdium morfológie povrchu dubového dreva po opracovaní gravírovacím CO ₂ laserom <i>Oak wood surface morphology inspected after engraving with a CO₂ laser</i>	5
Banski Adrián – Dudiak Michal: Energetická náročnosť procesu teplovzdušného sušenia brezových vlysov v komorových sušiarňach bez zmeny farby dreva <i>Energy demanding of the process of heat drying of birch friezes in chamber dryers without changing the wood color</i>	15
Deliiski Nencho – Dzurenda Ladislav – Trichkov Neno: An approach for estimating of the natural color change of logs subjected to thermal treatment	21
Deliiski Nencho – Trichkov Neno – Tumbarkova Natalia – Angeski Dimitar – Gochev Zhivko: Computing the average mass temperature of logs and the rate of its change during logs' freezing	29
Dudiak Michal – Dzurenda Ladislav: Acidita (pH) termicky a hydrotermicky upravovaného bukového dreva <i>Acidity (pH) of thermally and hydrothermally treated beech wood</i>	37
Dzurenda Ladislav: Teplovzdušné sušenie parených brezových vlysov v komorových sušiarňach pri zachovaní farby nadobudnutej procesom parenia <i>Hot air drying of steamed birch hairs in chamber dryers when preservation the color acquired by the steaming process</i>	41
Geffert Anton – Geffertová Jarmila – Dudiak Michal – Výbohová Eva: Influence of steaming temperature on chemical characteristics and colour of Alder wood	49
Geffert Anton – Geffertová Jarmila – Dudiak Michal: Comparison of the influence of steaming time and temperature on selected characteristics of birch and alder wood	57
Gochev Zhivko – Vitchev Pavlin: Determination of performance indicators of PCD abrasive wheels for sharpening of tungsten carbide tools	65
Klement Ivan – Uhrín Miroslav – Vilkovská Tatiana – Vilkovský Peter: High-temperature drying of spruce reaction wood	71
Konopka Aleksandra – Baranski Jacek – Orłowski Kazimierz A. – Chuchala Daniel: The effect of drying intensity on the color changes of pine wood (<i>Pinus Sylvestris L.</i>)	79

Novák Igor – Sedliačik Ján – Chodák Ivan – Kleinová Angela – Matyašovský Ján – Jurkovič Peter: Modifikácia vybraných druhov dreva účinkom nízкотеплотnej plazmy	85
Slabejová Gabriela – Šmidriaková Mária: Quality of finish on lightweight plywood	91
Slabejová Gabriela – Šmidriaková Mária: Colour of Thermally modified wood finished with transparent coatings	97
Vilkovská Tatiana – Klement Ivan – Vilkovský Peter – Uhrín Miroslav: The effect of drying temperatures on size of longitudinal contraction different wood species (<i>Fagus sylvatica</i> L. and <i>Picea abies</i> L.)	103
Vukov Georgi – Slavov Valentin – Vitchev Pavlin – Gochev Zhivko: Forced spatial vibrations of a wood shaper, caused by the cutting forces on the worn cutting tool	109



ŠTÚDIUM MORFOLÓGIE POVRCHU DUBOVÉHO DREVA PO OPRACOVANÍ GRAVÍROVACÍM CO₂ LASEROM

Michal Andrejko – Jozef Kúdela – Oľga Mišíková – Richard Kminiak

Abstract

The paper reports on experiments investigating morphological modification of beech wood surface engraved with a CO₂ laser performing at different power outputs and raster density values. The changes in surface morphology were evaluated and quantified through roughness parameters Ra and Rz, measured parallel with and perpendicular to the grain course. These changes were also studied on micro-slides examined with light microscopy. The results confirmed that, during CO₂ laser engraving, all the factors studied (power, density, anatomic direction) had significant effects on roughness parameters. The major influence on roughness variation was found for the raster density. Within the whole examined raster density range, the increasing density induced increasing roughness parameters in both directions: parallel and perpendicular to the grain. More pronounced roughness was recorded perpendicular to the grain course than parallel with it. There has also been confirmed that the oak wood surface roughness after a CO₂ laser irradiation also depended on the heterogeneous oak wood structure on its own. The laser beam track was deeper in the early wood with higher proportion of vessels than in the late wood in which the beam contacted libriform fibres.

Key words: CO₂ laser, oak wood, surface morphology, roughness

ÚVOD

Opracovanie CO₂ laserom sa dostáva do popredia kvôli množstvu výhod, ktoré táto technológia ponúka (rýchle bez trieskové opracovanie, nízke prevádzkové náklady, cieľená modifikácia farby na povrchu, atď.). Laserový lúč nahrádza vďaka úzkej šírke reznej škáry technológie rezania a víťania. Prináša však aj nové možnosti opracovania povrchu kovových aj nekovových materiálov gravírovaním (Patel *et al.* 2017, Yang *et al.* 2019). Výhodou pri opracovaní dreva laserom je, že pri známych koeficientoch absorpcie je možné stanoviť množstvo dodanej energie privedenej na povrch dreva laserovým lúčom s cieľovým dopadom na jeho štruktúru a vlastnosti (Kačík a Kubovský 2011, Vidholdová *et al.* 2017, Kúdela *et al.* 2019, 2020).

Pri gravírovaní dreva laserom dochádza k modifikácii povrchu dreva. Chemicko-fyzikálne a morfológické zmeny vlastností povrchu závisia od množstva energie dodávanej na povrch dreva prostredníctvom laserového lúča, ktorú je možné ovplyvniť výkonom lasera, rýchlosťou pohybu laserovej hlavy, ohniskovou vzdialenosťou, resp. hustotou rastrovania

(Lin *et al.* 2008, Kubovský and Kačík 2013, Haller *et al.* 2014, Gurau *et al.* 2017, Gurau and Petru 2018, Li *et al.* 2018, Sikora *et al.* 2018, Kúdela *et al.* 2020).

Pri gravírovaní dreva sa energia koncentrovaná v laserovom lúči, dodaná na konkrétne miesto, mení na teplo. V dôsledku vysokej teploty koncentrovanej v malom priemere laserového lúča na rozhraní s povrchom dreva, dochádza k okamžitej sublimácii tenkej povrchovej vrstvy dreva. Okrem veľkosti dodanej energie a jej koncentrácie, je hrúbka sublimovanej vrstvy do veľkej miery ovplyvnená tiež druhom dreva v dôsledku ich rozdielnej štruktúry a tvrdosti. (Arai and Kawasumi 1980, Barcikowski *et al.* 2006, Wust *et al.* 2005, Haller *et al.* 2014, Dolan 2014).

Ako vyplýva z mikroskopických pozorovaní (Haller *et al.* 2014, Dolan 2014), opracovanie povrchu dreva laserovým lúčom môže znížiť jeho drsnosť v dôsledku roztavenia buniek do hĺbky niekoľkých mikrometrov bez ich karbonizácie. V práci Kúdelu *et al.* (2019) sa uvádza, že k významným morfológickým zmenám, ktoré sa prejavili na zvýšení drsnosti, dochádzalo až pri dávke ožiarenia $75 \text{ J}\cdot\text{cm}^{-2}$ a to hlavne v dôsledku karbonizácie povrchovej vrstvy dreva. Pri gravírovaní povrchu dreva laserom sa však môže dosiahnuť opačný efekt (Gurau *et al.* 2017, Gurau and Petru 2018). Z posledne citovaných prác má na drsnosť povrchu dreva významný vplyv výkon lasera a rýchlosť pohybu skenovacej hlavice.

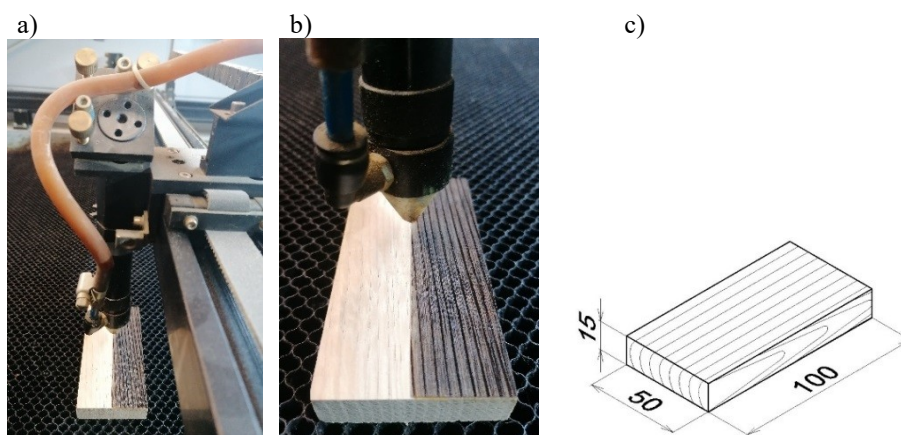
Kúdela *et al.* (2020) použitím CO_2 lasera aplikovaného na povrch bukoveho dreva zistili pri nižšom výkone lasera (4 %) mierny pokles parametrov drsnosti v smere vlákien. Merania ukazovali hodnoty nižšie, ako u brúsených referenčných vzoriek. Táto skutočnosť bola spôsobená odstránením uvoľnených bunkových elementov po brúsení. Pri vyššom výkone (8 %) posledne citovaní autori uvádzajú nárast drsnosti s rastúcou hustotou rastra. Hodnoty parametrov drsnosti boli významne vyššie v porovnaní s brúseným povrchom. Morfológia povrchu po ožarovaní CO_2 laserom je teda ovplyvnená technickými parametrami lasera, ako aj technológiou a zvolenou metodikou ožarovania. To znamená, že vhodnou voľbou parametrov ožarovania CO_2 laserom je možné cielene meniť morfológiu povrchu dreva.

Cieľom tejto práce bolo experimentálne sledovať morfológické zmeny povrchu dubového dreva prostredníctvom parametrov drsnosti, ktorý bol opracovaný gravírovacím CO_2 laserom, pri rôznych výkonoch lasera a pri rôznej hustote rastrovania. Ďalším cieľom práce bolo namerať e a vyhodnotiť parametre drsnosti takto opracovaných povrchov dvomi profilometrami pracujúcimi s odlišnými technikami.

MATERIÁL A METODIKA

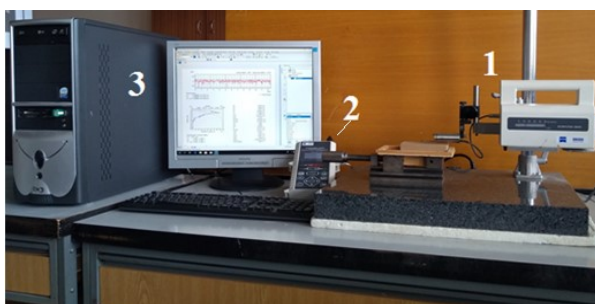
Na gravírovanie dreva sa použil CO_2 laser CM-1309 od firmy EAGLE s maximálnym výkonom 135 W (Obr. 1a, b). Ožarovanie laserom sa realizovalo na vzorkách z dubového dreva (*Quercus robur*) rozmerov $100 \text{ mm} \times 50 \text{ mm} \times 15 \text{ mm}$ (obr. 1c). Vzorky boli umiestnené vo vzdialenosti 17 mm pod ohniskom fokusačnej šošovky. Rýchlosť laserovej hlavice, ktorá sa pohybovala nad povrchom vzorky v smere vlákien, bola konštantná ($350 \text{ mm}\cdot\text{s}^{-1}$). Intenzita ožarovania sa menila so zmenou výkonu lasera a hustotou rastrovania (počet rastrov na jeden milimeter šírky). Jedna sada telies bola gravírovaná pri 8%, druhá pri 12% a tretia sada telies pri 16% výkone lasera. Gravírovanie prebiehalo kolmo na priebeh vlákien, pričom počet rastrov na jeden milimeter šírky bol 1, 2 a 5. Spolu to predstavovalo 9 kombinácií a každá kombinácia bola zastúpená tromi telesami, plus tri referenčné telesá. Každá sada telies bola za zvolených podmienok rovnomerne ožarovaná po celej dĺžke a šírke.

Zmeny morfológie povrchu dreva pri rôznych spôsoboch ožarovania CO₂ laserom sa sledovali prostredníctvom parametrov drsnosti, ako aj sledovaním zmien štruktúry ožiareného povrchu pomocou svetelnej mikroskopie. Drsnosť sa merala dvomi rozdielnymi metódami na ožiarených radiálnych plochách dubových telies rovnobežne s vláknami a kolmo na priebeh vlákien na základe hodnôt parametrov drsnosti R_a (stredná aritmetická odchýlka) a R_z (súčet výšky najväčšieho výstupku a hĺbky najnižšej ryhy v rámci základnej dĺžky).



Obr. 1 Gravírovanie povrchu dubového dreva laserom CM-1309 (a), detail (b), skúšobné teleso (c)

Na meranie drsnosti bol v jednom prípade použitý mechanický profilometer Surfcom 130A (Carl Zeiss, Germany), ktorý sa skladá z meracej a z vyhodnocovacej jednotky (obr. 2). Tento drsnomer umožňuje merať profil v rozmedzí od $-400\ \mu\text{m}$ do $+400\ \mu\text{m}$ od stredovej čiary (celkové možné merané výškové rozpätie profilu je $800\ \mu\text{m}$). Celková meraná dĺžka profilu sa skladala z úseku rozbehu hrota, z piatich základných dĺžok l_r (cutoff λ_c) a dojazdu l_p . Základné dĺžky sa volili v intervale $0,025\text{--}8\ \text{mm}$ na základe predbežne nameraných hodnôt parametrov drsnosti R_a a R_z . Pri vyhodnocovaní drsnosti nameranej uvedeným profilometrom sa odfiltrovala zo základného profilu vlnitosť a krivka drsnosti sa preniesla na základnú čiaru.



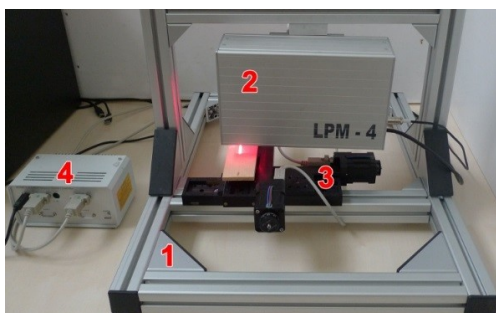
Obr. 2 Mechanický profilometer Surfcom 130A

- 1 – meracia jednotka,
- 2 – vyhodnocovacia jednotka,
- 3 – počítač

V druhom prípade bola použitá optická metóda (laserový profilometer LPM 4, Kvant, Slovakia) – obr. 3.. Laserový profilometer slúži na optické bezkontaktné meranie 2D profilu objektov pozdĺž definovaného rezu (redukovanej roviny). Pre tento účel využíva tzv. triangulačný princíp. Na meraný povrch je najprv premietaná laserová čiara (jej

zdrojom je laserová dióda ktorá produkuje modré svetlo o vlnovej dĺžke $\lambda = 450$ nm a výkone 10 mW), ktorá je následne snímaná digitálnou kamerou (o rozlíšení 1280×1024). Z každého zosnímaného obrazu je možné vyhodnotiť aktuálny 2D profil povrchu telesa. Nanesená laserová čiara vytvára virtuálny rez povrchom v mieste vybranom pre hodnotenie povrchu.

Laserový profilometer umožňuje tvorbu tzv. dlhých profilov do dĺžky 90 mm s výškou a hĺbkou profilu 3–1000 μm . Podstata tvorby dlhých profilov spočíva v tom že, laserový profilometer pri meraní zosníma základnú dĺžku 4 mm a následne dôjde k prestaveniu vzorky o 4 mm v smere merania (presnosť prestavenia vzorky 1 μm). Softvér laserového profilometra stotožní koncové body čiastkových 2D profilov povrchu telesa a vyskladá dlhý 2D profil povrchu (ktorý v našom prípade predstavoval 40 mm). Následné je daný profil virtuálne vyrovnaný, aby sa eliminoval sklon plochy vzorky a vzniknutý profil je podrobený analýze podľa metodiky uvedenej v norme ISO 4287.



Obr. 3 Laserový profilometer LPM-4
 1 – rámová konštrukcia umožňujúca manuálne nastavenie hlavy a systému vozíka,
 2 – laserová hlavica profilometra,
 3 – posuvný súradnicový systém,
 4 – ovládač radenia pracovných stolov

Mikroskopické preparáty pričných rezov sa robili zo vzoriek zmäkčených v glyceríne a modifikovaných transparentným lakom. Mikrorezy boli potom zaliate v euparale. Vzhľadom na veľmi nestabilnú zuhoľnatú vrstvu vrchných buniek, ktorá sa odlupovala pri uvedenej príprave mikrorezov, bola použitá ešte druhá príprava mikrorezov. Mikrorezy sa rezali z malých hranolčekov dubového dreva modifikovaných syntetickou živcou (Technovit). Mikrorezy boli následne zaliate v euparale.

VÝSLEDKY A DISKUSIA

Pri meraní geometrie povrchu dubového dreva mechanickým a optickým profilometrom boli pozorované rozdiely v hodnotách parametrov drsnosti. Obidvomi metódami merania drsnosti sa potvrdila významná zmena morfológie povrchu dreva počas jeho gravírovania CO_2 laserom. Sledované parametre drsnosti R_a a R_z sa so zvyšujúcim výkonom lasera a rastúcou hustotou rastrovania významne zvyšovali. Výraznejšie zmeny parametrov drsnosti boli zaznamenané pri optickej metóde. Základné štatistické charakteristiky parametrov drsnosti R_a a R_z v smere vlákien a kolmo na priebeh vlákien, zisťované obidvomi profilometrami, sú uvedené v tab. 1.

Rozdiely vo výsledkoch drsnosti meranej mechanickým a optickým profilometrom sa zväčšovali s rastúcim výkonom gravírovacieho lasera ako aj s hustotou rastra. Výraznejšie rozdiely boli pozorované v prípade parametra R_z a to hlavne pri meraní drsnosti kolmo na priebeh vlákien. Príčinou rozdielných hodnôt parametrov drsnosti, nameraných jedným a druhým profilometrom je rozdielna technika snímania profilu povrchu a tiež rozdielne nastavenie základnej a meranej dĺžky. Kvôli objektívnejšiemu hodnoteniu vplyvu

sledovaných faktorov gravírovania na drsnosť povrchu je preto vhodné použiť len jeden spôsobom snímania profilu drsnosti. Každá z použitých metód má svoje výhody i nevýhody. Pre viac obmedzený rozsah snímania vertikálneho profilu mechanický profilometer neumožňoval snímať profily drsnosti pri vyššom výkone a vyššej hustote rastra. Preto sa v našom prípade ukázalo vhodnejšie použiť optický profilometer, pomocou ktorého bolo možné snímať aj najvyššie dosiahnuté profily gravírovaného povrchu dubového dreva.

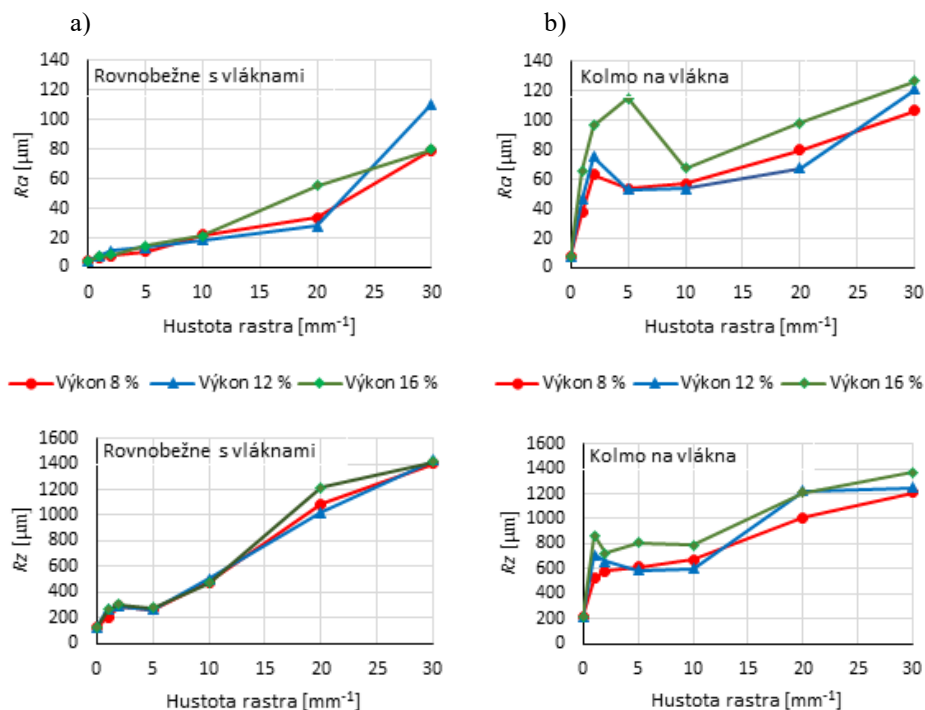
Tab. 1 Základné štatistické charakteristiky parametrov drsnosti rovnobežne s vláknami a kolmo na priebeh vlákien gravírovaného povrchu dubového dreva pri výkone lasera 8 a 12 %.

Hustota rastra [mm ⁻¹]		Parametre drsnosti pri výkone lasera 8 %							
		Rovnobežne s vláknami				Kolmo na priebeh vlákien			
		Mechanická metóda		Optická metóda		Mechanická metóda		Optická metóda	
		Ra	Rz	Ra	Rz	Ra	Rz	Ra	Rz
[µm]									
Refer.	\bar{x}	4,23502	29,2968	4,4866	123,0870	9,8328	86,8475	8,0401	219,498
	s	2,85375	18,6659	1,4490	49,5980	2,7941	25,9783	0,9077	149,214
1	\bar{x}	12,8811	87,7865	6,4870	206,2270	32,2210	225,7300	37,6302	522,1910
	s	3,1896	20,0108	1,5752	72,4315	3,3134	19,5405	2,6264	76,5297
2	\bar{x}	7,6978	53,7068	8,0784	292,4530	46,1406	249,174	62,9958	581,5280
	s	4,3320	30,7587	3,2961	117,7140	1,7625	7,3165	5,0553	77,1163
5	\bar{x}	14,1485	85,7063	10,8021	262,5120	42,9105	279,2280	53,6959	613,4590
	s	2,7445	19,2821	2,8147	63,8087	5,4687	37,7454	10,4749	53,9510
		Parametre drsnosti pri výkone 12 %							
		Rovnobežne s vláknami				Kolmo na priebeh vlákien			
		Mechanická metóda		Optická metóda		Mechanická metóda		Optická metóda	
		Ra	Rz	Ra	Rz	Ra	Rz	Ra	Rz
Refer.	\bar{x}	4,23502	29,2968	4,4866	123,0870	9,8328	86,8475	8,0401	219,498
	s	2,85375	18,6659	1,4490	49,5980	2,7941	25,9783	0,9077	149,214
1	\bar{x}	8,3638	54,2989	7,8090	271,1250	34,6484	224,481	46,2007	711,0300
	s	2,4301	15,5936	3,6329	188,8470	3,0507	9,7726	2,2380	119,9540
2	\bar{x}	11,4016	68,8696	11,5110	288,4770	51,5137	259,642	75,5088	662,236
	s	3,6284	19,9643	3,5358	93,7473	4,3090	19,4808	3,7295	53,2777
5	\bar{x}	22,3629	111,1050	13,4381	262,6530	40,3751	269,0190	53,1402	589,1250
	s	4,1936	16,5668	3,9408	95,6725	15,1150	100,2360	10,1854	74,3294
		Parametre drsnosti pri výkone 16 %							
		Rovnobežne s vláknami				Kolmo na priebeh vlákien			
		Mechanická metóda		Optická metóda		Mechanická metóda		Optická metóda	
		Ra	Rz	Ra	Rz	Ra	Rz	Ra	Rz
Refer.	\bar{x}	4,23502	29,2968	4,4866	123,0870	9,8328	86,8475	8,0401	219,498
	s	2,85375	18,6659	1,4490	49,5980	2,7941	25,9783	0,9077	149,214
1	\bar{x}	9,6640	68,9010	7,5430	262,2140	-	-	65,8235	867,5200
	s	5,8951	37,9037	3,0535	141,1540	-	-	8,2964	123,3830
2	\bar{x}	24,9843	141,0590	8,5765	303,1570	-	-	96,7483	723,3900
	s	3,2531	19,4747	2,7280	89,2026	-	-	8,8894	54,6062
5	\bar{x}	18,0873	102,6150	14,3972	277,5290	-	-	115,100	810,3670
	s	7,5397	37,1196	5,0935	62,9488	-	-	6,5722	54,5425

Dosiahnuté výsledky parametrov drsnosti optickým profilometrom boli vyhodnotené trojfaktorovou analýzou rozptylu. Pri gravírovaní CO₂ laserom sa sledoval vplyv výkonu lasera, hustoty rastra, ako aj vplyv anatomického smeru na uvedené parametre drsnosti. Výsledky trojfaktorovej analýzy rozptylu potvrdili významný vplyv všetkých troch testovaných faktorov na parametre drsnosti Ra a Rz.

Vplyv sledovaných faktorov na parametre drsnosti je znázornený na obr. 4. Ako vidieť z obr. 4, hodnoty oboch sledovaných parametrov drsnosti sa s rastúcou hustotou rastra zvyšovali a to tak v smere vlákien ako aj kolmo na priebeh vlákien. Toto sa nedá jednoznačne povedať o vplyve výkonu lasera. Hoci sa potvrdil významný vplyv aj výkonu lasera na parametre drsnosti, nedá sa jednoznačne povedať (platí to najmä pre pozdĺžny

smer), že sa drsnosť s rastúcim výkonom lasera zvyšuje. Kvalitatívne podobné výsledky pri rovnakých podmienkach ožarovania sa dosiahli aj v prípade bukového dreva (Kúdela *et al.* 2020).

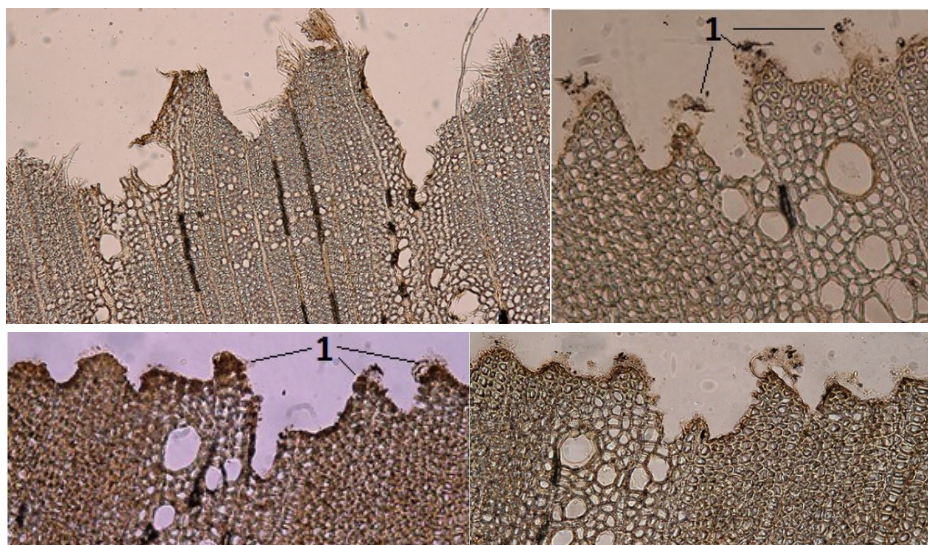


Obf. 4 Vplyv hustoty rastra na parametre drsnosti R_a a R_z gravírovaného povrchu dubového dreva meraných rovnoobežne s vláknami a kolmo na priebeh vlákien pri výkonoch lasera 8, 12 a 16 %

Vzhľadom na krátku vzdialenosť povrchu vzorky pod ohniskom fokusačnej šošovky, dochádzalo v priebehu gravírovania k odbúraniu a okamžitej sublimácii drevnej hmoty. To znamená, že teplota na povrchu vzoriek v kontakte so zväzkom laserového lúča musela byť výrazne nad 240 °C, čo potvrdili aj experimentálne merania teploty pomocou termokamery. Už pri výkone lasera 4 %, bola v mieste dopadajúceho zväzku laserového lúča nameraná teplota okolo 450 až 500 °C a pri výkone 8 % to bola teplota na hranici, ktorú mohla termokamera s horným rozsahom teploty do 1000 °C zaznamenať.

Šírka vygravírovanej stopy (0,14 mm) bola daná šírkou zväzku v mieste dopadu na povrch, bez rozdielu výkonu lasera. Pri konštantnej hustote rastra so zvyšujúcim výkonom hrúbka odstránenej vrstvy úmerne rástla, ale na drsnosť povrchu, ktorý ostal po ožiarení sa to významne neprejavilo, čo je v súlade s výsledkami prác Haller *et al.* (2014), Dolan (2014), Kúdela *et al.* (2019). Je však potrebné poznamenať, že podmienky ožarovania CO₂ v prípade citovaných autorov boli iné. Určité rozdiely v drsnosti pripisujeme rôznemu stupňu zuhoľnatenia vrchných buniek ako aj heterogenite povrchu dubového dreva. Raster na povrchu dreva zanechával stopy v podobe rýh, ktoré spôsobovali zvýšenie drsnosti. Pri hustote rastra 10 mm⁻¹ a vyššej, vzhľadom na šírku rastra dochádzalo k prekryvaniu týchto rastrov. To znamená, že tam, kde došlo k prekrytiu rastrov, bola na jedno miesto dodaná väčšia dávka energie, ktorá bola príčinou prehĺbenia ryhy.

Hĺbku a frekvenciu rýh kolmo na priebeh vlákien na povrchu dubového dreva pri výkone lasera 8 % a hustote rastra 20 mm^{-1} možno vidieť na obr. 5. Z obrázka tiež vidieť ako hĺbka rýh po gravírovaní je ovplyvnená aj samotnou heterogénnou štruktúrou dubového dreva. Dubové drevo je kruhovito-pórovité s veľkými lúmenmi najmä jarných ciev s tenkou bunkovou stenou, v porovnaní s librifonnými vláknami, ktoré majú malý priemer lúmenu a hrubú bunkovú stenu (Požgaj *et al.* 1997). Keďže sa jednalo o gravírované radiálne plochy, tak sa na týchto plochách striedalo jarné a letné drevo. Ako vidieť z obr. 5, laserový lúč zanechával v jarnom dreve hlbšiu stopu ako v letnom dreve. Táto skutočnosť sa odrazila najmä na hodnotách parametra R_z .



Obr. 5 Profil povrchu dubového dreva po gravírovaní CO_2 laserom kolmo na priebeh vlákien pri výkone lasera 8 % a hustote rastrovania 20 mm^{-1} .

1 – fragmenty zuhoľnatých buniek drevných vlákien

Množstvo energie dodávanej na povrch dubového dreva prostredníctvom laserového lúča a jej premena na tepelnú energiu nespôsobilo len sublimáciu dreva a zuhoľnatie vrchných drevných buniek, ale teplo difundovalo stržňovými lúčmi hlbšie do štruktúry dubového dreva, čo dokumentujú stmavnuté parenchamatické bunky stržňových lúčov (obr. 5).

Štúdium ožiareného povrchu dubového dreva CO_2 laserom ukázalo, že interakcie, ktoré prebiehajú na rozhraní drevo – laserový lúč, sú veľmi zložité. Na hlbšie pochopenie javov, ktoré sa odohrávajú na povrchu dreva počas gravírovania pri dodaní rôznych dávok energie, je potrebná hlbšia analýza štruktúry dreva povrchových vrstiev z anatomického aj chemického hľadiska.

ZÁVERY

Z analýzy výsledkov vyhodnotenia drsnosti povrchu dubového dreva po gravírovaní CO_2 laserom na základe parametrov drsnosti nameraných optickým profilometrom, možno vyvodit' nasledovné závery.

Potvrdil sa významný vplyv všetkých sledovaných faktorov počas gravírovania (výkon lasera, hustota rastra, vplyv anatomického smeru) na parametre drsnosti R_a a R_z .

Najvýznamnejší vplyv na zmenu drsnosti mala hustota rastra. S rastúcou hustotou rastra v celom sledovanom rozsahu sa parametre drsnosti zvyšovali v pozdĺžnom smere ako aj kolmo na priebeh vlákien. Vyššia drsnosť bola zaznamenaná kolmo na priebeh vlákien ako rovnobežne s vláknami.

Bolo tiež potvrdené, že na drsnosť povrchu dubového dreva po jeho ožarovaní CO_2 laserom, má vplyv aj samotná heterogénna štruktúra dubového dreva. V jarnom dreve s hlavným podielom jarných ciev, zväzok laserového lúča zanechával hlbšiu stopu ako v letnom dreve v kontakte s libriformnými vláknami.

PodĎakovanie: Táto práca bola podporená Agentúrou na podporu výskumu vývoja na základe Zmluvy č. APVV-16-0177 a Internou projektovou agentúrou TUZVO, č. projektu IPA 15/2020.

LITERATÚRA

Arai, I., Kawasumi, H. 1980: Thermal analysis of laser machining in wood III. Mokuzaï Gakkaishi, 26, 773–782.

Barcikowski, S., Koch, G., Odermatt, J. 2006: Characterisation and modification of the heat affected zone during laser material processing of wood and wood composites. Holz als Roh- u. Werkstoff, 64, 94–103.

Dolan, J. A. 2014: Characterization of Laser Modified Surfaces for Wood Adhesion. (Thesis for the degree of Master of Science In: Macromolecular Science and Engineering). The Faculty of Virginia Polytechnic Institute, Blacksburg, VA, 100 p.

Gurau, L., Petru, A. 2018: The influence of CO_2 laser beam power output and scanning speed on surface quality of Norway maple (*Acer platanoides*), BioResources, 13, 8168–8183.

Gurau, L., Petru, A., Varodi, A., Timar, M. C. 2017: The influence of CO_2 laser beam power output and scanning speed on surface roughness and colour changes of beech (*Fagus sylvatica*), BioResources, 12, 7395–7412.

Haller, P., Beyer, E., Wiedemann, G., Panzner, M., Wust, H. 2014: Experimental study of the effect of a laser beam on the morphology of wood surfaces. <https://www.researchgate.net/publication/237543545>

Kačík, F., Kubovský, I. 2011: Chemical changes of beech wood due to CO_2 laser irradiation. J. Photochem. Photobiol. A, 222, 105–110.

Kubovský, I., Kačík, F. 2013: Changes of the wood surface colour induced by CO_2 laser and its durability after the xenon lamp exposure. Wood Research. 58, 581–590.

Kúdela, J., Kubovský, I., Andrejko, M. 2020: Surface properties of beech wood after CO_2 laser engraving. Coatings, 10(1): 77.

Kúdela, J., Reinprecht, L., Vidholdová, Z., Andrejko, M. 2019: Surface properties of beech wood modified by CO_2 laser. Acta Facultatis Xylogologiae Zvolen, 61, 5–18.

- Li, R., Xu, W., Wang, X.A., Wang, C. 2018: Modelling and predicting of the color changes of wood surface during CO₂ laser modification, *J. Clean. Prod.*, 183, 818–823.
- Lin, C. J., Wang, Y. C., Lin, L. D., Chiou, C. R., Wang, Y. N., Tsai, M. J. 2008: Effects of feed speed ratio and laser power on engraved depth and color difference of Moso bamboo lamina. *J. Mater. Process. Technol.*, 198, 419–425.
- Patel, Ch., Patel, A. J., Patel, R. C. 2017: A Review on Laser Marking Process for Different Materials. *IJSRD*, 5(1): 147–150.
- Požgaj, A., Chovanec, D., Kurjatko, S., Babiak, M. 1997: Štruktúra a vlastnosti dreva. Bratislava: Príroda 1997, s. 269 – 276
- Sikora, A., Kačík, F., Gaff, M., Vondrová, V., Bubeníková, T., Kubovský, I. 2018: Impact of thermal modification on color and chemical changes of spruce and oak wood. *Inter. J. Wood Sci.*, 64: 406–416.
- Vidholdová, Z., Reinprecht, L., Igaz, R. 2017: Mold on laser-treated beech. *BioResources*, 12(2): 4177–4186.
- Wust, H., Haller, P., Wiedemann, G. 2005: Experimental study of the effect of a laser beam on the morphology of wood surfaces. In *Proceedings of the Second European Conference on Wood Modification*, Göttingen, Germany, 6-7 October 2005.
- Yang, Ch., Jiang, T., Yu, Y., Bai, Y., Song, M., Miao, Q., Ma, Y., Liu, J. 2019: Water-jet Assisted Nanosecond Laser Microcutting of Northeast China Ash Wood: Experimental Study. *BioResources*, 14, 128–138.



ENERGETICKÁ NÁROČNOSŤ PROCESU TEPLOVZDUŠNÉHO SUŠENIA BREZOVÝCH VLYSOV V KOMOROVÝCH SUŠIARŇACH BEZ ZMENY FARBY DREVA

Adrián Banski – Michal Dudiak

Abstract

The paper deals with the energy intensity of the process of hot air drying of birch friezes with emphasis on preserving the original color of the wood. The proposed mode is longer by $\Delta\tau = 26$ hours in comparison with the mode determined according to the ON 49 0651 standard. The prolongation of the drying time of the birch friezes is caused by the lower temperature of the drying medium during the evaporation of the free water. The normative of heat consumption of the proposed regime of drying of birch friezes has the value $QTZN = 264.85 \text{ kWh}\cdot\text{m}^{-3}$, which is 7.1 % more than the heat consumption during drying according to the standard. The increase in heat consumption for drying 1 m^3 of birch friezes is caused both by the extension of the actual drying time and by the consumption of heat to cover the heat losses of the dryer during the process.

Key words: birch friezes, hot air drying, chamber dryers, energy intensity of wood drying

ÚVOD

Sušenie dreva patrí k základným technologickým operáciám spracovania drevnej hmoty. Uvedená technologická operácia je značne komplikovaný hydrotermický proces, ktorý je stále riešený vedecko-výskumnými pracovníkmi a technológmi, aby bol stále efektívnejší a dokonalejší.

Sušenie brezových vlysov vykonávané v teplovzdušných komorových sušiarňach podľa sušiacich režimov ON 49 0651, či režimov sušenia odporúčaných firmami: KATRES s.r.o., Hildebrand Holztechnik GmbH, Mühlböck Holzrocknungsanlagen GmbH a iné, je bežne realizované pri teplotách $t = 50 - 70 \text{ }^\circ\text{C}$. Realizácia sušiaceho procesu pri uvedených teplotách vytvára v brezovom dreve podmienky nielen pre odstraňovanie vody z dreva, ale i pre priebeh chemických reakcií akými sú hydrolýza polysacharidov, extrakcia vodorozpustných akcesorických látok, depolymerizácia polysacharidov a chemické zmeny v ligníne vyvolávajúce modifikáciu chromoforneho systému dreva. (Bučko 1995, Trebula a Bučko 1996, Kačík 2001, Laurová a kol. 2004, Geffert a kol. 2020), ktoré vyvolávajú ireverzibilné zmeny brezového dreva. Jednou z takýchto zmien je zmena farby brezového dreva z pôvodnej bielo-žltej farby na viac či menej sýte odtiene hnedo-červenej farby. Mieru zmeny farby v procesoch hydrotermickej úpravy dreva definoval (Deliiski 1991) kritériom farebnej homogenizácie dreva S_{FH} , ktoré je číselne rovné veľkosti integrálnej plochy funkcie zmeny teploty dreva v procese hydrotermickej úpravy dreva. Jednotkou uvedeného kritéria je termosekunda [K.s].

Cieľom práce je stanovenie vplyvu navrhovaných zmien v procese teplotvzdušného sušenia brezových vlysov na energetickú náročnosť procesu sušenia.

MATERIAL A METÓDA

Návrh teplotvzdušného režimu pre sušenie brezových vlysov s rozmermi 38x100x800 mm, z vlhkosti $w_p = 50 \%$, na vlhkosť $w_k = 10 \%$ (Dzurenda 2020) a rozpis podmienok sušenia vlysov dreveniny Breza biela podľa normovaného režimu ON 49 0651 zohľadňujúceho parené a neparené brezové vlysy, uvádza Tab. 1.

Tab. 1 Rozpis podmienok sušenia brezových vlysov

Fázy sušenia	Rozmery brezových vlysov 38x100x800					
	režim navrhnutý			ON 49 0651		
	t_s [°C]	Δt [°C]	τ [hod]	t_s [°C]	Δt [°C]	τ [hod]
Ohrev	35	2	4	50	2	4
50 - 35	35	5	27	50	3	21
35 - 25	40	8	23	50	6	18
Kondicionovanie	50	3	6			
25 - 20	60	8	16	60	8	16
20 - 15	70	12	17	70	12	17
15 - 10	70	18	25	70	18	25
Ošetrenie	70	7	7	70	7	8
Ochladenie	30	7	4	30	7	4
Σ	-	-	129	-	-	113

Špecifická spotreba tepla na vysušenie $1m^3$ brezových vlysov v komorovej teplotvzdušnej sušiarňi KC 1/50 vyrábanej firmou SUSAR s.r.o navrhnutým režimom a režimom podľa ON 49 0651 je stanovená formou technicky zdôvodniteľnej normy (Q_{TZN}) prostredníctvom technického výpočtu normatívu spotreby tepla na vysušenie reziva v komorových sušiarňach (Dzurenda a Deliiski 2010).

Normatív spotreby tepla na proces sušenia brezových vlysov v komorovej sušiarňi kvantifikuje rovnica:

$$Q_{TZN} = \frac{Q_W + Q_V + Q_A + Q_L + Q_{HG} + Q_S}{V_D} \quad [kWh.m^3] \quad (1)$$

kde: Q_W – teplo potrebné na ohrev vlysov v sušiarňi, $[kWh.m^3]$,

Q_V – teplo potrebné na ohrev vlhkého vzduchu v komorovej sušiarňi a zvlhčovanie vo fáze ohrevu a konečného ošetrenia, $[kWh.m^3]$,

Q_A – teplo potrebné na ohrev konštrukcie komorovej sušiarne a prekladových latiek, $[kWh.m^3]$,

Q_L – teplo potrebné na ohrev vzduchu v sušiarňi za účelom odparenia vody z dreva, $[kWh.m^3]$,

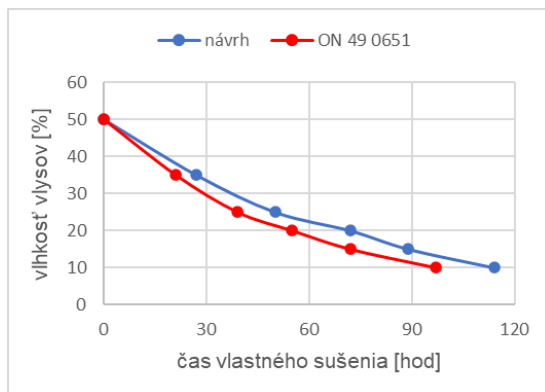
Q_{HG} – teplo na uvoľnenie hydroskopicky viazanej vody z dreva, $[kWh.m^3]$,

Q_S – teplo na krytie tepelných strát sušiarne, $[kWh.m^3]$,

V_D – objem sušeného dreva, $[m^3]$.

VÝSLEDKY A DISKUSIA

Priebeh procesu vlastného sušenia brezových vlysov podľa navrhnutého režimu a podľa ON 49 0651 je zobrazený na obr. 1.



Obr. 1 Krivka vlastného sušenia brezových vlysov

Podľa rozpisu teplôt a psychrometrických diferencií sušiacieho prostredia uvedeného režimu teplovzdušného sušenia brezových vlysov, sa uvedené režimy sušenia radia medzi tzv. režim so stúpajúcou teplotou a klesajúcou relatívnou vlhkosťou sušiacieho prostredia (Kollmann 1955, Trebula 1989).

Zníženie teploty sušiacieho prostredia počas odparovania voľnej vody z brezového dreva sa premieta v spomalení procesu sušenia a predĺžení vlastného času sušenia o 16 hod. Uvedená skutočnosť má negatívny dopad na kapacitné využitie komorovej sušiarne, ako uvádzajú aj práce (Trebula a Klement 2002, Dzurenda a Deliiski 2010).

Hodnoty technicko-zdôvodniteľnej normy spotreby tepla na vysušenie 1 m^3 brezových vlysov v stredno-kapacitnej komorovej sušiarňi KC 1/50, podľa navrhnutého režimu a režimu sušenia v zmysle normy ON 49 0651, z vlhkosti $w_p = 50 \%$ na vlhkosť $w_k = 10 \%$, pri počiatočnej teplote vlysov $t_r = 10 \text{ }^\circ\text{C}$ a pri priemernej teplote atmosférického vzduchu v okolí komorovej sušiarne $t_o = 10 \text{ }^\circ\text{C}$ uvádza tabuľka 2.

Tab. 2 Položky spotreby tepla na vysušenie 1 m^3 brezových vlysov v sušiarňi dreva KC 1/50

Položky bilancie spotreby tepla komorovej sušiarne dreva KC 1/50		Režim sušenia brezových vlysov			
		Navrhnutý		ON 49 0651	
		Špecifická spotreba tepla			
		kWh.m ⁻³	%	kWh.m ⁻³	%
Teplo na ohrev sušeného dreva	Q_W	31,56	11,92	33,20	13,49
Teplo na ohrev a zvlhčovanie. vzduchu v sušiarňi vo fáze ohrevu	Q_V	0,26	0,10	0,86	0,35
Teplo na ohrev konštrukcie sušiarne	Q_A	8,22	3,11	8,22	3,34
Teplo na ohrev vzduchu pre odparenie vody z dreva	Q_L	208,35	78,66	186,52	75,80
Teplo na uvoľnenie HG viazanej vody	Q_{HG}	2,96	1,12	2,96	1,20
Teplo na krytie tepelných strát sušiarne	Q_S	13,50	5,10	14,28	5,81
Normatív spotreby tepla $Q_{TZN} = \Sigma Q_i$		264,85	100,0	246,04	100,0

Teplovzdušné sušenie brezových vlysov podľa navrhnutého režimu v komorovej sušiarňi je z aspektu spotreby tepla charakterizované normatívom spotreby tepla $Q_{TZN} = 264,85 \text{ kWh.m}^{-3}$ a normatívom spotreby tepla $Q_{TZN} = 246,04 \text{ kWh.m}^{-3}$ pre režim sušenia podľa ON 49 0651. Z porovnania hodnôt normatívov spotreby tepla plynie, že v priebehu sušenia podľa navrhnutého režimu bez zmeny farby dreva sa spotrebuje o $18,81 \text{ kWh.m}^{-3}$ (7,1 %) viac tepla ako pri normovanom režime.

Z analýzy jednotlivých položiek vynaloženého tepla v procese sušenia plynie, že navrhovaný režim je síce úsporný: v spotrebe tepla na ohrev reziva o $Q_D = 1,64 \text{ kWh.m}^{-3}$ v spotrebe tepla na počiatočný ohrev a zvlhčenie sušiaceho média v sušiarňi o $Q_W = 0,6 \text{ kWh.m}^{-3}$, v spotrebe tepla na krytie tepelných strát sušiarne o $Q_S = 0,78 \text{ kWh.m}^{-3}$, ale zvýšená spotreba tepla v položke teplo na ohrev vzduchu pre odparenie vody z dreva o $Q_L = 21,83 \text{ kWh.m}^{-3}$, ktorá je niekoľko násobne vyššia než vyššie uvedené úspory rozhoduje vyššej energetickej náročnosti navrhovaného režimu nevyvolávajúcom zmenu farby dreva.

ZÁVER

Realizácia procesu odparovania voľnej vody z brezových vlysov počas sušenia v komorových teplovzdušných sušiarňach pri nižších teplotách, ako pri klasickom teplovzdušnom sušení podľa ON 49 0561 sa negatívne prejavuje na predlžovaní procesu sušenia brezových vlysov o $\Delta\tau = 16$ hod.

Uvedené skutočnosti sa premietajú i na spotrebe tepla. Normatív špecifickej spotreba tepla na vysušenie 1m^3 brezových vlysov v komorovej sušiarňi KC 1/50 podľa navrhnutého rozpisu je $Q_{TZN} = 264,85 \text{ kWh.m}^{-3}$. V porovnaní s normatívom spotreby tepla na sušenie brezových vlysov podľa režimu sušenia ON 49 0651 je normatív spotreby tepla o $18,81 \text{ kWh.m}^{-3}$ vyšší.

LITERATÚRA

1. BUČKO, J. (1995): Hydrolýzne procesy. Zvolen, Technická univerzita vo Zvolene, 116 s.
2. DELIISKI, N. (1991): Metod dlja ocenki stepeni oblagoraživanja bukovykh pilomaterialov vo vremja ich proparki. Súčasné problémy a perspektívy sušenia bukového reziva Zvolen: TU vo Zvolene, s. 37-44.
3. DZURENDA, L.(1993): Energetická náročnosť sušenia reziva v malokapacitných komorových sušiarňach. Sušenie dreva v malovýrobe. Zvolen: TU vo Zvolene, s. 97-111, ISBN 80-228-0224-7.
4. DZURENDA, L.; DELIISKI, N. (2010): Tepelné procesy v technológiách spracovania dreva. Zvolen: TU vo Zvolene, 274 s.
5. DZURENDA, L. (2020): Teplovzdušné sušenie parených brezových vlysov v komorových sušiarňach pri zachovaní farby pareného brezového dreva. Trieskové a beztrieskové obrábanie dreva, TU vo Zvolene, 12(1), s. 41-48.
6. GEFFERT, A.; GEFFERTO VÁ, J.; VÝBOHOVÁ, E.; DUDI AK, M. (2020): Impact of Steaming Mode on Chemical Characteristics and Colour of Birch Wood. Forests, 11, 478.

7. KAČÍK, F. (2001): Tvorba a chemické zloženie hydrolyzátov v systéme drevo – voda – teplo. Zvolen: TU vo Zvolene, 75 s.
8. KOLLMANN, F. (1955): Technologie des Holzes und der Holzwerkstoffe. 2 vyd. Berlin-Göttingen-Heidelberg-München, Springer – Verlag, 2 zv.
9. LAUROVÁ, M.; MAMOŇOVÁ, M.; KUČEROVÁ, V. (2004): Proces parciálnej hydrolýzy bukového dreva (*Fagus sylvatica* L.) parením a varením. Zvolen: TU Zvolen, 58 s.
10. TREBULA, P. (1989): Hydrotermická úprava a ochrana dreva, časť Hydrotermická úprava dreva. Zvolen: TU vo Zvolene, 301 s.
11. TREBULA, P.; BUČKO, J. (1996): Vákuové sušenie dreva, technické, technologické a ekologické aspekty. Zvolen: TU vo Zvolene, 70 s.
12. TREBULA, P.; KLEMENT, I. (2002): Sušenie a hydrotermická úprava dreva. Zvolen: TU vo Zvolene, 449 s.

POĎAKOVANIE:

Tento experimentálny výskum bol pripravený v rámci grantového projektu: *APVV-17-0456 „Termická modifikácia dreva sýtou vodnou parou za účelom cielenej a stabilnej zmeny farieb drevnej hmoty“* ako výsledok práce autora a značnej pomoci agentúry APVV.



AN APPROACH FOR ESTIMATING OF THE NATURAL COLOR CHANGE OF LOGS SUBJECTED TO THERMAL TREATMENT

Nencho Deliiski¹ – Ladislav Dzurenda² – Neno Trichkov¹

Abstract

An approach for estimating of the degree of change in the natural color of logs during their thermal treatment and subsequent conditioning in an air environment has been suggested. The approach is based on the integration of the solutions of own mathematical model for computing the 2D non-stationary temperature distribution in the longitudinal section of the logs during their thermal treatment. A software program has been prepared in the calculation environment of Visual FORTRAN Professional for solving of the model. With the help of the program, computations have been carried out for the determination of the integral temperature-time area on the logs' surface and also of 4 characteristic points in two beech logs with a diameter of 240 mm, length of 480 mm during their autoclave steaming and subsequent conditioning. The values of this area are used as a criterion for estimation of the degree of change in the natural color of the separate layers of the logs.

Key words: *beech logs, autoclave steaming, temperature-time area, color change*

INTRODUCTION

In the accessible specialized literature there are limited reports about the temperature distribution in subjected to thermal treatment logs aimed at their plasticizing in the production of rotary cut veneer (Chudinow 1968, Steinhagen 1986; Khattabi – Steinhagen 1993, Deliiski 2004, 2011; Deliiski – Dzurenda 2010; Hadjiski – Deliiski 2016) and there is no information about the approaches for quantitative determination of the degree of change in the natural color of the logs subjected to such treatment.

It is known that the market price of the plywood and other layered veneer products depends on the color of their surface layer. That is why the modeling and the study of the influence of the thermal treatment regimes of logs on the degree of change in the natural color of the veneer produced from them are of considerable scientific and practical interest.

The aim of this work is to suggest an approach for estimating the degree of change in the natural color of logs during their steaming and subsequent conditioning. The approach has to be based on the integration of the solutions of own non-linear model for calculation of the non-stationary 2D temperature field in the longitudinal section of logs during steaming.

¹ Faculty of Forest Industry, University of Forestry, Kliment Ohridski Bd. 10, 1797 Sofia, Bulgaria

² Technical University in Zvolen, T. G. Masaryka 24, 960 01 Zvolen
e-mail: deliiski@netbg.com, ntrichkov@gmail.com, dzurenda@tuzvo.sk

MATERIAL AND METHODS

Mathematical model of the 2D temperature distribution in non-frozen logs during their steaming and subsequent conditioning

When the length of the logs, L , is larger then their diameter, D , by not more then $3 \div 4$ times, for comuting the change of the temperature in the logs' longitudinal sections (i.e. along the coordinates r and z of these sections) during their steaming the following 2D mathematical model can be used (Deliiski 2004, 2011):

$$c \cdot \rho \frac{\partial T(r, z, \tau)}{\partial \tau} = \lambda_r \left[\frac{\partial^2 T(r, z, \tau)}{\partial r^2} + \frac{1}{r} \cdot \frac{\partial T(r, z, \tau)}{\partial r} \right] + \frac{\partial \lambda_r}{\partial T} \left[\frac{\partial T(r, z, \tau)}{\partial r} \right]^2 + \lambda_p \frac{\partial^2 T(r, z, \tau)}{\partial z^2} + \frac{\partial \lambda_p}{\partial T} \left[\frac{\partial T(r, z, \tau)}{\partial z} \right]^2 \quad (1)$$

with an initial condition

$$T(r, z, 0) = T_0 \quad (2)$$

and following boundary conditions:

a) During the staming process – at prescribed surface temperature of the logs:

$$T(r, 0, \tau) = T(0, z, \tau) = T_m(\tau), \quad (3)$$

b) During the conditioning process of the heated logs immedeately after their steaming – at convective heat exchange between the logs and surrounding air:

• Along the radial coordinate r on the logs' frontal surface:

$$\frac{\partial T(r, 0, \tau)}{\partial r} = - \frac{\alpha_p(r, 0, \tau)}{\lambda_p(r, 0, \tau)} \left[T(r, 0, \tau) - T_{\text{air}}(\tau) \right], \quad (4)$$

• Along the longitudinal coordinate z on the logs' cylindrical surface:

$$\frac{\partial T(0, z, \tau)}{\partial z} = - \frac{\alpha_r(0, z, \tau)}{\lambda_r(0, z, \tau)} \left[T(0, z, \tau) - T_{\text{air}}(\tau) \right]. \quad (5)$$

Equations (1) to (5) represent a common form of a mathematical model of the mutually connected processes of steaming and subsequent conditioning of logs, i.e. of the 2D temperature distribution in logs during these processes.

Mathematical description of thermo-physical properties of non-frozen wood

The thermo-physical properties and the density of the non-frozen wood, which participate in equations (1) ÷ (5), above the hygroscopic range, can be calculated according to following equations (Deliiski 2004, 2011):

$$c = \frac{1}{1+u} (2862u + 2.95T + 5.49u \cdot T + 0.0036T^2 + 555), \quad (6)$$

$$\rho = \rho_b(1+u) \text{ @ } u > u_{\text{fp}}, \quad (7)$$

$$\lambda = \lambda_0 \cdot [1 + \beta \cdot (T - 273.15)], \quad (8)$$

where

$$\lambda_0 = K_{\text{ad-}\lambda} \cdot v \cdot [0.165 + (1.39 + 3.8u) \cdot (3.3 \cdot 10^{-7} \rho_b^2 + 1.015 \cdot 10^{-3} \rho_b)], \quad (9)$$

$$\beta = 3.65 \left(\frac{579}{\rho_b} - 0.124 \right) \cdot 10^{-3}, \quad (10)$$

$$\nu = 0.1284 - 0.013u. \quad (11)$$

In Deliiski (2011) the precise values of the coefficient $K_{ad-\lambda}$ in eq. (9) for various wood species have been determined. For the beech wood the following values of the coefficient $K_{ad-\lambda}$ in eq. (9) have been obtained: in radial direction $K_{r-\lambda} = 1.35$ and in longitudinal direction $K_{l-\lambda} = 2.40$.

The heat transfer coefficients α_r in eq. (5) and α_p in eq. (4) of the subjected to air cooling beech logs after their autoclave steaming is equal to (Deliiski – Dzurenda 2010)

$$\alpha_r = 0.380 \cdot 1.026^{[T(0,z,\tau_{reg}) - T_{air}(\tau)]}. [T(0,z,\tau_{reg}) - T_{air}(\tau)], \quad (12)$$

$$\alpha_p = 0.676 \cdot 1.026^{[T(r,0,\tau_{reg}) - T_{air}(\tau)]}. [T(r,0,\tau_{reg}) - T_{air}(\tau)]. \quad (13)$$

Mathematical description of temperature-time area of the wood of logs subjected to thermal treatment and subsequent conditioning

For the determination of the change in the natural wood colour in the volume of logs subjected to thermal treatment and subsequent conditioning the suggested in (Deliiski 1991) approach can be modified and used. The approach is based on the solutions of the mathematical model (1) ÷ (5) and it consists of the calculation of the integral temperature-time area $S_j(\tau)$ (in K·s) of some characteristic points of the log according to the equation

$$S_j(\tau) = \int_0^\tau (T_{i,k}^n - T_{beg}) dt, \quad (14)$$

where j is the successive number of the corresponding characteristic point in the subjected to thermal treatment wood material; $T_{i,k}^n$ – current temperature in the j characteristic point with coordinates i along the radius and k along the length of the log, K; T_{beg} – the temperature at which the change in wood colour begins to take place, K, τ – time, s.

According to the equation (14) as a criterion for evaluation of the degree of wood colour change the integral area $S_j(\tau)$ is used. This area is found between the curves for the change in the temperature in separate characteristic points j during the wood thermal treatment process and a parallel line to the x -axis (axis measuring the time), corresponding to the temperature T_{beg} , at which the process of colour change from a natural colour begins.

RESULTS AND DISCUSSION

Computation of the 2D temperature distribution in logs during their freezing

The mathematical descriptions of $S_j(\tau)$ and of the thermo-physical characteristics of non-frozen logs given above were introduced in the mathematical model (1) to (5).

The model has been solved with the help of explicit schemes of the finite difference method in a way, equal to the one used and described in (Deliiski – Dzurenda 2010). For the numerical solving of the model, a software program was prepared in the calculation environment of Visual FORTRAN Professional developed by Microsoft.

With the help of the program computations were made for the determination of the 2D non-stationary change of the temperature in the longitudinal sections of two beech (*Fagus Sylvatica* L.) logs named below as Log 1 and Log 2. The calculation mesh has been built on $\frac{1}{4}$ of the longitudinal section of the logs due to the circumstance that this $\frac{1}{4}$ is mirror symmetrical towards the remaining $\frac{3}{4}$ of the same section.

The model was solved for logs with a diameter $D = 240$ mm, length $L = 480$ mm, basic density $\rho_b = 560$ kg·m⁻³, moisture content $u = 0.6$ kg·kg⁻¹, fiber saturation point $u_{\text{fsp}}^{293.15} = 0.31$ kg·kg⁻¹ (Deliiski – Dzurenda 2010) and with the following values of the log's temperature in the beginning of the steaming process:

- $t_0 = 0$ °C for Log 1,
- $t_0 = 20$ °C for Log 2.

The participating in eq. (14) temperature T_{beg} , at which the change in wood colour begins to take place, was accepted equal to 333.15 K, i.e. to 60 °C.

During the solving of the model, 3-stage regimes for autoclave steaming of the logs were used. The typical temperature time profile of the processing medium temperature t_m in a steaming autoclave and of the air medium for the subsequent conditioning of the heated wood materials is shown in (Deliiski 2011, Deliiski – Dzurenda 2010).

During the first stage of the steaming regimes input of water steam is accomplished in the autoclave, with situated inside logs, until the temperature of the processing medium $t_m = 132$ °C at steam pressure of 0.2 MPa is reached. After reaching $t_m = 132$ °C, this temperature is maintained unchanged by reducing the input of steam flux inside the autoclave until the calculated by the model average mass temperature of the wood, t_{avg} , reaches a value of 90 °C.

After reaching $t_{\text{avg}} = 90$ °C the input of steam in the autoclave is terminated and the second stage of the steaming regime begins. During this stage, by using the accumulated heat in the autoclave, the further heating and plasticizing of the logs is accomplished, thus resulting in gradual reduction of the temperature t_m for about 2 hours down to around 110 °C. Afterwards, the cranes directing the steam and condensed water out of the autoclave are opened, which initiates the third stage of the steaming regime. This stage ends after about 2 hours, when t_m reaches approximate value of around 85 °C. After that a conditioning of the logs under external aerial medium is realized. During the time of conditioning of the heated logs a redistribution and equalization of the temperature in their volume takes place, which is especially appropriate for the obtaining of quality rotary cut veneer.

Using the software program, computations were made for determination of the 2D non-stationary temperature change in 4 characteristic points in the longitudinal section of the logs during their autoclave steaming and subsequent conditioning. Point 1 was with coordinates $r = 30$ mm and $z = 120$ mm; Point 2: with $r = 60$ mm and $z = 120$ mm; Point 3: with $r = 90$ mm and $z = 180$ mm and Point 4: with $r = 120$ mm and $z = 240$ mm (center of the log). These coordinates of the characteristic points allow for the determination of the 2D temperature distribution in logs during their steaming and subsequent conditioning.

It is well known that for the obtaining of quality veneer from plasticized beech wood it is needed that the temperature of all characteristic points of the logs during the veneer cutting process stays between the optimal values of $t_{\text{min}} = 62$ °C and $t_{\text{max}} = 90$ °C (Deliiski 2004, Deliiski – Dzurenda 2010). The duration of the steaming regimes of the studied logs was chosen taking into account of that requirement.

On Fig. 1 and Fig. 2 the calculated change in t_m , t_s , and t of the pointed 4 characteristic points of the Log 1 and Log 2 during their autoclave steaming and subsequent conditioning at $t_{\text{air}} = 20$ °C is presented. It can be seen that the duration of the steaming regimes are equal to 10 h for Log 1 and to 9 h for Log 2 respectively.

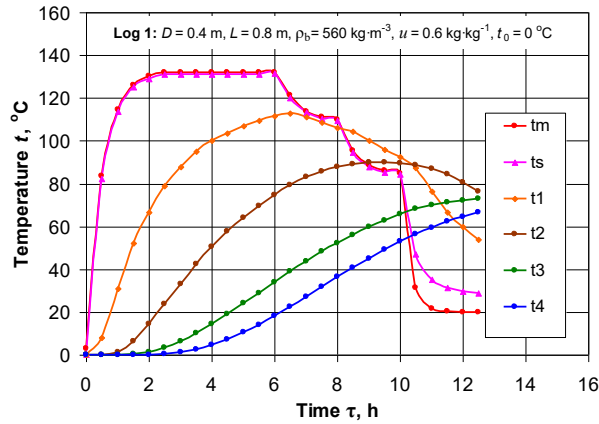


Figure 1. Change in t_m , t_s , and t in 4 characteristic points of the Log 1 with $t_0 = 0\text{ °C}$ during its steaming in an autoclave and its subsequent conditioning at $t_{\text{air}} = 20\text{ °C}$

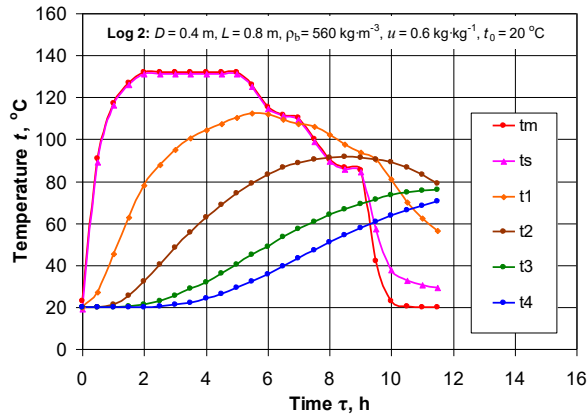


Figure 2. Change in t_m , t_s , and t in 4 characteristic points of the Log 2 with $t_0 = 20\text{ °C}$ during its steaming in an autoclave and its subsequent conditioning at $t_{\text{air}} = 20\text{ °C}$

After approximately 1.5 h conditioning of the heated logs the temperature of all characteristic points enter in the range from 62 °C and 90 °C. Due to the very large heat transfer coefficient between the logs and condensed on their surfaces water steam, the surface temperature of the logs, t_s , is equal to the processing medium temperature, t_m , in the autoclave. Significantly lower value of the convective heat transfer coefficient during the conditioning of the logs causes difference between t_s and $t_m = t_{\text{air}}$ after the steaming.

On Fig. 3 and Fig. 4 the calculated change in the integral temperature-time area on the logs' surface, S_s , and also S of the 4 characteristic points of the Log 1 and Log 2 during their autoclave steaming and subsequent conditioning is presented.

The analysis of the obtained results leads to the following statements:

1. The change in the integral temperature-time area on the logs' surfaces, S_s , and in all characteristic points, S_1 , S_2 , S_3 , and S_4 happens on complex curves.
2. At the end of the autoclave steaming of the logs the areas S_s and S_1 , S_2 , S_3 , and S_4 reach the following values:

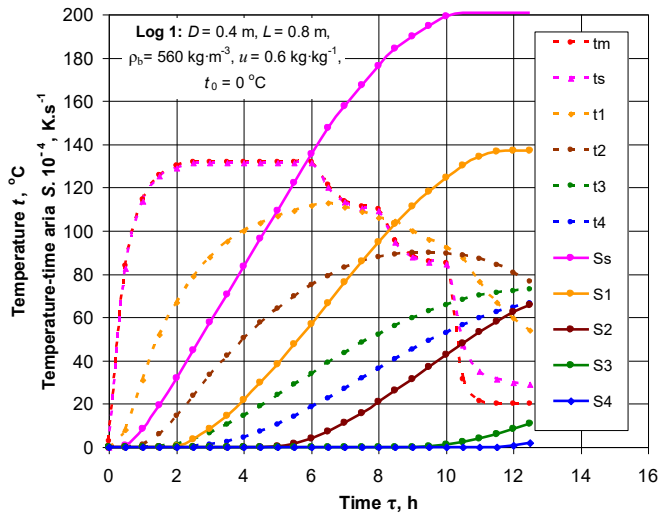


Figure 3. Change in S_s and S in 4 characteristic points of the Log 1 with $t_0 = 0\text{ }^\circ\text{C}$ during its steaming in an autoclave and its subsequent conditioning at $t_{\text{air}} = 20\text{ }^\circ\text{C}$

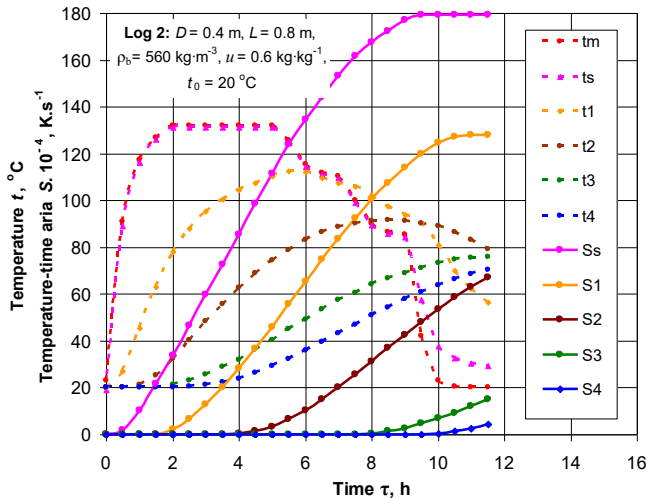


Figure 4. Change in S_s and S in 4 characteristic points of the Log 2 with $t_0 = 20\text{ }^\circ\text{C}$ during its steaming in an autoclave and its subsequent conditioning at $t_{\text{air}} = 20\text{ }^\circ\text{C}$

- For Log 1 after 10 h steaming: $S_s = 1.993 \cdot 10^6\text{ K}\cdot\text{s}^{-1}$, $S_1 = 1.244 \cdot 10^6\text{ K}\cdot\text{s}^{-1}$, $S_2 = 0.426 \cdot 10^6\text{ K}\cdot\text{s}^{-1}$, $S_3 = 0.027 \cdot 10^6\text{ K}\cdot\text{s}^{-1}$, and $S_4 = 0\text{ K}\cdot\text{s}^{-1}$;

- For Log 2 after 9 h steaming: $S_s = 1.770 \cdot 10^6\text{ K}\cdot\text{s}^{-1}$, $S_1 = 1.140 \cdot 10^6\text{ K}\cdot\text{s}^{-1}$, $S_2 = 0.426 \cdot 10^6\text{ K}\cdot\text{s}^{-1}$, $S_3 = 0.027 \cdot 10^6\text{ K}\cdot\text{s}^{-1}$, and $S_4 = 0\text{ K}\cdot\text{s}^{-1}$.

3. At the end of 2.5 h conditioning in an air environment of the heated logs the areas S_s and $S_1, S_2, S_3,$ and S_4 reach the following values:

- For Log 1: $S_s = 2.007 \cdot 10^6\text{ K}\cdot\text{s}^{-1}$, $S_1 = 1.372 \cdot 10^6\text{ K}\cdot\text{s}^{-1}$, $S_2 = 0.658 \cdot 10^6\text{ K}\cdot\text{s}^{-1}$, $S_3 = 0.108 \cdot 10^6\text{ K}\cdot\text{s}^{-1}$, and $S_4 = 0.020\text{ K}\cdot\text{s}^{-1}$;

▪ For Log 2: $S_s = 1.793 \cdot 10^6 \text{ K} \cdot \text{s}^{-1}$, $S_1 = 1.280 \cdot 10^6 \text{ K} \cdot \text{s}^{-1}$, $S_2 = 0.670 \cdot 10^6 \text{ K} \cdot \text{s}^{-1}$, $S_3 = 0.149 \cdot 10^6 \text{ K} \cdot \text{s}^{-1}$, and $S_4 = 0.044 \text{ K} \cdot \text{s}^{-1}$.

4. The comparison of these results with the pointed in (Deliiski 1991) values of S for pink, pink-red, and dark-red color of beech lumber after its steaming shows that:

- The surface layers of the steamed and conditioned logs have dark-red color;
- Part of the inner layers of the logs have red and part of them – pink color;
- The central layers do not change their natural color after the autoclave steaming.

This conclusion must be taken into consideration in the production of plywood and layered wood products with desired surface color from rotary cut veneer, which is received from logs after their steaming in an autoclave.

CONCLUSIONS

This paper describes an approach for estimation of the degree of change in the natural color of logs during their thermal treatment and subsequent conditioning in an air environment. The approach is based on the integration of the solutions of own mathematical model for computing the 2D temperature distribution in the longitudinal section of logs subjected to thermal treatment. For the numerical solution of the model and for the applying of the suggested approach a software program has been prepared, which has been input in the calculation environment of Visual FORTRAN Professional developed by Microsoft.

With the help of the program, computations have been carried out for the determination of the integral temperature-time area on the logs' surface and also of 4 characteristic points of two beech logs with a diameter of 240 mm and length of 480 mm during their autoclave steaming and subsequent conditioning. The values of that area are used as a criterion for estimation of the degree of change in the natural color of the separate layers of the logs.

The obtained results can be used for scientifically based determination of the change in the color of different layers of subjected to thermal treatment logs from various wood species and dimensions. They could be taken into consideration in the production of plywood or layered wood products with desired color of their surface veneer layer, which is received from logs, plasticized in an autoclave or in other equipment for thermal treatment.

Symbols:

- c – specific heat capacity, $\text{J} \cdot \text{kg}^{-1} \cdot \text{K}^{-1}$
 D – diameter, m
 L – length, m
 r – radial coordinate: $0 \leq r \leq D/2$, m
 S – area, m^2
 T – temperature, K: $T = t + 273.15$
 u – moisture content, $\text{kg} \cdot \text{kg}^{-1} = \% / 100$
 z – longitudinal coordinate: $0 \leq z \leq L/2$, m
 α – heat transfer coefficients between log surfaces and the surrounding air, $\text{W} \cdot \text{m}^{-2} \cdot \text{K}^{-1}$
 λ – thermal conductivity, $\text{W} \cdot \text{m}^{-1} \cdot \text{K}^{-1}$
 ρ – density, $\text{kg} \cdot \text{m}^{-3}$
 τ – time, s

Subscripts and superscripts:

avg	– average (for logs' mass temperature or for root square mean error)
b	– basic (for wood density)
beg	– beginning
fsp	– fiber saturation point
i	– knot of the calculation mesh for solving of the mathematical model in the direction along the logs' radius: $i = 1, 2, 3, \dots, 21$
k	– knot of the calculation mesh for solving of the model in longitudinal direction of the logs: $k = 1, 2, 3, \dots, 41$
m	– medium (for temperature of the processing medium in an autoclave)
n	– current number of the step $\Delta\tau$ along the time coordinate for model's solving: $n = 0, 1, 2, \dots$
0	– initial
p	– parallel to the wood fibers
r	– radial direction
s	– surface
293.15	– at 293.15 K, i.e. at 20 °C

REFERENCES

1. CHUDINOV, B. S., 1968: Theory of Thermal Treatment of Wood. Nauka, Moscow, 255 p. (in Russian).
2. DELIISKI, N. 1991: An approach for estimating the degree of ennoblement of beech lumber during its steaming. Proc. of the Int. Conf. „Contemporary problems and perspectives of drying beech wood“, Zvolen, Czechoslovakia, pp. 37-44.
3. DELIISKI, N. 2004: Modelling and Automatic Control of Heat Energy Consumption Required for Thermal Treatment of Logs. *Drvna Industrija*, 55 (4): 181-199.
4. DELIISKI, N., 2011: Transient Heat Conduction in Capillary Porous Bodies. In: *Convection and Conduction Heat Transfer*. InTech Publishing House, Rieka, 149-176.
5. DELIISKI, N., DZURENDA, L. 2010: Modelling of the Thermal Processes in the Technologies for Wood Thermal Treatment. TU Zvolen, Slovakia, 224 p. (in Russian).
6. HADJISKI M., DELIISKI N. 2016: Advanced Control of the Wood Thermal Treatment Processing. *Cybernetics and Information Technologies*, Bulgarian Academy of Sciences, 16(2): 179–197.
7. KHATTABI, A., STEINHAGEN, H. P. 1993: Analysis of Transient Non-linear Heat Conduction in Wood Using Finite-difference Solutions. *Holz als Roh- und Werkstoff*, 51(4): 272-278, <http://dx.doi.org/10.1007/BF02629373>.
8. STEINHAGEN, H. P. 1986: Computerized Finite-difference Method to Calculate Transient Heat Conduction with Thawing. *Wood Fiber Science*, 18(3): 460-467.

Acknowledgements

This document was supported by the APVV Grant Agency as part of the project: APVV-17-0456 as a result of work of authors and the considerable assistance of the APVV agency.



COMPUTING THE AVERAGE MASS TEMPERATURE OF LOGS AND THE RATE OF ITS CHANGE DURING LOGS' FREEZING

Nencho Deliiski – Neno Trichkov – Natalia Tumbarkova – Dimitar Angeski
– Zhivko Gochev

Abstract

An approach for computing the average mass temperature of logs subjected to freezing and the rate of its change has been suggested. The approach is based on the use of the solutions of own 2D non-linear model of the logs' freezing process. A software program has been prepared in the calculation environment of Visual FORTRAN Professional for solving of the model. With the help of the program, the 2D non-stationary temperature field in the longitudinal section of two poplar logs with a diameter of 240 mm, length of 480 mm, and moisture content above the hygroscopic range during their 50 h freezing in a freezer at approximately $-30\text{ }^{\circ}\text{C}$ has been calculated. After integration of the temperature fields, the average mass temperatures total for the whole volume of the studied logs and separately for their non-frozen and frozen zones, and also the rate of the change in these average mass temperatures have been calculated, visualized, and analyzed.

Key words: *poplar logs, freezing, average mass temperature, non-frozen zone, frozen zone*

INTRODUCTION

It is known that the duration and the energy consumption of the thermal treatment of frozen logs in the winter, aimed at their plasticizing for the production of veneer, depend on the degree of the logs' icing (Chudinov 1968; Shubin 1990; Požgaj et al.1997; Trebula – Klement 2002; Videlov 2003; Deliiski 2004; Pervan 2009; Deliiski – Dzurenda 2010).

In the accessible specialized literature there are limited reports about the temperature distribution in subjected to defrosting frozen logs (Steinhagen 1986, 1991; Khattabi – Steinhagen 1992, 1993, 1995; Deliiski 2004, 2011; Deliiski – Dzurenda 2010; Hadjiski – Deliiski 2016) and there is very little information about research of the temperature distribution in logs during their freezing (Deliiski – Tumbarkova 2016, 2017, 2019).

For different engineering and technological calculations it is necessary to be able to determine some energy characteristics of subjected to freezing logs, depending on their average mass temperature. In the available literature for hydrothermal treatment of frozen wood materials, there is no information about the approaches for quantitative determination of the logs' average mass temperature during their freezing.

The aim of the present work is to suggest an approach for computing the average mass temperature of logs subjected to freezing and the rate of its change. The approach have to

be based on the integration of the solutions of own non-linear model for calculation of the non-stationary 2D temperature field in the longitudinal section of logs during their freezing.

MATERIAL AND METHODS

Mathematical model of the 2D temperature distribution in logs during their freezing

When the length of the logs, L , is larger than their diameter, D , by not more than $3 \div 4$ times, for computing the change of the temperature in the logs' longitudinal sections (i.e. along the coordinates r and z of these sections) during their freezing in air medium the following 2D mathematical model can be used (Deliiski and Tumbarkova 2017):

$$c_{\text{we-f}} \cdot \rho_w \frac{\partial T(r, z, \tau)}{\partial \tau} = \lambda_{\text{wr}} \left[\frac{\partial^2 T(r, z, \tau)}{\partial r^2} + \frac{1}{r} \cdot \frac{\partial T(r, z, \tau)}{\partial r} \right] + \frac{\partial \lambda_{\text{wr}}}{\partial T} \left[\frac{\partial T(r, z, \tau)}{\partial r} \right]^2 + \lambda_{\text{wp}} \frac{\partial^2 T(r, z, \tau)}{\partial z^2} + \frac{\partial \lambda_{\text{wp}}}{\partial T} \left[\frac{\partial T(r, z, \tau)}{\partial z} \right]^2 + q_v \quad (1)$$

with an initial condition

$$T(r, z, 0) = T_{w0} \quad (2)$$

and boundary conditions for convective heat transfer:

- along the radial coordinate r on the logs' frontal surface during the freezing process:

$$\frac{\partial T(r, 0, \tau)}{\partial r} = - \frac{\alpha_{\text{wp-f}}(r, 0, \tau)}{\lambda_{\text{wp}}(r, 0, \tau)} \left[T(r, 0, \tau) - T_{\text{m-f}}(\tau) \right], \quad (3)$$

- along the longitudinal coordinate z on the logs' cylindrical surface during the freezing:

$$\frac{\partial T(0, z, \tau)}{\partial z} = - \frac{\alpha_{\text{wr-f}}(0, z, \tau)}{\lambda_{\text{wr}}(0, z, \tau)} \left[T(0, z, \tau) - T_{\text{m-f}}(\tau) \right]. \quad (4)$$

Equations (1) to (4) represent a common form of a mathematical model of the logs' freezing process, i.e. of the 2D temperature distribution in logs subjected to freezing.

Mathematical description of the average mass temperature of the logs and the rate of its change

For the calculation of some energy characteristics of logs during their freezing it is needed to have an information about the current values of the average mass temperature separately for the non-frozen and frozen zones of the logs, and also for their entire volume.

The average mass temperature of the non-frozen zone of the logs' volume during the freezing can be calculated through integration of the 2D non-stationary temperature distribution in the non-frozen part of the log's longitudinal section using the following equation:

$$T_{\text{avg-nf}}^n = \frac{1}{S_w} \iint_{S_w} T_{i,k}^n dS_w \quad @ \quad 272.15 \text{ K} < T_{i,k}^n \leq T_{w0}, \quad (5)$$

Analogously, the average mass temperature of the frozen zone of the logs' volume during the freezing can be calculated through integration of the 2D non-stationary

temperature distribution in the frozen part of the log's longitudinal section with the help of the following equation:

$$T_{\text{avg-fr}}^n = \frac{1}{S_w} \iint_{S_w} T_{i,k}^n dS_w \quad @ \quad T_{w\text{-fr-avg}} \leq T_{i,k}^n \leq 272.15 \text{ K}. \quad (6)$$

The average mass temperature of the entire volume of the logs during their freezing is calculated through integration of the 2D non-stationary temperature distribution in the whole log's longitudinal section using the following equation (Deliiski 2011):

$$T_{\text{avg-total}} = \frac{1}{S_w} \iint_{S_w} T_{i,k}^n dS_w \quad @ \quad T_{w\text{-fr-avg}} \leq T_{i,k}^n \leq T_{w0}. \quad (7)$$

It is needed strictly to take into account the temperature ranges in eqs. (5), (6), and (7) for each step along the time coordinate τ and for each knot of the calculation mesh used for solving of the mathematical model (1) to (4).

During the solving of the model, simultaneously with the computation of the average wood temperatures, $T_{\text{avg-nfr}}^n$, $T_{\text{avg-fr}}^n$, and $T_{\text{avg-total}}$, it is possible to calculate the current values of the rate of their change, $\frac{dT_{\text{avg-nfr}}}{d\tau}$, $\frac{dT_{\text{avg-fr}}}{d\tau}$, and $\frac{dT_{\text{avg-total}}}{d\tau}$ respectively.

RESULTS AND DISCUSSION

Computation of the 2D temperature distribution in logs during their freezing

The mathematical descriptions of the average mass temperature of the logs and the rate of its change given above, and also of the thermo-physical characteristics of the logs subjected to freezing given in (Deliiski 2004, 2009, 2013; Deliiski – Dzurenda 2010; Deliiski – Tumbarkova 2017, 2019) were introduced in the mathematical model (1) to (4).

The model has been solved with the help of explicit schemes of the finite difference method in a way, equal to the one used and described in (Deliiski and Tumbarkova 2019).

For the numerical solving of the model, a software program was prepared in the calculation environment of Visual FORTRAN Professional developed by Microsoft.

With the help of the program computations were made for the determination of the 2D non-stationary change of the temperature in the longitudinal sections of two poplar (*Populus nigra* L.) logs named below as Log 1 and Log 2. The calculation mesh has been built on $\frac{1}{4}$ of the longitudinal section of the logs due to the circumstance that this $\frac{1}{4}$ is mirror symmetrical towards the remaining $\frac{3}{4}$ of the same section.

The model was solved with the same initial and boundary conditions, as they were during the experimental research described in (Deliiski and Tumbarkova 2016, 2017, 2019). The logs were with a diameter $D = 240$ mm, length $L = 480$ mm, fiber saturation point $u_{\text{fip}}^{293.15} = 0.35 \text{ kg} \cdot \text{kg}^{-1}$ (Deliiski – Dzurenda 2010) and with the following values of the initial conditions in the beginning of the freezing process:

- for Log 1: $\rho_b = 359 \text{ kg} \cdot \text{m}^{-3}$, $u = 1.44 \text{ kg} \cdot \text{kg}^{-1}$, and $t_{w0} = 19.8 \text{ }^\circ\text{C}$;
- for Log 1: $\rho_b = 364 \text{ kg} \cdot \text{m}^{-3}$, $u = 1.78 \text{ kg} \cdot \text{kg}^{-1}$, and $t_{w0} = 20.5 \text{ }^\circ\text{C}$.

Using the software program, computations were made for determination of the 2D temperature change in 4 characteristic points in the longitudinal section of the logs during their 50 h freezing in a freezer at approximately $-30 \text{ }^\circ\text{C}$. Point 1 was with coordinates $r = 30$ mm and $z = 120$ mm; Point 2: with $r = 60$ mm and $z = 120$ mm; Point 3: with $r = 90$ mm

and $z = 180$ mm and Point 4: with $r = 120$ mm and $z = 240$ mm (center of the log). These coordinates of the characteristic points allow for the determination of the 2D temperature distribution in logs during their freezing.

Figure 1 presents the calculated change in the freezing medium temperature t_{m-fr} , log's surface temperature t_s , and t of 4 characteristic points in the studied poplar logs.

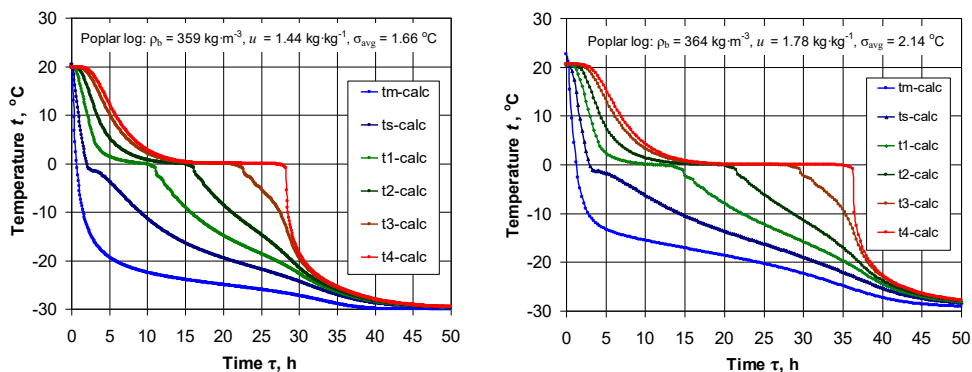


Figure 1. Calculated change in t_m , t_s , and t in 4 points of the studied poplar logs during their 50 h freezing

The comparison of the curves on Fig. 1 with analogical empirical curves of t in the characteristic points presented in (Deliiski and Tumbarkova 2017) show good qualitative and quantitative conformity between the calculated and experimentally determined changes in the very complicated temperature field of the studied logs during their freezing. Values of Root Square Mean Error (*RSME*), equal to $\sigma_{avg} = 1.66$ °C for Log 1 and $\sigma_{avg} = 2.14$ °C for Log 2 overall for the studied 4 characteristic points of the logs have been obtained.

During our wide simulations with the mathematical model, we observed good compliance between computed and experimentally established temperature fields during the freezing of logs from various wood species and different moisture content.

The overall *RSME* for the studied 4 characteristic points in the logs does not exceed 5% of the temperature ranges between the initial and the end temperatures of the logs subjected to freezing. In general, the larger the unevenness of the moisture content in the logs' volume is the larger value of *RSME* is obtained.

Computation of the logs' average mass temperatures and their rates of change

Simultaneously with the solution of the 2D model, calculations of $T_{avg-nfr}$, T_{avg-fr} , and $T_{avg-total}$, and also of the derivatives $\frac{dT_{avg-nfr}}{d\tau}$, $\frac{dT_{avg-fr}}{d\tau}$, and $\frac{dT_{avg-total}}{d\tau}$ have been carried out.

On Figure 2 the calculated change in the average mass temperatures $t_{avg-nfr}$, t_{avg-fr} , and $t_{avg-total}$ of Log 1 and Log 2 during their 50 h freezing is presented.

On Figure 3 the calculated change in the rates of the average mass temperatures $t_{avg-nfr}$, t_{avg-fr} , and $t_{avg-total}$ of the studied logs during their 50 h freezing is shown.

The obtained results show that through the freezing process of the logs the change of all studied average mass temperatures and their rates of change go on according to complex curves.

The average mass temperature $t_{avg-nfr}$ starts from a value, which is equal to the initial wood temperature of the logs t_{w0} . By increasing the freezing time the temperature $t_{avg-nfr}$

decreases and gradually approaches asymptotically to a value of $-1\text{ }^{\circ}\text{C}$, at which the freezing of the free water in the logs ends (Deliiski – Tumbarkova 2016).

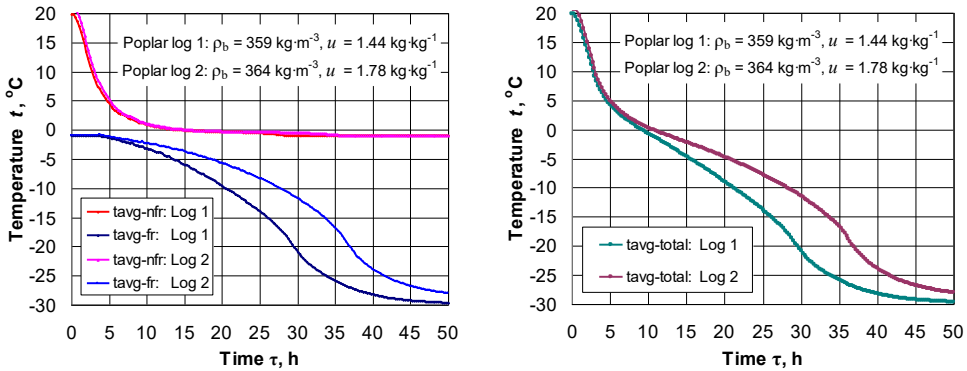


Figure 2. Change in $t_{\text{avg-nfr}}$ and $t_{\text{avg-fr}}$ (left) and $t_{\text{avg-total}}$ (right) of the studied logs during their 50 h freezing in a freezer at approximately $-30\text{ }^{\circ}\text{C}$

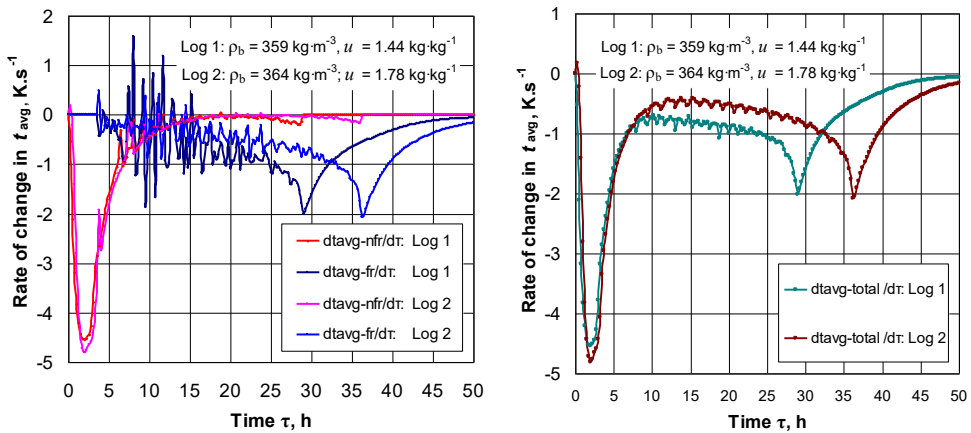


Figure 3. Change in $dt_{\text{avg-nfr}}/dt$ and $dt_{\text{avg-fr}}/dt$ (left) and $dt_{\text{avg-total}}/dt$ (right) of the studied logs during their 50 h freezing at approximately $-30\text{ }^{\circ}\text{C}$

The average mass temperature $t_{\text{avg-fr}}$ starts from a value of $-1\text{ }^{\circ}\text{C}$, at which the freezing of the bound water in the logs begins. By increasing the freezing time the temperature $t_{\text{avg-fr}}$ decreases, gradually approaching to the freezing medium temperature, which is equal to approximately $-30\text{ }^{\circ}\text{C}$.

The average mass temperature $t_{\text{avg-total}}$ starts from a value, which is equal to t_{w0} . By increasing the freezing time it decreases, gradually approaching to the freezing medium temperature of about $-30\text{ }^{\circ}\text{C}$.

At the beginning of the freezing process a sharply decreasing of $\frac{dt_{\text{avg-nfr}}}{d\tau}$ and $\frac{dt_{\text{avg-total}}}{d\tau}$ is observed (Fig. 3). Two hours from the beginning of the logs' freezing these derivatives reach values, equal to $-4.55\text{ K}\cdot\text{s}^{-1}$ for Log 1 and $-4.80\text{ K}\cdot\text{s}^{-1}$ for Log 2. This sharply decreasing correspond to the initial very step section of the dependences $t_{\text{avg-nfr}} = f(\tau)$ and $t_{\text{avg-total}} = f(\tau)$ (refer to Fig. 2).

During the first 3.75 h of the freezing process the derivative $\frac{dt_{\text{avg-fr}}}{d\tau}$ is equal to 0 because of the circumstance that then $t_{\text{avg-fr}}$ is constant and equal to -1 °C.

After 2nd h of the freezing process the rate of change in $t_{\text{avg-nfr}}$ sharply increases and gradually approaches asymptotically to a value of $0 \text{ K}\cdot\text{s}^{-1}$.

After 3.75th h the rate of change in $t_{\text{avg-fr}}$ fluctuates between $1.6 \text{ K}\cdot\text{s}^{-1}$ and $-1.9 \text{ K}\cdot\text{s}^{-1}$ and gradually decreases until reaching the minimal value of $-2.0 \text{ K}\cdot\text{s}^{-1}$. Such minimal value of $-2.0 \text{ K}\cdot\text{s}^{-1}$ reaches also the derivative $\frac{dt_{\text{avg-total}}}{d\tau}$. This is observed at 29th h of the freezing

process for Log 1 and at 32nd h for Log 2 when the inflexed points of the curves $t_{\text{avg-fr}} = f(\tau)$ and $t_{\text{avg-total}} = f(\tau)$ are coming (refer to Fig. 2). The fluctuations of $\frac{dt_{\text{avg-fr}}}{d\tau}$ are caused by the uneven increase during the time of the number of knots of the calculation mesh, which reflects the freezing of the bound water in the logs and determines an unevenness of the derivative $dt_{\text{avg-fr}}/d\tau$.

After reaching the minimal value of $-2.0 \text{ K}\cdot\text{s}^{-1}$, the derivatives $\frac{dt_{\text{avg-fr}}}{d\tau}$ and $\frac{dt_{\text{avg-total}}}{d\tau}$ increase gradually and reach a value of $0.06 \text{ K}\cdot\text{s}^{-1}$ for Log 1 and of $0.16 \text{ K}\cdot\text{s}^{-1}$ at the end of 50 h logs' freezing.

CONCLUSIONS

This paper describes a numerical approach for the computation of the average mass temperature of logs subjected to freezing and the rate of its change during the freezing process. The approach is based on the integration of the solutions of own non-linear mathematical model for calculation of the non-stationary 2D temperature distribution in the longitudinal section of the logs. The average mass temperatures separately for the non-frozen and frozen zones of the logs and also of the rate of their change have been calculated too.

For the numerical solution of the model and for the applying of the suggested approach a software program has been prepared, which has been input in the calculation environment of Visual FORTRAN Professional developed by Microsoft. With the help of the program, computations have been carried out for the determination of the mentioned above average wood mass temperatures and of the rate of their change for two poplar logs with a diameter of 240 mm, length of 480 mm, and moisture content above the hygroscopic range during their 50 h freezing in a freezer at approximately -30 °C.

The obtained results can be used for scientifically based determination of different energy characteristics of subjected to freezing and subsequent defrosting logs from various wood species.

Symbols:

- c – specific heat capacity, $\text{J}\cdot\text{kg}^{-1}\cdot\text{K}^{-1}$
- D – diameter, m
- L – length, m
- q – internal heat source, $\text{W}\cdot\text{m}^{-3}$
- r – radial coordinate: $0 \leq r \leq D/2$, m
- S – area, m^2
- T – temperature, K: $T = t + 273.15$

t	– temperature, °C: $t = T - 273.15$
u	– moisture content, $\text{kg}\cdot\text{kg}^{-1} = \%/100$
z	– longitudinal coordinate: $0 \leq z \leq L/2$, m
α	– heat transfer coefficients between log surfaces and the surrounding air, $\text{W}\cdot\text{m}^{-2}\cdot\text{K}^{-1}$
λ	– thermal conductivity, $\text{W}\cdot\text{m}^{-1}\cdot\text{K}^{-1}$
ρ	– density, $\text{kg}\cdot\text{m}^{-3}$
Σ	– root square mean error (<i>RSME</i>), °C
τ	– time, s
@	– at

Subscripts:

avg	– average (for logs' mass temperature or for root square mean error)
b	– basic (for wood density)
fr	– frozen or freezing
fsp	– fiber saturation point
i	– knot of the calculation mesh in the direction along the logs' radius: $i = 1, 2, \dots, 21$
k	– knot of the calculation mesh in longitudinal direction of the logs: $k = 1, 2, \dots, 41$
m	– medium (for freezing air environment)
nfr	– non-frozen
0	– initial
p	– parallel to the wood fibers
r	– radial direction
total	– total (for average mass temperature of the logs)
w	– wood
we	– wood effective (for specific heat capacity)

Superscripts:

293.15	– at 293.15 K, i.e. at 20 °C
n	– current number of the step along the time coordinate during the solving of the mathematical model: $n = 0, 1, 2, \dots$

REFERENCES

1. CHUDINOV, B. S., 1968: Theory of Thermal Treatment of Wood. Nauka, Moscow, 255 p. (in Russian).
2. DELIISKI, N. 2004: Modelling and Automatic Control of Heat Energy Consumption Required for Thermal Treatment of Logs. *Drvna Industrija*, 55 (4): 181-199.
3. DELIISKI, N., 2011: Transient Heat Conduction in Capillary Porous Bodies. In: *Convection and Conduction Heat Transfer*. InTech Publishing House, Rieka, 149-176.
4. DELIISKI, N., 2013: Computation of the Wood Thermal Conductivity during Defrosting of the Wood. *Wood research*, 58 (4): 637-650.
5. DELIISKI, N., DZURENDA, L., 2010: Modelling of the Thermal Processes in the Technologies for Wood Thermal Treatment. TU Zvolen, Slovakia, 224 p. (in Russian).

6. DELIISKI, N., TUMBARKOVA, N. 2016: A Methodology for Experimental Research of the Freezing process of logs. *Acta Silvatica et Lignaria Hungarica*, Vol. 12, № 2: 145-156, <http://dx.doi.org/10.1515/aslh-2016-0013>.
7. DELIISKI, N., TUMBARKOVA, N. 2017: An Approach and an Algorithm for Computation of the Unsteady Icing Degrees of Logs Subjected to Freezing. *Acta Facultatis Xilologiae Zvolen*, 59(2): 91-104, https://df.tuzvo.sk/sites/default/files/09-02-17_3_0_0_0_0.pdf
8. DELIISKI, N., TUMBARKOVA, N. 2019: Numerical Solution to Two-dimensional Freezing and Subsequent Defrosting of Logs. In Iranzo A editor. *Heat and Mass Transfer - Advances in Science and Technology Applications*, IntechOpen, 20 p., DOI: 10.5772/intechopen.84706, <http://mts.intechopen.com/articles/show/title/numerical-solution-to-two-dimensional-freezing-and-subsequent-defrosting-of-logs>
9. HADJISKI, M., DELIISKI, N. 2016: Advanced Control of the Wood Thermal Treatment Processing. *Cybernetics and Information Technologies*, Bulgarian Academy of Sciences, 16 (2): 179–197, <http://dx.doi.org/10.1515/cait-2016-0029>.
10. KHATTABI, A., STEINHAGEN, H. P. 1992: Numerical Solution to Two-dimensional Heating of Logs. *Holz als Roh- und Werkstoff*, 50 (7-8): 308-312, <http://dx.doi.org/10.1007/BF02615359>.
11. KHATTABI, A., STEINHAGEN, H. P. 1993: Analysis of Transient Non-linear Heat Conduction in Wood Using Finite-difference Solutions. *Holz als Roh- und Werkstoff*, 51(4): 272-278, <http://dx.doi.org/10.1007/BF02629373>.
12. KHATTABI, A., STEINHAGEN, H. P. 1995: Update of “Numerical Solution to Two-dimensional Heating of Logs”. *Holz als Roh- und Werkstoff*, 53(1): 93-94, <http://dx.doi.org/10.1007/BF02716399>.
13. PERVAN, S. 2009: *Technology for Treatment of Wood with Water Steam*. University in Zagreb (in Groatian).
14. SHUBIN, G. S., 1990: *Drying and Thermal Treatment of Wood*. Lesnaya promyshlennost, Moscow, URSS, 337 p., 1990 (in Russian).
15. STEINHAGEN, H. P. 1986: Computerized Finite-difference Method to Calculate Transient Heat Conduction with Thawing. *Wood Fiber Science*, 18(3): 460-467.
16. STEINHAGEN, H. P., 1991: Heat Transfer Computation for a Long, Frozen Log Heated in Agitated Water or Steam – A Practical Recipe. *Holz als Roh- und Werkstoff*, 49(7-8): 287-290, <http://dx.doi.org/10.1007/BF02663790>.
17. TREBULA, P., KLEMENT, I., 2002: *Drying and Hydrothermal Treatment of Wood*, TU in Zvolen, Slovakia, 449 p. (in Slovak).
18. VIDELOV, H., 2003: *Drying and Thermal Treatment of Wood*, University of Forestry in Sofia, Bulgaria, 335 p. (in Bulgarian).



ACIDITA (*pH*) TERMICKY A HYDROTERMICKY UPRAVOVANÉHO BUKOVÉHO DREVA

Michal Dudiak – Ladislav Dzurenda

Abstract

The paper presents the acidity values of beech wood in wet and dry state, without thermal treatment and after thermal treatment by steaming with water saturation with temperature $t = 125 \pm 2.5$ °C during $\tau = 7.5$ hours. Wet beech wood in the fresh state is slightly acidic, $pH = 5.18 \pm 0.15$. Through the process of technological treatment of beech wood by steaming, due to the hydrolysis of mainly hemicelluloses and extraction of water-soluble substances, the acidity of beech wood increases to the value of $pH = 4.01 \pm 0.25$. Hot air drying of beech wood at temperatures $t = 70 - 80$ °C causes a decrease in pH. The acidity of native beech wood decreased by $\Delta pH = 0.53$ by drying and by drying of steamed beech wood by $\Delta pH = 0.66$.

Key words: *beech wood, saturated water steam, acidity, tactile method of pH measurement*

ÚVOD

Hodnota pH je miera koncentrácie iónov H^+ v roztoku a používa sa na stanovenie kyslého, neutrálneho alebo zásaditého správania chemickej reakcie. Hodnoty pH sú veľmi dôležitými fyziologickými parametrami pre rastliny, ľudí a zvieratá. Vo výrobných procesoch sa zmena acidity využíva na riadenie technologických procesov.

V lúmenoch buniek mokrého dreva sa nachádza zriedený vodný roztok cukrov, organických kyselín a solí vápnika, horčíka, draslíka, sodíka anorganických kyselín, ktoré sú koreňovým systémom dopravované do žijúceho stromu (Čudinov 1968; Blažej *a kol.* 1975; Zevenhoven 2001, Pňakovič a Dzurenda 2015), v dôsledku čoho má tento roztok určitú aciditu. Acidita dreva listnatých, roztrúseno-pórovitých drevín s vlhkosťou nad bodom nasýtených vlákien (BNV) je v rozmedzí hodnôt $pH = 5,5 - 4,8$ (Sandermann a Rothkamm 1956; Irlé 2012; Solár 2014; Geffert *a kol.* 2019).

Kyslá reakcia dreva väčšiny drevín je spôsobená voľnými kyselinami a kyslými skupinami, ktoré sa ľahko odštiepujú, t.j. prevažne kyselinou octovou a acetylovými skupinami. Kyslosť dreva rastie počas skladovania vo vlhkom prostredí a s rastúcou teplotou.

Cieľom práce je stanovenie acidity vysušeného a pareného bukového dreva na vlhkosť $w = 10$ %, priamou metódou merania pH - plošnou elektródou SenTix Sur.

MATERIÁL A METODA

Materiál

Z dreva dreviny (*Fagus sylvatica* L.) bezprostredne po ťažbe boli vyrobené prírezy s rozmermi: hrúbkou $h = 27$ mm, šírkou $\delta = 60$ mm a dĺžkou $d = 550$ mm v počte 45 kusov. Bukové prírezy mali vlhkosť $w \approx 60,5$ %. Hustota bukového dreva v suchom stave bola stanovená v zmysle STN 49 0108 (1993) Drevo – stanovenie hustoty.

Prírezy boli rozdelené do 3 skupín po 15 kusov v každej skupine. Prírezy prvej skupiny neboli termicky upravované. Prírezy druhej a tretej skupiny boli tepelne ošetrené nasýtenou vodnou parou pri teplote $t = 125 \pm 2,5$ °C v dĺžke trvania 7,5 hodín. Tepelná úprava bukového dreva sýtou vodnou parou bola vykonaná v tlakovom autokláve APDZ 240 (Himmasch AD, Haskovo, Bulharsko) inštalovanom v spoločnosti Sundermann s.r.o. Banská Štiavnica (Slovensko). Termicky upravené bukové vlisy parením sýtou vodnou parou, ako i termicky neupravené bukové prírezy prvej skupiny boli vysušené na vlhkosť $w = 10$ % v teplovzdušnej komorovej sušiarňi KC 1/50 vyrábanej firmou SUSAR s.r.o. Sušenie bukových prírezov sa realizovalo teplovzdušným režimom podľa ON 49 0651 pri teplotách $t = 70 - 80$ °C.

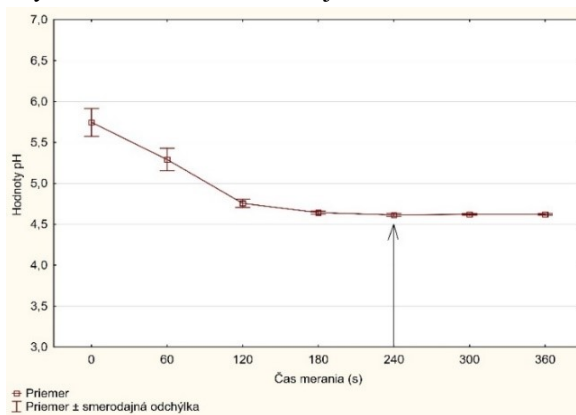
Meranie vlhkosti

Vlhkosť natívneho, pareného i vysušeného bukového dreva bola stanovená gravimetrickou metódou podľa normy STN EN 13183-1 (2003).

Meranie acidity

Meranie acidity mokrého i vysušeného termicky natívneho i termicky upravovaného bukového dreva sa vykonávalo na ohobľovanom povrchu pomocou pH-metra pH7110 s plošnou elektródou SenTix Sur.

Meranie acidity mokrého bukového dreva sa vykonávalo priložením plošnej elektródy SenTix Sur pH-metra typ: pH7110 na povrch dreva. Hodnota acidity sa odčítala po ustálení hodnoty pH na displeji pH-metra. V mieste merania pH suchého dreva plošnou elektródou SenTix Sur sa najprv pomocou kvapkadla kvapla jedna kvapka destilovanej vody na povrch dreva a následne bola plošná dotyková elektróda pritlačená k povrchu dreva v mieste kvapnutej kvapky, čím sa vytvoril kontakt elektródy z povrchom dreva. Hodnota pH sa odčítala po cca 240 sekundách stabilizácie elektródy na pH-metri pH7110. Záznam priebehu merania acidity suchého bukového dreva je na obr. 1.



Obr. 1 Meranie pH na povrchu suchého bukového dreva po jeho zvlhčení kvapkou vody

Namerané hodnoty acidity bukového dreva sú uvádzané formou zápisu $x = \bar{x} \pm s_x$ t.j. priemernej nameranej hodnoty a smerodajnej odchýlky.

VÝSLEDKY A DISKUSIA

Hustota bukového dreva v suchom stave $\rho_0 = 683 \pm 36 \text{ kg.m}^{-3}$, stanovená meraním zo vzoriek bukových prírezov čo predstavuje priemernú hodnotu hustoty zdravého, hubami, či plesňami nepoškodeného bukového dreva. Obdobné hodnoty hustoty bukového dreva pre územie Strednej Európy uvádzajú práce: (Požgaj *a kol.* 1997; Makovíny 2010; Kurjatko *a kol.* 2010). Na základe uvedeného konštatovania je možné aciditu bukového dreva, ako aj jej zmeny dosiahnuté termickou, či hydrotermickou úpravou označiť prívlastkom reprezentatívne (štandardné).

Výsledky merania acidity natívneho bukového dreva v čerstvom stave, termicky upravovaného sýtou vodnou parou a vysušeného nepareného a pareného bukového dreva sú v tab. 1.

Tab. 1 Namerané hodnoty pH mokrého a vysušeného bukového dreva, pareného a vysušeného bukového dreva v teplovzdušnej sušiarňi

Bukové prírezy	Vlhkosť dreva	Acidita bukového dreva
Bukové drevo mokré	$60,5 \pm 0,8$	$5,18 \pm 0,15$
Bukové drevo po vysušení	$10,4 \pm 0,6$	$4,65 \pm 0,12$
Bukové drevo po termickej úprave - parením	$51,8 \pm 1,2$	$4,01 \pm 0,25$
Parené bukové drevo po vysušení	$10,2 \pm 0,5$	$3,35 \pm 0,15$

Nami nameraná hodnota acidity bukového dreva v čerstvom stave $\text{pH} = 5,18 \pm 0,15$ je obdobný údaj, ako uvádza (Geffert *a kol.* 2019) pre mokrého bukového dreva stanovený pH metrom SI 600 s vpichovou elektródou LanceFET+H od firmy SENTRON.

Nížšia nameraná hodnota acidity termicky upravovaného bukového dreva parením $\text{pH} = 4,01 \pm 0,25$ je potvrdením známych poznatkov o priebehu hydrolýzy predovšetkým hemicelulóz v mokrom dreve listnatých drevín pôsobením tepla na mokré drevo, ako ich uvádzajú práce: (Melcer *a kol.* 1989; Laurová *a kol.* 2004; Sundqvist *a kol.* 2006; Samešová *a kol.* 2018; Geffert *a kol.* 2019).

Technologickým procesom sušenia bukového dreva nedochádza len k úbytku hmotnosti z dôvodu odparovania vody z dreva ale pôsobením tepla na drevo počas odparovania voľnej vody aj k miernej hydrolýze polysacharidov a to predovšetkým hemicelulóz. Z odštiepených acetylových skupín sa tvorí predovšetkým kyselina octová, ako aj kyselina mravčia, ktoré zostávajú v dreve aj po odparení vody. Zvlhčením dreva sa tieto kyseliny aktivujú, čo potvrdzujú i merania pH vysušeného pareného i nepareného bukového dreva. Acidita nepareného bukového dreva sušením poklesla o $\Delta\text{pH} = 0,53$ a sušením pareného bukového dreva o $\Delta\text{pH} = 0,66$.

ZÁVER

V príspevku sú prezentované hodnoty acidity mokrého bukového dreva v čerstvom stave, termicky upravovaného bukového dreva sýtou vodnou parou a vysušeného bukového dreva na vlhkosť $w = 10 \%$.

Namerané hodnoty acidity bukového dreva sú $pH = 5,18 - 4,01$. Kým mokré drevo v čerstvom stave je mierne kyslé $pH = 5,18 \pm 0,15$, tak procesy termickej úpravy a hydrotermickej úpravy kyslosť dreva zvyšujú. Termickou úpravou mokré bukové drevo parením - sýtou vodnou parou s teplotou $t = 125 \pm 2,5$ °C počas $\tau = 7,5$ hod sa acidita bukového dreva znižuje na úroveň $pH = 4,01 \pm 0,25$.

Aj proces teplovzdušného sušenia bukového dreva spôsobuje pokles hodnoty pH. Acidita nepareného bukového dreva sušením poklesla o $\Delta pH = 0,53$ a sušením pareného bukového dreva o $\Delta pH = 0,66$.

LITERATÚRA

1. BLAŽEJ, A., ŠUTÝ, L., KOŠÍK, M., KRKOŠKA, P. GOLIS, E. (1975): *Chémia dreva*. ALFA, Bratislava. 221 s.
2. ČUDINOV, B. S., STEPANOV, V. L. (1968): *Phasenzusammensetzung der Wassers in gefrorenem Holz*. In: *Holztechnologie*, 9(1): 14-18 s.
3. GEFFERT, A., GEFFERTOVÁ, J., DUDIAK, M. (2019). *Direct Method of Measuring the pH Value of Wood*. In: *Forests* 10(10), 852; doi:10.3390/f10100852.
4. IRLE, M. (2012): pH and why you need to know it. *Wood Based Panels International* Available online: <http://www.wbpionline.com/features/ph-and-why-you-need-to-know-it/>
5. KURJATKO, S., et al. (2010): *Parametre kvality dreva určujúce jeho finálne použitie*. Technická univerzita vo Zvolene, Zvolen, 352 s.
6. MAKOVÍNY, I. (2010). *Úžitkové vlastnosti a použitie rôznych druhov dreva*. Zvolen: Technická univerzita Zvolen, 104 s.
7. MELCER, I., MELCEROVÁ, A., SOLÁR, R., KAČÍK, F. (1989). *Chemizmus hydrotermickej úpravy listnatých drevín*. Zvolen: Vysoká škola lesnícka a drevárska, 2/1989, 76 s.
8. PŇAKOVIČ, E., DZURENDA, L. (2015): *Combustion characteristics of fallen fall leaves from ornamental trees in city and forest parks*. *BioResources*, 10(3): 5563-5572. DOI: 10.15376/biores.10.3.5563-5572.
9. POŽGAJ, A., CHOVANEC, D., KURJATKO, S., A BABIAK M. (1997): *Štruktúra a vlastnosti dreva*. Príroda, Bratislava, 485 s.
10. LAUROVA, M., MAMONOVA, M., KUČEROVA, V. (2004): *Proces parciálnej hydrolyzy bukového dreva (Fagus sylvatica L.) parením a varením*. Zvolen: TU Zvolen. 58 s.
11. SAMEŠOVÁ, D., DZURENDA, L., JURKOVIČ, P. (2018): *Kontaminácia kondenzátu produktmi hydrolyzy a extrakcie v termickom procese farebnej modifikácie roztrúsenopórovitých listnatých drevín*. In: *Trieskové a beztrieskové obrábanie dreva*, 11(1): 235–239. ISSN 2453-904X
12. SANDERMAN, W., ROTHKAMM, M. (1959): *The determination of pH values of woods and their practical importance* In: *Holz Roh- Werkstoff*, 17: 433-441.
13. SOLÁR, R. (2004): *Chémia dreva*, Technická univerzita vo Zvolene, Zvolen. 102 s.
14. SUNDQVIST, B., KARLSSON, O., WESTREMARK, U. (2006): *Determination of formic-acid and acid concentrations formed during hydrothermal treatment of birch wood and its relation to color, strength and hardness*, In: *Wood Sci Technol* 40(7):549-561.
15. ZEVENHOVEN, M. (2001): *Ash-forming matter in biomass fuels*. Åbo Akademi University. 88 s. ISBN 952-12-0813-9.

POĎAKOVANIE

Tento experimentálny výskum bol pripravený v rámci grantového projektu: *APVV-17-0456 „Termická modifikácia dreva sýtou vodnou parou za účelom cielenej a stabilnej zmeny farby drevnej hmoty“* ako výsledok práce autorov a značnej pomoci agentúry APVV.



TEPLOVZDUŠNÉ SUŠENIE PARENÝCH BREZOVÝCH VLYSOV V KOMOROVÝCH SUŠIARŇACH PRI ZACHOVANÍ FARBY NADOBUDNUTEJ PROCESOM PARENIA

Ladislav Dzurenda

Abstract

The paper presents a hot air regime for drying steamed birch friezes with dimensions: 38x100x800 mm from the initial moisture content $W_p \approx 50\%$ to the final humidity $W_k = 10\%$, while maintaining the color of wood obtained in the process of steaming with saturated steam. The drying process is divided into two parts. Evaporation of free water from wet wood at drying medium temperatures $t_s = 35 \div 40$ °C and relative air humidity $\varphi = 70 - 60$ %, when there are no chemical changes in the lignin-saccharide complex of birch wood manifested by a change in color. Evaporation of bound water from birch wood below the hygroscopicity limit is performed at temperatures $t_s = 60 - 70$ °C. The color coordinates of steamed birch wood after drying by a given regime in the CIE color space $L^* a^* b^*$ are: $L^* = 67.1 \pm 1.6$; $a^* = 12.3 \pm 0.9$; $b^* = 18.4 \pm 0.9$. Total color difference $\Delta E^* = 1.6$. According to the categorization of wood color changes in thermal processes of wood (Cividini et al. (2007), this change belongs to small (insignificant) color changes.

Key words: steamed birch friezes, hot air drying, chamber dryers, wood color.

ÚVOD

Breza biela je roztrúsenopórovitá drevina. Drevo je stredne ťažké, mierne tvrdé, pružné, pevné v ohybe a ťahu. Podľa autorov *Perelygin (1965)*, *Makoviny (2010)*, *Klement – Réh – Detvaj (2010)* brezové drevo má svetlu bielo-hnedú farbu. Vo farebnom priestore CIE- $L^* a^* b^*$, autori: *Babiak – Kubovský – Mamoňova (2004)*, farbu brezového dreva popisujú hodnotami súradníc: $L^* = 78,07$; $a^* = 5,92$; $b^* = 20,02$. V práci: *Wood colour of central European wood species: CIELAB characterisation and colour intensification*, autori: *Meints – Teischinger – Stingl – Hansmann (2016)* farbu brezového dreva udávajú hodnotami súradníc: $L^* = 80,7$; $a^* = 7,8$; $b^* = 25,3$.

Parením mokrého brezového dreva sa jeho farba mení. Drevo nadobúda hnedú farbu, ktorej tmavosť sa so zvyšujúcou teplotou procesu parenia a predlžovaním času parenia zvyšuje *Dzurenda (2019)*. Vyššie uvedené tvrdenie o zmene farby a poklese svetlosti dreva v procese parenia je v súlade s poznatkami o parení, či inej termickej úprave mokrého dreva listnatých drevín *Tolvaj et al. (2009)*, *Dzurenda (2014,2018)*, *Barčík et al. (2015)*, *Hadjirski – Deliiski (2016)*, *Baranski et al. (2017)*, *Hrčkova et al. (2018)*, *Geffert et al. (2020)*.

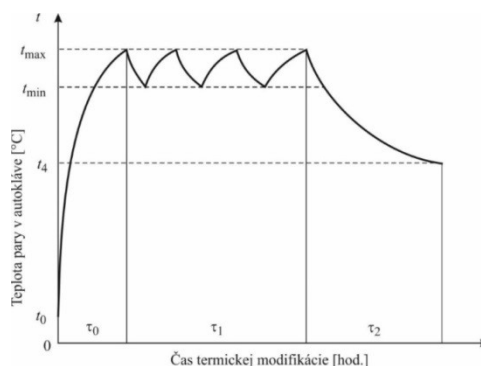
Sušenie dreva je hydrotermický proces v ktorom sa z dreva odstraňuje voda. Sušenie reziva a vlysov v teplovzdušných komorových sušiarňach sa vykonáva prostredníctvom sušiacich režimov ON 49 0651, GOST, či vlastných režimov sušenia jednotlivých firiem KATRES s.r.o., Hildebrand Holztechnik GmbH, Mühlböck Holz Trocknungsanlagen GmbH, NARDI. Sušenie brezového reziva a vlysov je bežne realizované pri teplotách $t = 50 \div 70$ °C. Realizácia procesu sušenia pri uvedených teplotách vytvára podmienky nielen pre odstraňovanie vody z dreva, ale v mokrom dreve i podmienky pre priebeh chemických reakcií akými sú: hydrolýza hemicelulózy dreva, depolymerizácia polysacharidov a chemické zmeny v ligníne vyvolávajúce modifikáciu chromoforného systému v lignín-sacharidickom komplexe dreva *Bučko (1995)*, *Trebula – Bučko (1996)*, *Cividini et al. (2007)*, *Dzurenda – Deliiski (2012)*, *Dzurenda – Dudiak (2020)*, prejavujúce sa zmenou farby dreva.

Cieľom tejto práce je prezentácia režimu teplovzdušného sušenia parených brezových vlysov s rozmermi: 38x100x800 mm z počiatočnej vlhkosti $W_p \approx 50$ % na konečnú vlhkosť $W_k = 10$ % v komorových sušiarňach reziva, z aspektu zmeny farby dreva a kvality vysušených vlysov navrhnutým režimom sušenia.

MATERIÁL A METODA

Parenia brezových vlysov

Brezové vlysy boli pred sušením parené. Proces parenia sýtou vodnou parou za účelom zmeny pôvodnej svetlej bielo - hnedej farby na hnedú farbu bol realizovaný v tlakovom autokláve APDŽ 240 (Chimmaš AD, Haskovo, Buluharsko) vo firme Sundermann s.r.o. Banská Štiavnica. Priebeh procesu parenia – termickej modifikácie farby brezových vlysov obr. 1. a technicko-technologické parametre režimu parenia uvádza tabuľka 1.



Obr. 1 Režim pre modifikáciu farby brezových vlysov parením

Tab. 1 Parametre režimu pre modifikáciu farby dreva brezových vlysov parením

Režimy	Teplota sýtej pary [°C]			Čas technologickej operácie [hod]		
	t_{min}	t_{max}	t_4	τ_1 - fáza I	τ_2 - fáza II	Celkový čas
Režim parenia	122,5	127,5	100	6,0	1,5	7,5

Sušenie parených brezových vlysov bez vplyvu na zmenu farby dreva

Pokles vlhkosti dreva parených vlysov na vlhkosť $w_2 \approx 10$ % bol vykonaný dvoma spôsobmi: - sušením v klimatizovanom priestore,
- sušením v teplovzdušnej sušiarňi reziva, navrhnutým režimom.

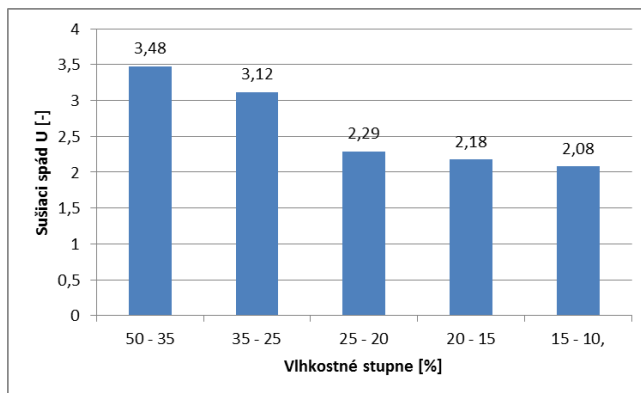
Sušenie v klimatizovanom priestore, 20 ks parených brezových vlysov bolo realizované v klimatizovanom priestore pri teplote vzduchu $t = 20^{\circ}\text{C}$ a relatívnej vlhkosti vzduchu $\varphi = 60\%$. Hodnoty farebných súradníc L^* , a^* , b^* na ohobľovanom povrchu vysušených vlysov vo farebnom priestore CIE $L^*a^*b^*$ sú označená prívlastkom – *referenčná hodnota*.

Sušenie parených brezových vlysov navrhnutým režimom bolo vykonané v teplovzdušnej komorovej sušiarňi KC 1/50 vyrábanej firmou SUSAR s.r.o. Rozpis vonkajších podmienok pre sušenie parených brezových vlysov s rozmermi: $38 \times 100 \times 800$ mm z vlhkosti $W_p \approx 50\%$ na vlhkosť $W_k = 10\%$ v komorovej sušiarňi reziva uvádza tabuľka 2. Proces sušenie je rozdelený na dva časti. Sušenie počas adiabatického odparovania voľnej vody z mokrého dreva je navrhované pri teplotách vlhkého vzduchu $t = 35 \div 40^{\circ}\text{C}$ a relatívnej vlhkosti vzduchu $\varphi = 70 - 60\%$. Pri uvedených teplotách nie sú vytvorené podmienky pre chemické reakcie lignínu v lignín-sacharidickom komplexe prejavujúce sa zmenou chromoforného systému vyvolávajúce zmenu farby brezového dreva. Na konci uvedenej fázy je zaradené kondicionovanie za účelom čiastkovej eliminácie vlhkosťného spádu vytvoreného v dreve vlysov počas odparovania vody z lúmenov buniek. Kondicionovanie je realizované zvýšením relatívnej vlhkosti vzduchu na $\varphi = 84\%$ a teploty vzduchu $t = 50^{\circ}\text{C}$. Sušenie brezového dreva pod medzou hygroskopicity je realizované pri teplotách vlhkého vzduchu $t = 60 - 70^{\circ}\text{C}$.

Tab. 2 Rozpis vonkajších podmienok sušenia pre parené brezové vlysy pri zachovaní farby dreva nadobudnutej procesom parenia

Fáza sušenia	Vlysov s rozmermi: $38 \times 100 \times 800$ mm		
	t_s [$^{\circ}\text{C}$]	Δt [$^{\circ}\text{C}$]	τ [hod]
Ohrev	35	2	4
50 ÷ 35	35	5	40
35 ÷ 25	40	8	25
Kondicionovanie	50	3	6
25 ÷ 20	60	8	13
20 ÷ 15	70	11	15
15 ÷ 10	70	16	20
Ošetrovanie	70	7	7
Ochladzovanie	30	7	4

Miera tvrdosti režimu sušenia parených brezových vlysov vyjadrená formou sušiaceho spádu ($U = w/w_{rov}$) v jednotlivých vlhkosťných stupňoch je zobrazené na obr. 2.



Obr. 2 Hodnoty sušiacich spádov pre jednotlivé vlhkosťné stupne sušenia parených brezových vlysov

Kontrola farby a kvality vysušených parených brezových vlysov

Farba vysušených vlysov na ohobľovanom povrchu sa merala kolorimetrom Color Reader CR-10. Vplyv režimu sušenia na zmenu farby brezového dreva bol vyhodnocovaný:

- Stanovením hodnôt L^* , a^* , b^* farebného priestoru CIE $L^*a^*b^*$ pareného brezového dreva. Hodnoty farebných súradníc sú uvádzané formou zápisu: $x = \bar{x} \pm s_x$ t.j. priemernej nameranej hodnoty a smerodajnej odchýlky.
- Porovnávaním hodnôt na súradniciach L^* , a^* , b^* vysušeného dreva teplovzdušným režimom sušenia s referenčnými hodnotami súradnice L^* , a^* , b^* brezového dreva vysušeného v klimatizovanom priestore.
- Stanovením celkovej farebnej diferencie ΔE kvantifikovanej vzťahom:

$$\Delta E^* = \sqrt{(L_1^* - L^*)^2 + (a_1^* - a^*)^2 + (b_1^* - b^*)^2} \quad (1)$$

kde: L^* , a^* , b^* hodnoty na súradniciach farebného priestoru brezového dreva vysušeného v klimatizovanom priestore.

L_1^* , a_1^* , b_1^* hodnoty na súradniciach farebného priestoru brezového dreva vysušeného navrhnutým režimom sušenia v sušiarňi KC 1/50.

Kontrola kvality vysušených vlysov bola po ukončení procesu sušenia vykonaná stanovením: odchýlky konečnej vlhkosti od požadovanej vlhkosti w_0 , kolísanie konečnej vlhkosti w_{k0} a vlhkosťným spádom Δw .

Odchýlka konečnej vlhkosti od požadovanej vlhkosti bola stanovovaná prostredníctvom vzťahu:

$$w_0 = \frac{\sum_{i=1}^n w_{ik}}{n} - w_k \quad [\%], \quad (2)$$

kde: n – počet kontrolných vzoriek [-],

w_{ik} – konečná vlhkosť vzoriek [%],

w_k – požadovaná konečná vlhkosť dreva [%].

Kolísanie konečnej vlhkosti sa hodnotilo rozdielom hodnôt maximálnej a minimálnej vlhkosti vzoriek podľa vzťahu:

$$w_{k0} = w_{\max} - w_{\min} \quad [\%], \quad (3)$$

kde: w_{\max} – maximálna vlhkosť v sušiacich vzorkách [%],

w_{\min} – minimálna vlhkosť v sušiacich vzorkách [%].

Vlhkosťný spád v rezive bol stanovený z rozdielu vlhkosti stredovej vrstvy a priemeru oboch povrchových vrstiev:

$$\Delta w = w_s - w_{\text{pov}} \quad [\%], \quad (4)$$

kde: w_s – vlhkosť stredovej vrstvy [%],

w_{pov} – vlhkosť povrchových vrstiev [%].

VÝSLEDKY A DISKUSIA

Referenčné hodnoty súradníc farby vo farebnom priestore CIE $L^*a^*b^*$, dreva parených brezových vlysov vysušených na vlhkosť $w \approx 10\%$ v klimatizovanom priestore pri teplote vzduchu $t = 20\text{ }^\circ\text{C}$ a relatívnej vlhkosti vzduchu $z \varphi = 60\%$, na ohobľovanom povrchu uvádza tabuľka 3.

Tab. 3 Hodnoty súradníc farby pareného brezového dreva sušeného v klimatizovanom priestore (Referenčná hodnota)

Parené brezové vlysy sušené v klimatizovanom priestore	Farebné súradnice		
	L^*	a^*	b^*
počet meraní [-]	40	40	40
hodnota súradnice [-]	68,4 ± 1,5	11,8 ± 1,0	19,2 ± 1,1

Po ukončení procesu sušenia parených brezových vlysov v teplovzdušnej komorovej sušiarňi KC 1/50 bola meraná farba brezových vlysov na ohobľovanom povrch 36 ks vlysov a vykonaná kontrola kvality na 12 ks vysušených vlysoch.

Hodnoty farebných súradníc: L^* , a^* , b^* vysušeného brezového dreva meraných na ohobľovanom povrchu oboch ložných plôch uvádza tabuľka 4.

Tab. 4 Hodnoty súradníc farby pareného brezového dreva sušeného v komorovej sušiarňi reziva, navrhnutým režimom sušenia

Parené brezové vlysy sušené v komorovej sušiarňi reziva	Farebné súradnice		
	L^*	a^*	b^*
počet meraní [-]	72	72	72
hodnota súradnice [-]	67,1 ± 1,6	12,3 ± 0,9	18,4 ± 0,9

Rozdiely medzi farbou vysušeného pareného brezového dreva v sušiarňi a farbou vysušeného pareného brezového dreva v klimatizovanom priestore (referenčná hodnota) uvádza tabuľka 5.

Tab. 5. Porovnanie hodnôt na súradniciach farebného priestoru CIE $L^*a^*b^*$ vysušeného brezového dreva s referenčnou hodnotou a celková farebná diferencia ΔE^*

Súradnice farebného priestoru CIE $L^*a^*b^*$	L^*	a^*	b^*	ΔE^*
Drevo vysušené v sušiarňi	67,1	12,3	18,4	----
Referenčná hodnota – drevo sušené v klimat. priestore	68,4	11,8	19,2	----
Diferencie na súradniciach ΔL^* , Δa^* , Δb^* a ΔE^*	- 1,3	+ 0,5	- 0,8	1,6

Hodnoty na farebných súradniciach vysušeného brezového dreva v sušiarňi v porovnaní s referenčnými hodnotami brezového dreva vysušeného v klimatizovanom priestore sa nepatrne líšia. Poklesla belosť brezového dreva o $\Delta L^* = -1,3$, zvýšila sa hodnota na súradnici červenej farby o $\Delta a^* = +0,5$ a poklesla hodnota na súradnici žltej farby $\Delta b^* = -0,8$. Hodnota celkovej farebnej diferencie je $\Delta E^* = 1,6$. Podľa kategorizácie zmien farieb dreva v tepelných procesoch uvádzaných autormi (Cividini et al. (2007), celková farebná diferencia zaraďuje zmenu farby $\Delta E^* = 1,6$ pareného brezového dreva do kategórie $\Delta E = 0,2 - 2,0$ t.j. malé (nevýrazné) zmeny farby.

Výsledky analýz hodnotiacich kvality vysušených parených brezových vlysov uvádza tabuľka 5.

Tab. 6 Hodnotenie kvality vysušeného brezových vlysov

Kvalitatívny znak		Nameraná hodnota
Odchýlka konečnej vlhkosti od požadovanej vlhkosti dreva	w_0	1,2 %
Kolísanie konečnej vlhkosti dreva	w_{k0}	1,8 %
Vlhkostný spád v dreve vlysov	Δw	1,4 %

Z porovnania nameraných hodnôt kvality sušeného dreva parených brezových vlysov s hodnotami pre stanovenie kvality vysušeného reziva uvádzanými v práci Trebula – Klement [25] vyplýva, že vysušené parené brezové vlysy spĺňajú požiadavky kvalitatívnych parametrov jednotlivých tried nasledovne:

- odchýlka konečnej od požadovanej vlhkosti, *II. trieda kvality* ($w_0 = 0,6 - 1,5\%$),
- konečná zmena obsahu vlhkosti, *I. trieda kvality* ($w_{k0} \leq 2,0\%$),
- gradient vlhkosti, *I. trieda kvality* ($\Delta w \leq 1,5\%$).

Negatívnou stránkou prezentovaného režimu sušenia parených brezových vlysov bez vplyvu na zmenu farby dreva dosiahnutú procesom parenia je cca 22 % predĺženie času sušenia v porovnaní s režimom sušenia neparených brezových vlysov podľa ON 49 0651 pri teplotách $t = 50 \div 70$ °C. Predĺženie času sušenia je spôsobené realizáciou procesu sušenia dreva parených vlysov do BNV pri nižších teplotách.

ZÁVER

V príspevku je prezentovaný režim pre sušenie dreva parených brezových vlysov s rozmermi: 38x100x800 mm z vlhkosti $W_p \approx 50$ % na konečnú vlhkosť $W_k = 10$ %, bez vplyvu na zmenu farby pareného brezového dreva.

Súradnice farby vysušeného pareného brezového dreva daným režimom vo farebnom priestore CIE L*a*b* sú: $L^* = 67,1 \pm 1,6$; $a^* = 12,3 \pm 0,9$; $b^* = 18,4 \pm 0,9$. Zmena farby pareného brezového dreva vyvolaná procesom sušenia vyjadrená formou celkovej farebnej diferencie ΔE^* v porovnaní s farbou pareného brezového dreva vysušenom v klimatizovanom priestore je $\Delta E^* = 1,6$. Uvedená zmena farby, podľa kategorizácie zmien farby dreva v tepelných procesoch uvádzaných autormi (Cividini et al. (2007) zaraďuje zmenu farby pareného brezového dreva vplyvom sušenia do kategórie $\Delta E^* = 0,2 - 2$, t.j. malé (nevýrazné) zmeny farby.

Negatívnou stránkou uvedeného režimu sušenia je cca 22 % predĺženie času sušenia parených brezových vlysov v porovnaní s režimom sušenia neparených brezových vlysov podľa ON 49 0651 pri teplotách $t = 50 \div 70$ °C. Predĺženie času sušenia je spôsobené realizáciou procesu sušenia dreva parených vlysov do BNV pri nižších teplotách.

Literatúra

1. BABIAK, M., KUBOVSKÝ, I., MAMOŇOVÁ, M.(2004): Farebný priestor vybraných domácich drevín. In: Interaction of wood with various Forms of Energy. Technická univerzita vo Zvolene, (2004), 113 – 117.
2. BARAŇSKI, J., KLEMENT, I., VILKOVSKÁ, T., KONOPKA, A. (2017): High temperature drying process of beech wood (*Fagus sylvatica* L.) with different zones of sapwood and red false heartwood. *BioResources* 12(1), 1861-1870.

3. BARCIK, Š., GAŠPARÍK, M., RAZUMOV, E. Y. (2015): Effect of thermal modification on the colour changes of oak wood. In: *Wood Research*. 60 (3):385-396.
4. BUČKO, J. (1995): *Hydrolyzálne procesy*. Zvolen: Vydavateľstvo TU Zvolen, 116 s.
5. CIVIDINI, R., TRAVAN, L., ALLEGRETTI, O. (2007): White beech: A tricky problem in drying process. In *International Scientific Conference on Hardwood Processing*, Quebec City, Canada.
6. DZURENDA, L. (2019): Technical-technological characteristics of the thermal process of color modification of birch wood with saturated water steam. In *Acta facultatis technicae* 24 (2): 61-73.
DZURENDA, L., DELIISKI, N. (2012): Convective Drying of Beech Lumber without Color Changes of Wood. *Drvna industrija*. 63 (2), 95– 103.
7. DZURENDA, L. (2014): Colouring of Beech Wood during Thermal Treatment using Saturated Water Steams. In: *Acta facultatis xylogologiae Zvolen*, 56 (1):13 – 22.
8. DZURENDA, L. (2018). The Shades of Color of *Quercus robur* L. Wood Obtained through the Processes of Thermal Treatment with Saturated Water Vapor. In: *BioResources* 13(1), 1525 - 1533; doi: 10.1063/biores.13.1.1525-1533
9. DZURENDA, L., DUDIÁK, M. (2020): The Effect of the Temperature of Saturated Water Steam on The Colour Change of Wood *Acer Pseudoplatanus* L. *Acta Facultatis xylogologiae Zvolen*, 62 (1), 19 – 28.
10. DZURENDA, L., GEFFERT, A., GEFFERTOVÁ, J., DUDIÁK, M. (2020): Evaluation of the Process Thermal Treatment of Maple Wood Saturated Water Steam in Terms of Change of pH and Color of Wood. *BioResources* 15(2), 2550-2559. DOI: 10.15376/biores.15.2.2500-2559.
11. GEFFERT, A., VÝBOHOVÁ, E., GEFFERTOVÁ, J., DUDIÁK, M. (2020): Impact of Steaming Mode on Chemical Characteristics and Colour of Birch Wood. In: *Forests* 11(4): 478, doi:10.3390/f11040478
12. HADJISKI, M., DELIISKI, N. (2016): Advanced Control of the Wood Thermal Treatment Processing. In: *Cybernetics and Information Technologies*. Bulgarian Academy of Sciences 16(2):176-197.
13. KLEMENT, I., RÉH, R., DETVAJ, J. (2010): *Základné charakteristiky lesných drevín – spracovanie drevnej suroviny v odvetví spracovania dreva*. NLC Zvolen.
14. MAKOVÍNÝ, I. (2010): *Úžitkové vlastnosti a použitie rôznych druhov dreva*. Zvolen: Technická univerzita Zvolen, 84 s.
15. MEINTS, T., TEISCHINGER, A., STINGL, R., HANSMANN, C. (2016): Wood colour of central European wood species: CIELAB characterisation and colour intensification, *Eur. J. Wood Prod.* 75, 499- 509
16. MELCER, I., MELCEROVÁ, A., SOLÁR, R., KAČÍK, F. (1989): *Chémia hydrotermálneho spracovania dreva listnatých drevín*. Zvolen: Vysoká škola lesnícka a drevárska, 76 s
17. PERELYGIN, L., M. (1965): *Náuka o dreve*, Bratislava: SVTL, 444 s.
18. HRČKOVÁ, M., KOLEDA, P., KOLEDA, P., BARCÍK, Š., ŠTEFKOVÁ, J. (2018): Color change of selected wood species affected by thermal treatment and sanding. *BioResources*. 13(4), 8956-8975.
19. TOLVAJ, L., NEMETH, R., VARGA, D., MOLNAR, S. (2009). Colour homogenisation of beech wood by steam treatment. In: *Drewno*. 52 (181): 5-17.

20. TREBULA, P., BUČKO, J. (1996): Vákuové sušenie dreva, technické, technologické a ekologické aspekty: In: Vedecké štúdie 5/1996/B, Zvolen, Vydavateľstvo Technickej univerzity vo Zvolene, 70 s.
21. TREBULA, P., KLEMENT, I. (2002): Sušenie a hydrotermická úprava dreva. Zvolen. Vydavateľstvo TU vo Zvolene. 441 s.

POĎAKOVANIE: Tento experimentálny výskum bol pripravený v rámci grantového projektu: *APVV-17-0456 „Termická modifikácia dreva sýtou vodnou parou za účelom cielenej a stabilnej zmeny farieb drevnej hmoty“* ako výsledok práce autora a značnej pomoci agentúry APVV.



INFLUENCE OF STEAMING TEMPERATURE ON CHEMICAL CHARACTERISTICS AND COLOUR OF ALDER WOOD

Anton Geffert¹ – Jarmila Geffertová¹ – Michal Dudiak² – Eva Výbohá¹

Abstract

*The aim of the work was to evaluate changes of the chemical components in alder wood (*Alnus glutinosa* L.) caused by steaming with saturated steam at three temperatures – 105 °C, 125 °C and 135 °C. Selected chemical characteristics were determined in the samples of the original wood and wood after steaming, and the wood was analyzed by ATR-FTIR spectroscopy. The greatest changes in the alder wood characteristics were observed at 135 °C. The differential spectrum of the alder wood samples showed the significant changes of extractives and also the degradation of hemicelluloses, what points on the colour changes as well as deterioration of wood mechanical properties. A decrease unconjugated and an increase conjugated carbonyls was seen at all steaming temperature. The findings also confirmed the changes in the lignin of alder wood with elevated steaming temperature, as well as the course of the thermal oxidation reactions and the formation of new carbonyls. The changes of the hemicelluloses and extractive substances in alder wood during steaming were well-correlated with the measured pH values and wood colour.*

Key words: alder wood, saturated steam, chemical characteristics, pH, CIEL^{*}a^{*}b^{*}, ATR-FTIR spectroscopy

INTRODUCTION

Hydrothermal treatment is method often applied to pretreat wood properties. During hydrothermal treatment, wood is mostly treated with water vapor at different modes - temperature, pressure, time, hydro module (Šutý 1982). The presence of moisture in the wood is a necessary condition for the course of chemical reactions. Saturated steam at lower temperature and at higher humidity of wood was used for obvious discoloration with no effect on polysaccharide components (Chen *et al.* 2012). Goal-directed changes in colour by hydrothermal treatment of full volumes of wood have practical importance, especially in the production of furniture, decorative products and other wood products (Dzurenda *et al.* 2020).

The basic chemical processes taking place in the hydrothermal treatment of wood include catalytic hydrolytic reactions of polysaccharides, lignin–saccharide bond disruption and the hydrolysis of lignin. Water-soluble extractives (inorganic salts, mono- and oligosaccharides, various polysaccharides - e.g. starch and pectins, cyclic alcohols, dyes, tannins and some low molecular weight phenols) are extracted from wood during hydrothermal action (Melcer *et al.* 1989, Kačík 2001).

At low steaming temperatures (below 100 °C), there are negligible chemical and structural changes in the basic wood components. Increasing the temperature of the hydrothermal reaction to 100 to 150 °C deepens the chemical and physicochemical changes of all components of the wood substance (Solár 1997).

The hydrothermal treatment of wood is accompanied by changes in the colour, which are caused by reactions of the wood substance degradation products, as well as chemical changes in the extractives and lignin. The mechanism of colour change is complex and involves a number of overlapping reactions of the basic wood components and their degradation products (Fengel and Wegener 1983, Solár 2001).

Wood colour changes are believed to occur as a result of intramolecular dehydration reactions and are associated with a conjugated system of multiple bonds and the free electron pairs of oxygen in the phenolic hydroxyl group. Increasing the content of phenolic hydroxyl groups in lignin may result in the formation of other chromophores, such as carbonyl and carboxyl groups (Solár 1997).

An increased intensity of the degradation reactions in the wood is achieved by increasing the temperature and the concentration of hydronium ions. The gradual increase in acidity of the environment is caused by cleavage of the acetyl and formyl groups from hemicelluloses.

The mechanism of the combined effect of heat and water on the properties of lignin in wood is a complex, multifactor process in which changes in the polysaccharide fraction play an important role too. At temperatures below 100 °C, the simultaneous course of competitive depolymerization and condensation reactions of lignin have been demonstrated. Assessing the effect of lignin condensation in the later stages of hydrothermal action is complicated by the fact that at temperatures of 80 to 140 °C, the degradation of the hemicellulose fraction also occurs. The amount of hemicellulose degradation products is approximately twice that of the amount of lignin, suggesting a higher rate of their degradation (Solár 1997).

The cellulose content of the wood increases relatively to the duration of the hydrothermal treatment in the temperature range of 80 to 140 °C and is in proportion to the decrease in the hemicellulose and lignin components. At temperatures above 100 °C, partial depolymerization of the cellulose begins (Solár 1997).

The aim of this work was to evaluate changes in selected chemical characteristics of alder wood caused by steaming with saturated steam under operating conditions for 12 hours at three different temperatures – 105 °C, 125 °C and 135 °C – and also to identify and explain the changes of select chemical characteristics using ATR-FTIR spectroscopy.

MATERIAL AND METHODS

The samples of alder wood (*Alnus glutinosa* L.) supplied from an industrial plant Sundermann Ltd. Banská Štiavnica were used to investigate chemical changes that occurred in different steaming treatments. Alder wood samples with dimensions of 32 × 90 × 600 mm and humidity $w_a > 45\%$ were thermally treated with saturated steam in an APDZ 240 pressure autoclave (Dzurenda 2018). Alder wood was steamed for 12 hours at 105, 125 and 135 ± 2.5 °C.

Disintegrated samples of the original alder wood and the wood after steaming were used to monitor the chemical changes (0.5–1.0 mm fraction of sawdust prepared from completely disintegrated boards including surface and centre part).

In the samples of the original wood and the wood after steaming, the following chemical characteristics were determined:

Extractives	Standard Test Method for Ethanol-Toluene Solubility of Wood (ASTM D 1107 – 96)
Polysaccharide fraction	Chlorite isolation method of Wise <i>et al.</i> (Kačík and Solár 2000)
Cellulose	Kürschner-Hoffer method (Kačík and Solár 2000)
<u>Lignin</u>	<u>ASTM D 1106 – 96</u>

(Note: The content of hemicelluloses was determined as the difference between the holocellulose and cellulose content.)

The pH measurement of the original alder wood and the wood after steaming was performed by the direct method according to Geffert *et al.* (2019).

The original and thermally treated alder wood samples were analyzed by ATR-FTIR spectroscopy. The measurements were carried out using a Nicolet iS10 FTIR spectrometer equipped with Smart iTR attenuated total reflectance (ATR). The resolution was set at 4 cm⁻¹, 32 scans were recorded for each analysis, and the wavenumber range was from 4000 cm⁻¹ to 650 cm⁻¹. Six analyses were performed per sample. The spectra were evaluated using the OMNIC 8.0 software.

Colour measurement was performed on the treated original alder wood and on the wood after steaming using the Color Reader CR-10. Six measurements were performed on each sample, where the lightness L* and the colour coordinates a* and b* were evaluated. The total colour difference ΔE* was determined from the difference of the colour coordinates (ΔL*, Δa* and Δb*) according to the following equation (ISO/CIE 11664-4):

$$\Delta E^* = \sqrt{(L_2^* - L_1^*)^2 + (a_2^* - a_1^*)^2 + (b_2^* - b_1^*)^2} \quad (1)$$

where (L₂*-L₁*) change in value of black-white coordinate (specific lightness)
(a₂*-a₁*) change in value of green-red coordinate
(b₂*-b₁*) change in the value of blue-yellow coordinate

RESULTS AND DISCUSSION

The chemical analysis results of the original alder wood samples and wood samples after steaming in each mode are shown in Figure 1.

The greatest changes in the alder wood after steaming were observed in the polysaccharides content, with the greatest decrease at temperature of 135 °C. The cellulose content was relatively stable and small changes was caused by the degradation of the more labile wood components was apparent.

The lignin content increased slightly compared to the original alder wood sample, and this increase was also attributable to the degradation of the more labile wood components.

The changes recorded in the content of extractives can be attributed to a large number of parallel reactions, in addition to the degradation of existing substances and new degradation products being formed. The overall increase in the content of extractives was

predominantly due to the degradation and destruction of the hemicellulose portion of the polysaccharide fraction in the wood.

The main role in hydrothermal action is played by nascent organic acids - acetic acid and formic acid. These volatile organic acids mainly cause the destruction of hemicelluloses and the amorphous cellulose too, dissolve the lignin and, in later phases, degrade monosaccharides. Organic acids released from wood catalyze various hydrolytic, dehydration and degradation reactions of carbohydrates and their products, but they also participate in condensation reactions (Kačík 2001).

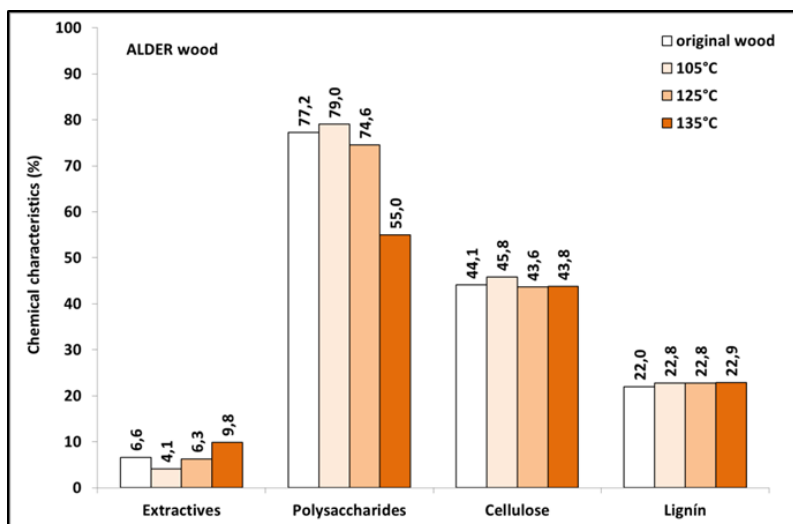


Fig. 1 Chemical characteristics of original alder wood and after steaming

Figure 2 shows the changes in the polysaccharide fraction in alder wood in dependence to the steaming temperature.

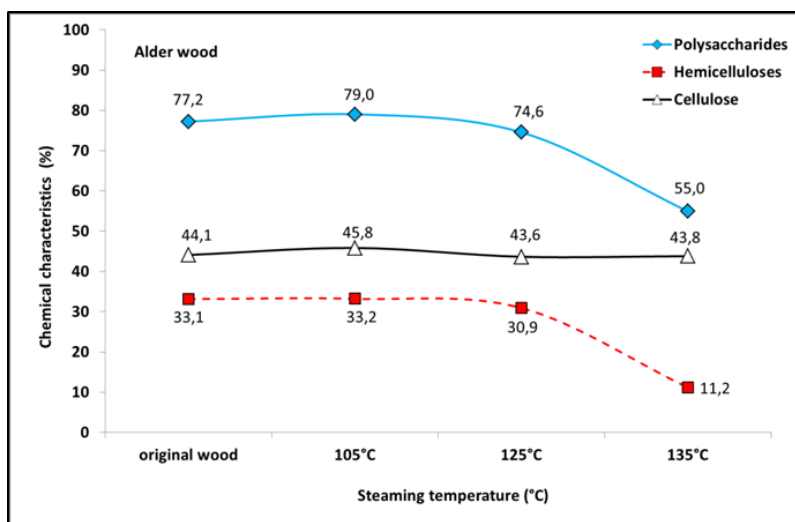


Fig. 2 Changes in polysaccharide fraction of alder wood according to steaming temperature

Total proportion of polysaccharides has decreased with elevated steaming temperature, while the degradation of polysaccharides accelerated. An increase was first observed of 1.8% at 105 °C, then it was a decrease of 2.6% at 125 °C and up to 22.2% at 135 °C. The results obtained are in good agreement with the conclusions of Kačík (1997), according to which the loss of holocellulose in hydrothermally treated wood occurs mainly through the degradation of non-cellulosic polysaccharides.

The process of releasing acidic components from wood and the associated change in pH at individual steaming temperatures is illustrated in Figure 3. The weakly acidic pH 4.87 of the original wood shifted toward the acidic region with increasing steaming temperature due to the more intense formation of acidic components, with the pH decreasing to 3.13 at 135 °C.

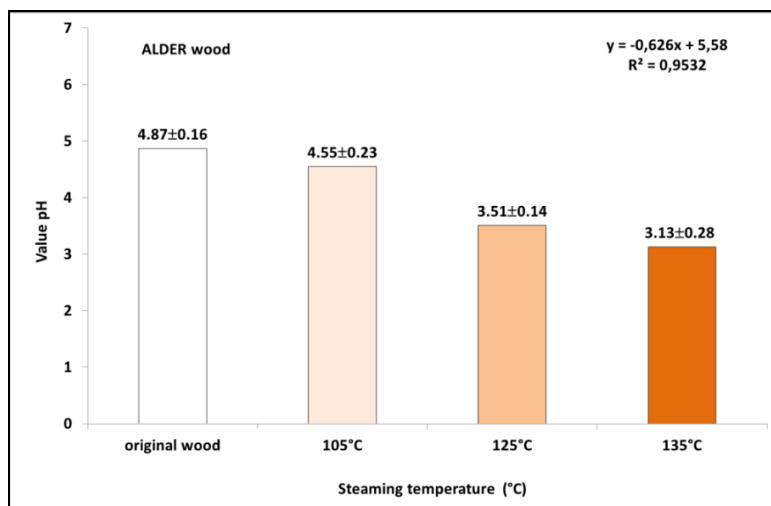


Fig 3 Change in the pH value according to steaming temperature

The differences in ATR-FTIR absorption spectra were used to further elucidate the changes in chemical substances of alder wood during steaming (Figure 4). The differential spectra were normalized to the maximum band at 1373 cm^{-1} (i.e., the band characterizing stable C—H cellulose binding) according to Nemeth *et al.* (2016). In the spectra, there were monitored the changes of the functional groups and bonds responsible for the colour change of the steamed wood (Polleto *et al.* 2012, Zhang *et al.* 2018).

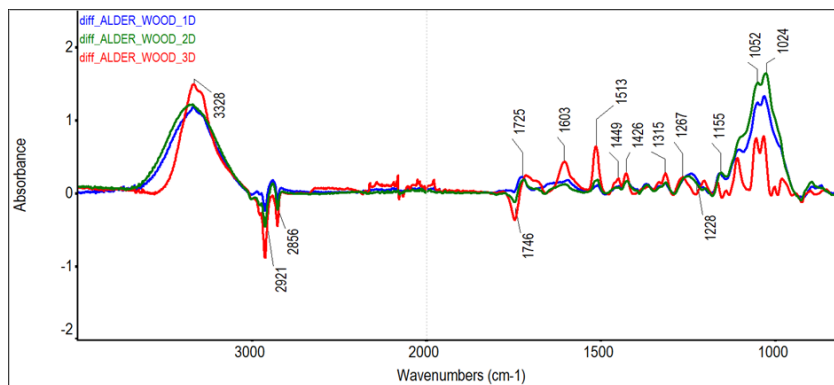


Fig. 4 The absorption difference spectra of alder wood

Positive bands at 3200 to 3500 cm^{-1} suggest an increase of intermolecular hydrogen bonds via devolatilization of original extractive substances and the changes in the carbohydrate components of wood - mainly from the significant degradation of hemicelluloses and the subsequent dehydration reactions. The decrease in absorption bands at 2921 and 2856 cm^{-1} is mainly attributed to carboxylic groups, whose contents decreased with the increasing steaming temperature. The bands around 1700 cm^{-1} , which characterize the carbonyl groups, showed an interesting course. The content of conjugated carbonyls increased and content of unconjugated carbonyls decreased partially. According to Chen *et al.* (2014), the increase in conjugated C=O groups and red colour is presumably due to hydrolysis and oxidative transformation of polyphenols to dark colour polymers.

The positive bands at 1603 and 1513 cm^{-1} suggested the changes of the lignin and forming of the quinone structures in alder wood with elevated steaming temperature.

Figure 5 illustrate the course of the colour changes of the wood expressed as the colour coordinates L^* , a^* and b^* according to steaming condition.

The lightness L^* decreased from 76.8 to 45.9 steadily with increasing steaming temperature due to the dehydration reactions of hemicelluloses and formation of secondary coloured substances (furfural and its condensation products). The value of the blue-yellow coordinate b^* decreased from 22.3 to 16.0. The value of the green-red coordinate a^* increased from the original value of 9.6 to 13.4. The change in a^* can be attributed to the air oxidation of water-insoluble polyaromatic structures (Chen *et al.* 2014).

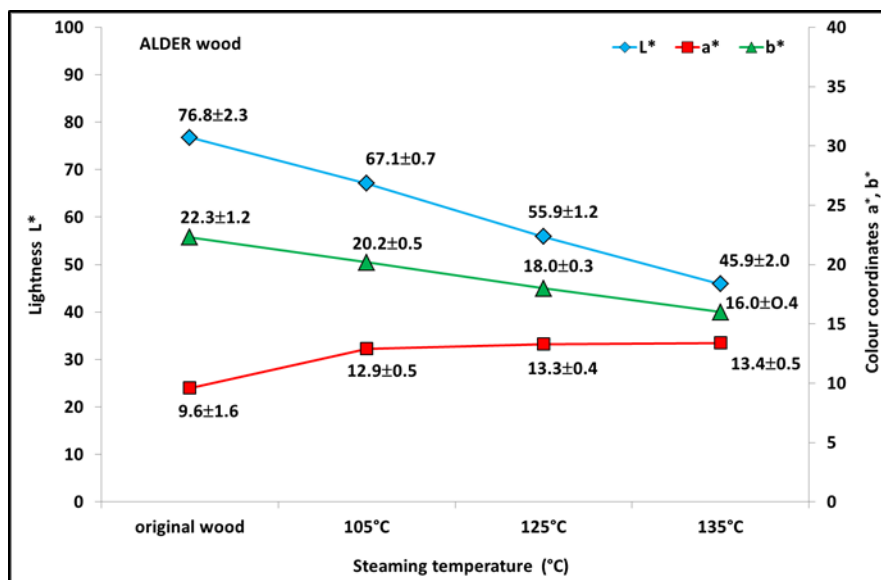


Fig. 5 Colour coordinates L^* , a^* , b^* according to steaming condition

To evaluate the colour changes of wood, the total colour difference ΔE^* is often used, which involves changes of all three colour coordinates (L^* , a^* , b^*). Table 1 shows the strong dependence of the total colour difference ΔE^* on the content of hemicelluloses, extractives and pH value.

Table 1 Influence of steaming temperature on selected characteristics of alder wood

Steaming temperature (°C)	Extractives (%)	Hemicelluloses (%)	pH	ΔE^*
-	6.6	33.1	4.87	-
105	4.1	33.2	4.55	10.5
125	6.3	30.9	3.51	21.7
135	9.8	11.2	3.13	31.7

The original and secondary extractives play a significant role in the formation of secondary colour compounds during hydrothermal treatment. According to previous studies, colour changes of wood are due to the formation of new chromophore groups that arise in hydrothermal treatment process of wood (Chen *et al.* 2014, Banadics and Tolvaj 2019).

CONCLUSION

The obtained results showed that the change in colour of the wood depends on the steaming conditions and is closely related to changes in its chemical characteristics. The greatest changes in alder wood steaming using saturated steam were observed at 135 °C, which resulted in a significant decrease in polysaccharide content, a slight increase in lignin content and an increase in extractive content.

The pH shift to the acidic region was accompanied by greater degradation of hemicelluloses and an increased production of extractives. The dependence of the total colour difference on the pH of wood is a suitable tool for evaluating the achieved colour shade before further technological processing.

The differential spectrum of the alder wood samples showed the significant changes of extractives and also the degradation of hemicelluloses, what points on the colour changes as well as deterioration of the mechanical properties of the wood. A decrease unconjugated and an increase conjugated carbonyls was seen at all steaming temperature. The findings also confirmed the changes in the lignin of alder wood with elevated steaming temperature, as well as the course of the thermal oxidation reactions and the formation of new carbonyls.

REFERENCES

- ASTM D 1106–96. Standard Test Method for Acid Insoluble Lignin in Wood; ASTM International: West Conshohocken, PA, USA, 2013. Available online: www.astm.org (accessed on 23 August 2019).
- ASTM D 1107–96. Standard Test Method for Ethanol-Toluene Solubility of Wood; ASTM International: West Conshohocken, PA, USA, 2013. Available online: www.astm.org (accessed on 23 August 2019).
- Banadics, E.A.; Tolvaj, L. Color modification of poplar wood by steaming for brown color. *Eur. J. Wood Prod.* 2019, *77*, 717–719.
- Chen, Y.; GaO, J.M.; Fan, Y.M.; Tshabalala, M.A.; Stark, N.M. Heat-induced chemical and color changes of extractive-free black locust (*Robinia Pseudoacacia*) wood. *Bioresources* 2012, *7*, 2236–2248.

- Chen, Y.; Tshabalala, M.A.; Gao, J.M.; Stark, N.M.; Fan, Y.M. Color and surface chemistry changes of extracted wood flour after heating at 120 °C. *Wood Sci. Technol.* 2014, 48, 137–150.
- Dzurenda, L. The Shades of Color of *Quercus robur* L. Wood Obtained through the Processes of Thermal Treatment with saturated Water Vapor. *BioResources* 2018, 13, 1525–1533.
- Dzurenda, L.; Geffert, A.; Geffertová, J.; Dudiak, M. Evaluation of the Process Thermal Treatment of Maple Wood Saturated Water Steam in Terms of Change of pH and Color of Wood. *Bioresources* 2020, 15, 2550–2559.
- Fengel, D.; Wegener, G. *Wood: Chemistry, Ultrastructure, Reactions*, 2nd ed.; Walter de Gruyter: Berlin, Germany, 1989; p. 613.
- Geffert, A.; Geffertová, J.; Dudiak, M. Direct method of measuring the pH value of wood. *Forests* 2019, 10, 852.
- ISO/CIE 11664-4:2008 en. *Colorimetry—Part 4: CIE 1976 L*a*b* Colour Space*; CEN: CIE International Commission on Illumination: Brussels, Belgium, 2013. Available online: www.iso.org (accessed on 13 March 2020).
- Kačík, F. *Creation and Chemical Composition of Hydrolysates in the Wood-Water-Heat System*, 1st ed.; Technical University in Zvolen: Zvolen, Slovakia, 2001; p. 75.
- Kačík, F. *Influence of Temperature and Humidity on Carbohydrate Changes*, 1st ed.; Technical University in Zvolen: Zvolen, Slovakia, 1997; p. 69.
- Kačík, F.; Solár, R. *Analytical Chemistry of Wood*, 1st ed.; Technical University in Zvolen: Zvolen, Slovakia, 2000; p. 369.
- Melcer, I.; Melcerová, A.; Solár, R.; Kačík, F. *Chemism of Hydrothermal Treatment of Hardwoods*, 1st ed.; Technical University in Zvolen: Zvolen, Slovakia, 1989; p. 76.
- Nemeth, R.; Hill, C.A.S.; Takats, P.; Tolvaj, L. Chemical changes of wood during steaming measured by IR spectroscopy. *Wood Mater. Sci. Eng.* 2016, 11, 95–101.
- Poletto, M.; Zattera, A.J.; Santana, R.M.C. Structural Differences between Wood Species: Evidence from Chemical Composition, FTIR Spectroscopy, and Thermogravimetric Analysis. *J. App. Polym. Sci.* 2012, 126, E336–E343.
- Solár, R. *Lignin Changes in Hydrothermal Wood Treatment Processes*, 1st ed.; Technical University in Zvolen: Zvolen, Slovakia, 1997; p. 57.
- Zhang, P.; Wei, Y.; Liu, Y.; Gao, J.; Chen, Y.; Fan, Y. Heat-Induced Discoloration of Chromophore Structures in Eucalyptus Lignin. *Materials* 2018, 11, 1686.
- Solár, R. *Wood Chemistry*, 1st ed.; Technical University in Zvolen: Zvolen, Slovakia, 2001; p. 101.
- Šutý, L. Autohydrolysis of wood. In *Proceedings of the International Research Conference in Zvolen, Zvolen, Slovakia, 1–3 September 1982*; pp. 259–263.

Acknowledgments: This experimental research was carried out under the grant project APVV-17-0456 “Thermal modification of wood with water vapor for purposeful and stable change of wood colour”.



COMPARISON OF THE INFLUENCE OF STEAMING TIME AND TEMPERATURE ON SELECTED CHARACTERISTICS OF BIRCH AND ALDER WOOD

Anton Geffert¹ – Jarmila Geffertová¹ – Michal Dudiak²

Abstract

The aim of this work was to compare changes in the wood properties of two deciduous trees - birch and alder, caused by steaming with saturated steam under operating conditions for 6 and 12 hours at three different temperatures – 105 °C, 125 °C and 135 °C. In the samples of the original wood and wood after steaming, selected chemical (extractives, polysaccharides, cellulose, lignin and hemicelluloses) and physical characteristics (pH, ΔE^) were determined. A comparison of the hydrothermal treated birch and alder wood showed that the depth of the ongoing changes in the wood depends on specific conditions (time, temperature) as well as on the chemical composition of the treated wood. The changes in the colour of the wood take place during steaming simultaneously with chemical changes. Compared woods - birch and alder are showing higher values of ΔE^* in birch recorded at 6 hours, while at 12 hours the changes of ΔE^* in both trees were similar. The increasing differences in the colour of the wood during steaming showed a very good correlation with the content of extractives and especially hemicelluloses, but also with the pH values.*

Key words: alder, birch, saturated steam, chemical characteristics, pH, CIEL^{*}a^{*}b^{*}, ΔE^*

INTRODUCTION

Possible expansion of using the domestic wood raw material base. by suitable modification of the colour of less attractive wood species was studied.

Hydrothermal treatment is method often applied to pretreat wood properties, mainly for adjusting the colour shade of wood. Goal-directed changes in colour by hydrothermal treatment of full volumes of wood have great practical importance, especially in the production of furniture, decorative products and other wood products (Dzurenda *et al.* 2020).

The hydrothermal treatment of wood is accompanied by changes in the colour, which are caused by reactions of the wood substance degradation products, as well as chemical changes in the extractives and lignin. The mechanism of colour change is complex and involves a number of overlapping reactions of the basic wood components and their degradation products (Fengel and Wegener 1989, Solár 2001).

The presence of moisture in the wood is a necessary condition for the course of chemical reactions. Saturated steam at lower temperature and at higher humidity of wood

was used for obvious discolouration with no effect on polysaccharide components (Chen *et al.* 2012).

During the hydrothermal treatment of wood, several parallel processes take place, e.g. extraction of water-soluble substances, hydrolysis of non-cellulosic polysaccharides associated with the formation of acetic and formic acid, disruption of lignin-saccharide bonds and also hydrolysis of lignin (Fengel and Wegener 1989, Melcer *et al.* 1989, Kačík 2001, Sundqvist *et al.* 2006).

The aim of this work was to compare changes in the wood properties of two deciduous trees - birch and alder, caused by steaming with saturated steam under operating conditions for 6 and 12 hours at three different temperatures – 105 °C, 125 °C and 135 °C.

MATERIAL AND METHODS

The samples of birch wood (*Betula pendula* Roth) and alder wood (*Alnus glutinosa* L.) supplied from an industrial plant Sundermann Ltd. Banská Štiavnica were used to investigate chemical changes that occurred in different steaming treatments. The wood samples with dimensions of 32 × 90 × 600 mm and humidity $w_a > 45\%$ were thermally treated with saturated steam in an APDZ 240 pressure autoclave during 6 and 12 hours at 105, 125 and 135 ± 2.5 °C (Dzurenda 2018).

To monitor the chemical changes, disintegrated samples of the original wood and the wood after steaming were used (0.5–1.0 mm fraction of sawdust prepared from completely disintegrated boards including surface and centre part).

In the wood samples, the following chemical characteristics were determined:

Extractives	Standard Test Method for Ethanol-Toluene Solubility of Wood (ASTM D 1107 – 96)
Polysaccharide fraction	Chlorite isolation method of Wise <i>et al.</i> (Kačík and Solár 2000)
Cellulose	Kürschner-Hoffer method (Kačík and Solár 2000)
Lignin	Standard Test Method for Acid Soluble Lignin in Wood (ASTM D 1106 – 96).

The pH measurement of the original wood and the wood after steaming was performed by the direct method according to Geffert *et al.* (2019).

Colour measurement was performed on the wood samples using the Color Reader CR-10. Six measurements were performed on each sample and from the difference of the colour coordinates (ΔL^* , Δa^* and Δb^*), the total colour difference ΔE^* was determined according to the following equation (ISO/CIE 11664-4):

$$\Delta E^* = \sqrt{(L_2^* - L_1^*)^2 + (a_2^* - a_1^*)^2 + (b_2^* - b_1^*)^2} \quad (1)$$

where $(L_2^* - L_1^*)$ change in value of black-white coordinate (specific lightness)
 $(a_2^* - a_1^*)$ change in value of green-red coordinate
 $(b_2^* - b_1^*)$ change in the value of blue-yellow coordinate

RESULTS AND DISCUSSION

The monitored deciduous wood species - birch and alder, belong to the sapwood species characterized by a one-coloured zone of wood, as well as an even distribution of chemical components across the cross section.

The results of chemical analysis of the original birch and alder wood and wood samples of the monitored wood species after steaming in individual modes are shown in the following figures 1 and 2.

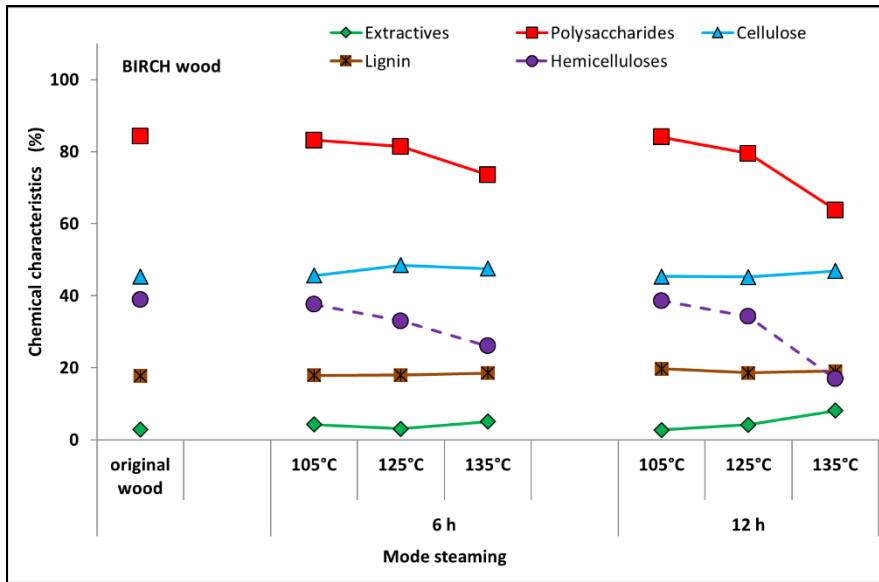


Fig. 1 Chemical characteristics of original birch wood and after steaming

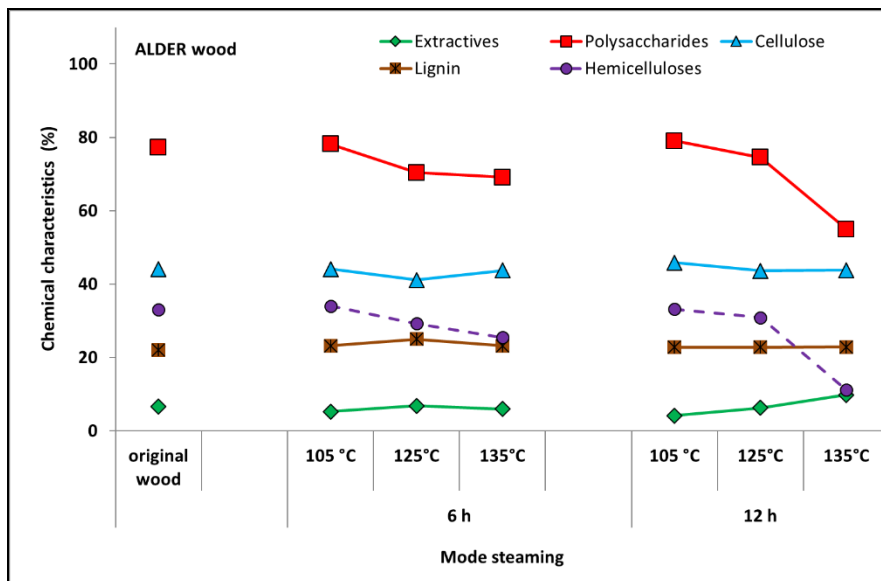


Fig. 2 Chemical characteristics of original alder wood and after steaming

The content of extractives showed an overall increase during steaming, although there were small irregularities. However, such fluctuations occur relatively frequently for a heterogeneous raw material as wood. The reason is the uneven distribution of the original extractives in the wood, as well as the uneven formation of secondary extractables and their entry into subsequent reactions.

The original and secondary extractives play a significant role in the formation of secondary colour compounds during hydrothermal treatment. According to previous studies, colour changes of wood are due to the formation of new chromophore groups that arise in hydrothermal treatment process of wood (Chen *et al.* 2014, Banadics and Tolvaj 2019).

The hemicellulose content calculated from the difference between the polysaccharide content and the cellulose content was showing a permanent decrease depending on the steaming conditions. The decrease in hemicelluloses content was associated with the formation of secondary extractables which are, able to participate in the formation of new colour compounds.

An increased intensity of the degradation reactions in the wood is achieved by increasing the temperature and the concentration of hydronium ions. The gradual increase in acidity of the environment is caused by cleavage of the acetyl and formyl groups from hemicelluloses.

The content of polysaccharides in wood during steaming showed a permanent decrease, which according to the results of previous studies (Kačík 1997, Geffert *et al.* 2020a, Geffert *et al.* 2020b) can be attributed mainly to the hydrolysis of hemicelluloses.

The content of cellulose, which is the most stable component of wood, changed only minimally during steaming.

The lignin content showed a relatively small increase during steaming including the removal of a small part of the water-soluble lignin in the initial stages of steaming.

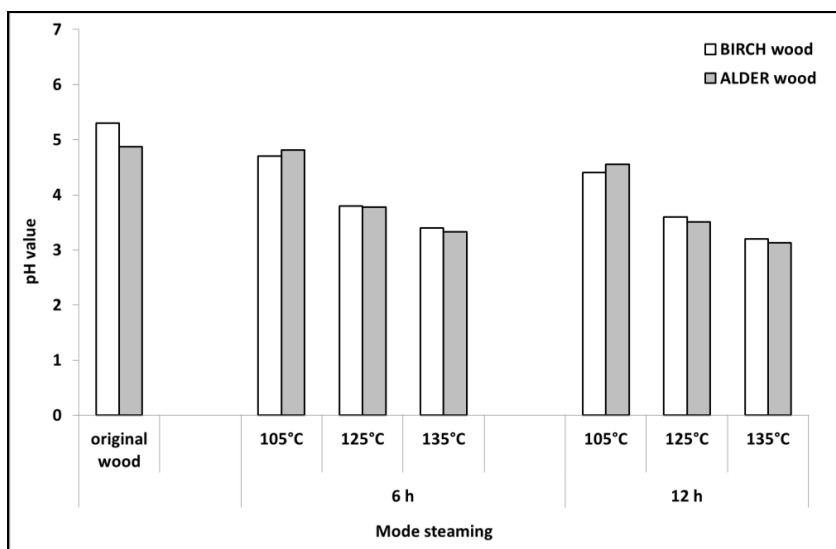


Fig 3 Change in the pH values according to steaming mode

The process of releasing acidic components from wood and the associated change in pH at individual steaming temperatures is illustrated in Figure 3. The weakly acidic pH (5.2 of the original birch wood and 4.9 of the original alder wood) shifted toward the acidic

region with increasing of steaming temperature due to more intense formation of acidic components (acetic-acid and formic-acid), with the pH value decreased to 3.2 for birch or 3.1 for alder at 135 °C respectively.

The colour changes of the monitored wood species, expressed by the coordinates L^* , a^* and b^* , are shown in Figure 4.

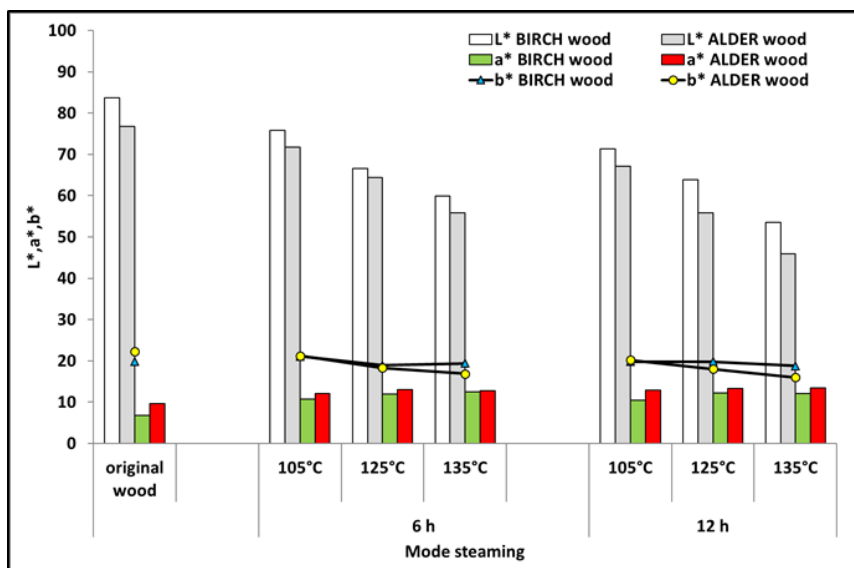


Fig. 4 Changes of the coordinates L^* , a^* and b^* according to steaming mode

The lightness L^* in both monitored wood species showed a clear decrease with increasing temperature and prolonged steaming time. A slight increase of the value of the green-red coordinate a^* was observed and the value of the blue-yellow coordinate b^* decreased slightly, although small fluctuations were observed in this behavior.

The decrease in lightness L^* is caused by the formation of coloured degradation products from extractives and hemicelluloses. At the same time, these degradation products are partially leached from the wood during steaming and leaching is more intense at temperatures above 120 °C. The air oxidation of the water-soluble polyaromatic extractants present (tannins, flavonols) is attributed to an increase in the a^* coordinate causing redness, but due to the low stability of the formed substances the value of a^* passes through the maximum. The observed slight increase in a^* with increasing temperature can be attributed to the degradation products of hemicelluloses and their subsequent reactions. The decrease in the value of the b^* coordinate is generally attributed to devolatilization or thermal degradation of dioxane extractives (Chen *et al.* 2014, Nemeth *et al.* 2016, Banadics and Tolvaj 2019).

The total colour difference ΔE^* is often used to evaluate the colour changes of wood. Figure 5 shows the dependence of the total colour difference ΔE^* according to steaming conditions - time and temperature.

Compared woods - birch and alder are showing higher values of ΔE^* in birch recorded at 6 hours, while at 12 hours the changes of ΔE^* in both trees were similar and correlated very well with changes in pH and hemicellulose content.

In addition, it can be deduced from the changes ΔE^* that the desired colour shade of the wood can be achieved by several steaming modes. Therefore, when choosing the modes, it

would be appropriate to choose those resulting to as minimal as possible deterioration of steam wood strength properties.

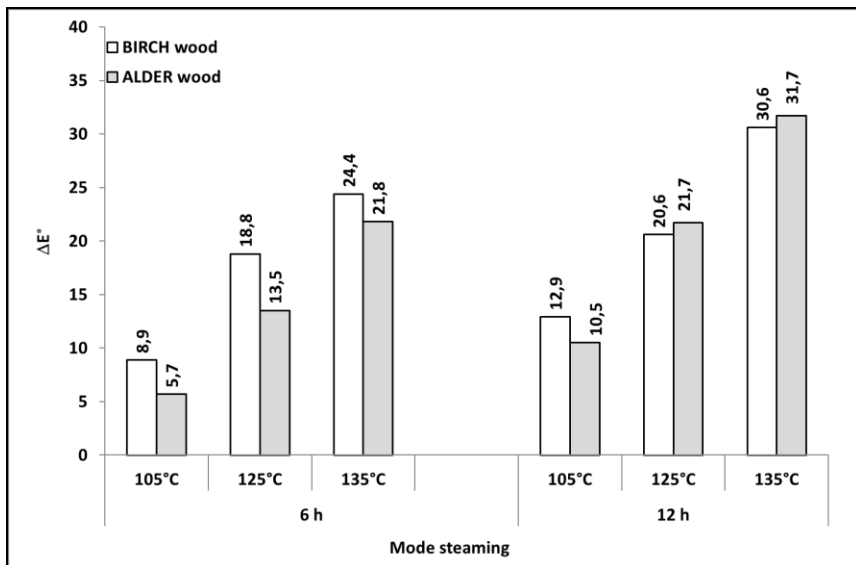


Fig. 5 Change in the ΔE^* values according to steaming mode

A demonstration of the change in the colour shades of birch and alder wood during steaming is presented in Figure 6.

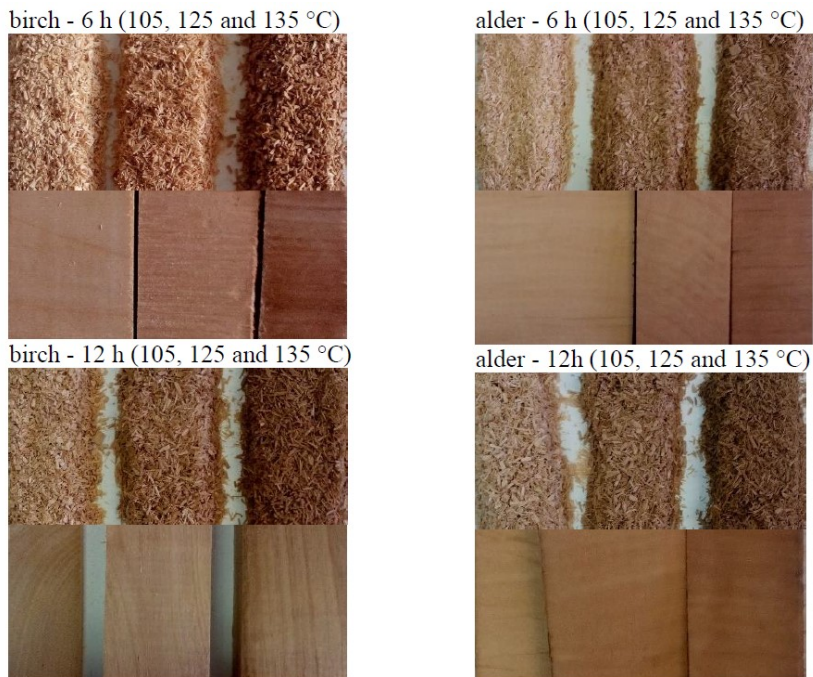


Fig. 6 Change in the colour shades of birch and alder wood during steaming

CONCLUSION

A comparison of the hydrothermal treatment of birch and alder wood with saturated water vapor showed that the depth of the ongoing changes in the birch and alder wood depends not only on specific conditions (time, temperature), but also significantly depends on the chemical composition of the treated wood.

The content of individual types of extractives and hemicelluloses plays a fundamental role in changing the colour of wood. Lignin and the method of binding the lignin-saccharide complex also play an important role.

The changes in physical properties as required change of wood colour are occurring simultaneously with chemical changes during steaming. At the same time, the changes in other physical and strength properties of the treated wood can be expected and significantly influence the subsequent process of processing the hydrothermally treated wood and on the quality of the final product.

The lightness L^* in both monitored wood species showed a clear decrease with increasing temperature and prolonged steaming time, the value of the green-red coordinate a^* increased slightly and the value of the blue-yellow coordinate b^* decreased slightly.

Compared woods - birch and alder are showing higher values of ΔE^* in birch recorded at 6 hours, while at 12 hours the changes of ΔE^* in both trees were similar.

The increasing differences in the colour of the wood during steaming showed a very good correlation with the content of extractives and especially hemicelluloses, as well as with the pH values. In the future, this knowledge could be used to control and manage the steaming process.

REFERENCES

- ASTM D 1106–96. Standard Test Method for Acid Insoluble Lignin in Wood; ASTM International: West Conshohocken, PA, USA, 2013. Available online: www.astm.org (accessed on 23 August 2019).
- ASTM D 1107–96. Standard Test Method for Ethanol-Toluene Solubility of Wood; ASTM International: West Conshohocken, PA, USA, 2013. Available online: www.astm.org (accessed on 23 August 2019).
- Banadics, E.A.; Tolvaj, L. Color modification of poplar wood by steaming for brown color. *Eur. J. Wood Prod.* 2019, *77*, 717–719.
- Chen, Y.; Gao, J.M.; Fan, Y.M.; Tshabalala, M.A.; Stark, N.M. Heat-induced chemical and color changes of extractive-free black locust (*Robinia Pseudoacacia*) wood. *Bioresources* 2012, *7*, 2236–2248.
- Chen, Y.; Tshabalala, M.A.; Gao, J.M.; Stark, N.M.; Fan, Y.M. Color and surface chemistry changes of extracted wood flour after heating at 120 °C. *Wood Sci. Technol.* 2014, *48*, 137–150.
- Dzurenda, L. The Shades of Color of *Quercus robur* L. Wood Obtained through the Processes of Thermal Treatment with saturated Water Vapor. *BioResources* 2018, *13*, 1525–1533.
- Dzurenda, L.; Geffert, A.; Geffertová, J.; Dudiak, M. Evaluation of the Process Thermal Treatment of Maple Wood Saturated Water Steam in Terms of Change of pH and Color of Wood. *Bioresources* 2020, *15*, 2550–2559.

- Fengel, D.; Wegener, G. *Wood: Chemistry, Ultrastructure, Reactions*, 2nd ed.; Walter de Gruyter: Berlin, Germany, 1989; p. 613.
- Geffert, A.; Geffertová, J.; Dudiak, M. Direct method of measuring the pH value of wood. *Forests* 2019, 10, 852.
- Geffert, A.; Geffertová, J.; Výbohová, E.; Dudiak, M. Impact of Steaming Mode on Chemical Characteristics and Colour of Birch Wood. *Forests* 2020a, 11, 478.
- Geffert, A.; Geffertová, J.; Dudiak, M.; Výbohová, E. Influence of Steaming Temperature on Chemical Characteristics and Colour of Alder Wood. In *Chip and Chpless Woodworking Processes*, Tu in Zvolen 2020b, 12(1), 8 p.
- ISO/CIE 11664-4:2008 en. *Colorimetry–Part 4: CIE 1976 L*a*b* Colour Space*; CEN: CIE International Commission on Illumination: Brussels, Belgium, 2013. Available online: www.iso.org (accessed on 13 March 2020).
- Kačík, F. *Creation and Chemical Composition of Hydrolysates in the Wood-Water-Heat System*, 1st ed.; Technical University in Zvolen: Zvolen, Slovakia, 2001; p. 75.
- Kačík, F. *Influence of Temperature and Humidity on Carbohydrate Changes*, 1st ed.; Technical University in Zvolen: Zvolen, Slovakia, 1997; p. 69.
- Kačík, F.; Solár, R. *Analytical Chemistry of Wood*, 1st ed.; Technical University in Zvolen: Zvolen, Slovakia, 2000; p. 369.
- Melcer, I.; Melcerová, A.; Solár, R.; Kačík, F. *Chemism of Hydrothermal Treatment of Hardwoods*, 1st ed.; Technical University in Zvolen: Zvolen, Slovakia, 1989; p. 76.
- Nemeth, R.; Hill, C.A.S.; Takats, P.; Tolvaj, L. Chemical changes of wood during steaming measured by IR spectroscopy. *Wood Mater. Sci. Eng.* 2016, 11, 95–101.
- Solár, R. *Wood Chemistry*, 1st ed.; Technical University in Zvolen: Zvolen, Slovakia, 2001; p. 101.
- Sundqvist, B.; Karlsson, O.; Westermark, U. Determination of formic-acid and acid concentrations formed during hydrothermal treatment of birch wood and its relation to color, strength and hardness. *Wood Science and Technology* 2006, 40(7), 549-561.

Acknowledgments: This experimental research was carried out under the grant project APVV-17-0456 “Thermal modification of wood with water vapor for purposeful and stable change of wood colour”.



DETERMINATION OF PERFORMANCE INDICATORS OF PCD ABRASIVE WHEELS FOR SHARPENING OF TUNGSTEN CARBIDE TOOLS

Zhivko Gochev – Pavlin Vitchev

Abstract

The article presents some results of the research on the performance of various diamond abrasive wheels. Diamond wheels with metal coated and aggregated grains with organic bonds were used. The studies were performed at two levels of intensified, multi-pass sharpening of TC (tungsten carbide) knives type K20, part of a cutter head for longitudinal flat milling. The results obtained were analyzed and relevant conclusions and recommendations made.

Key words: *sharpening, diamond abrasive wheel, knives, tungsten carbide tipped*

INTRODUCTION

The diamond sharpening of TC tools provides a significant increase in the productivity, accuracy, quality of surfaces, reliability, and durability of their cutting elements. The cost of maintaining them is significantly reduced. Due to their high hardness, diamond grains penetrate the hard alloy relatively lightly, deforming the surface layer slightly and causing no high stresses.

The performance of diamond wheels is an indicator that characterizes both the quality of the abrasive tool itself and the results of its impact on the sharpened TC tools (Zaharenko, 1981).

This article aims to study the performance of diamond wheels under various sharpening conditions.

MATERIAL AND METHODS

For the research, a cutter head with replaceable knives and TC edges was used for the preliminary and fine longitudinal planing of solid wood and wood-based materials (Fig. 1) (<https://www.zmm-sm.com/zmmsm/english/wood.htm>).

The basic parameters of the cutter head and the replaceable knives are given in Table 1. The tool body is made of aluminum and planer knives are with TC edges type K20 and heat-treated to hardness HRA 92.

Table 1. Basic parameters of the cutter head and knives

D , mm	d , mm	L , mm	B , mm	s , mm	z , mm	β , °	Type
120	30	120	30	3	4	45	TCT – K20

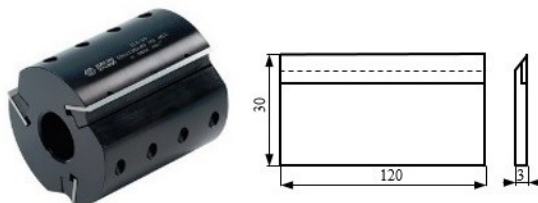


Figure 1 Assembled cutter head with insert knives and TC cutting edges, type K20

The indications in Table 1 correspond to:

D – Diameter of the cutter head;

d – Bore size;

L – Length of the knife;

B – Width of the knife;

s – Thickness of the knife;

z – Number of knives;

β – Angle of sharpening;

TCT – Tungsten carbide teeth.

The cutter head is designed for shaper machines and four-side processing machines. The TC edges type K20 (ISO grade classifications) consists of 94% tungsten carbide (WC) and 6% cobalt (Co) with a tungsten grain size of 1.0-2.0 μm (<http://carbide.ultra-met.com/viewitems/iso-grades/iso-grade-classifications-tungsten-carbide>).

The abrasive PCD grinding wheel (Fig. 2) has 12A2-45 shapes (conical cup - CC) and works with its front surface (manufacturing of Russia).

The characteristics of the experimental disks according to the FEPA (Federation of European Producers of Abrasives) are given in Table 2 and Fig. 2.

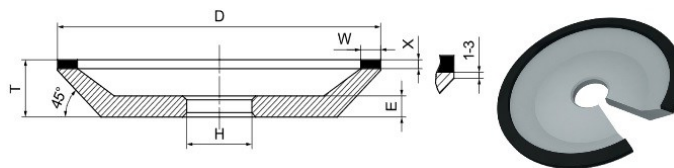


Figure 2 Abrasive grinding wheel shape 12A2-45 (conical cup)

Table 2. Characteristics of experimental diamond abrasive wheels

Shape and dimensions	Abrasive type	Mesh Size	Bond Type	Concentration	Hardness	Work conditions
12A2-45 125x5x3x32	SDC 2	D126	B2-01	K100	R	s
12A2-45 125x5x3x32	SDC 2	D126	B1-13	K100	R	s
12A2-45 125x5x3x32	SDC 4	D126	B2-01	K100	R	s
12A2-45 125x5x3x32	SDC 4	D126	B1-13	K100	R	s

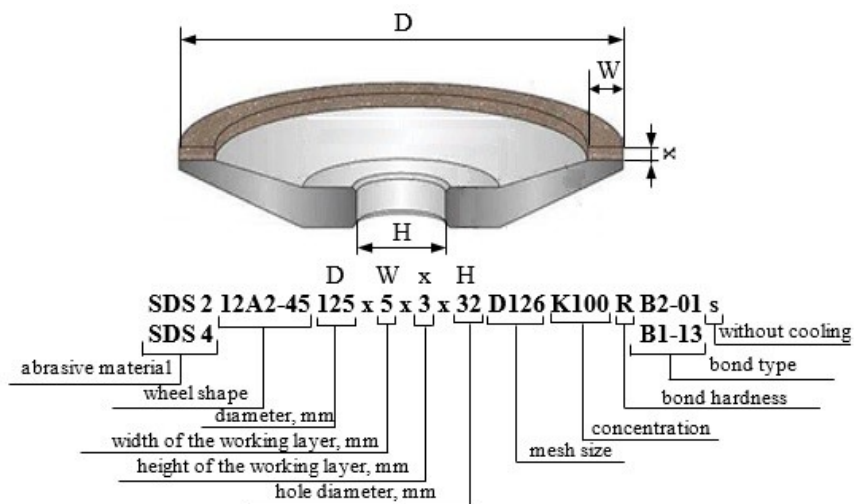


Figure 3 Abrasive wheel indication

The indications of Fig. 3 correspond to:

SDC 2 – Metal-coated synthetic diamond with aggregated grains and ordinary strength;
 SDC 4 – Metal-coated synthetic diamond with aggregated grains and increased strength;

D126 – Mesh size 125/100;

K100 – Concentration of diamond grains 100%;

R – Hard bond;

B2-01 – Phenol-formaldehyde-based organic bond with boron carbide filler enhancing self-sharpening process

B1-13 - Phenol-formaldehyde-based organic bond with barium sulphate filler and talc for clean sharpening and smoothing

Metal-coated diamond grains are better retained by the organic bond due to the presence of a metal film on their surface. This film protects the grains from shavings and ruptures, increases their strength and improves the conditions of heat removal from the sharpening zone. This results in a reduction in the specific diamond consumption and increases sharpening performance.

Aggregated grains (up to 10 pieces in one aggregate) have a significantly larger unfolded surface (regardless of the initial abrasive mesh size). Such diamond grain aggregates are better retained by the organic bond and withstand much higher loads. Abrasive wheels have better cutting abilities. (Kurdyukov, 2014).

The investigations were carried out with the intensified multi-pass sharpening of a sharpening machine model HMS 700 of HOLZMANN - Austria, under the following conditions:

- Cutting speed (V) – 18 m/s;
- Longitudinal feed speed (V_l) – 2,0; 2,5 m/min;
- Cross feed speed (V_{dm}) – 0,03; 0,05 mm/double motion.

The following indicators for evaluating the performance of diamond wheels in a multi-pass sharpening of TC tools have been determined (Ostrovskii, 1981; Zaharenko, 1981; Gochev, 2008; Gochev, 2019):

- Relative consumption of SDC determined by the weight method - Q_r , mg/g;

- Coefficient of cutting capacity - C_c ;
- Effective sharpening power of direct motion - \vec{N}_e , W;
- Relative power consumption of sharpening - $E_{r.e}$, kWh/kg;
- Complex performance indicator - $C_{c.i}$, mm³/g/min.kg.

The first four indicators were determined using the methodology set out in the Ohrid and Zagreb publications (Gochev, 2019).

Some researchers determine the performance of diamond wheels using a Grinding Ratio (Zaharenko, 1981; Rowe, 2009; Korotovskikh, 2012; Korotovskikh, 2017).

The complex performance indicator takes into account the diamond wheel's durability, productivity, conditions, and sharpening mode and can be defined as:

$$C_{c.i} = c \frac{P_{ac}}{Q_r} \quad (1)$$

Where c is a coefficient dependent on the magnitude of the cross feed speed ($c = 0,2$ at $W = 5$ mm и $V_{dm} < \text{mm/double motion}$):

P_{ac} – Actual sharpening performance, mm³/min;

RESULTS AND DISCUSSION

Table 3 shows the summary results of studies of synthetic diamond wheels with metal-coated and aggregated grains with organic bond with intensified multi-pass sharpening without cooling of TC edges type K20.

The study was conducted at two levels of sharpening modes. In mode 2, the theoretical productivity (P_{th}) was increased to the maximum possible - 1050 mm³/min.

The comparison of the results shows that the performance indicators of the studied diamond wheels are comparable and practically are in the same confidence intervals. Diamond wheels with metal-coated and aggregated abrasive grains have high cutting properties.

Table 3. Performance indicators for intensified multi-pass sharpening without cooling of TC edges type K20

Diamond wheels	Mode №	V_1	V_{dm}	P_{th}	Performance indicators				
					C_c	Q_r	$C_{c.i}$	\vec{N}_e	$E_{r.e}$
SDC 2 D126 B2-01 K100 s	1	2,0	0,03	504	0,91	0,24	382	295	41
	2	2,5	0,05	1050	0,88	1,60	116	610	40
SDC 2 D126 B1-13 K100 s	1	2,0	0,03	504	0,92	0,21	442	260	39
	2	2,5	0,05	1050	0,89	1,19	157	560	29
SDC 4 D126 B2-01 K100 s	1	2,0	0,03	504	0,92	0,23	403	230	36
	2	2,5	0,05	1050	0,89	1,27	147	490	32
SDC 4 D126 B1-13 K100 s	1	2,0	0,03	504	0,93	0,19	439	250	40
	2	2,5	0,05	1050	0,90	0,72	263	430	32

Organic bond, type B2-01 provides more efficient operation of diamond grains when sharpening under mode 1. At the same time, this type of bonding does not allow us to take advantage of metal-coated diamond grains (especially for the SDC 4 brand) as it does not provide reliable grains retention under heavier mode 2.

The use of diamond wheels with bond type B1-13 results in lower relative consumption of diamond, effective power of sharpening of direct motion and relative power consumption.

Diamond wheels with this type of bond can operate in cross-feeding up to 0,03 mm/double motion, below 1 mg/g relative consumption of SDC and large values of the complex performance indicator.

CONCLUSIONS

The analysis shows that when sharpening TC knives type K20, the SDC wheels with organic bond type B1-13 have a high coefficient of cutting capacity and the main work is done in the direct motion of the longitudinal feeding. Diamond grains retain well from the bond and do not fall out before they become blunt. This is confirmed by the relatively low relative consumption of SDC. Analysis of the results also shows that:

- Sharpening processes by multi-pass grinding without cooling can be intensified to a productivity greater than 500 mm³ / min using diamond discs with metal-coated and aggregated grains type SDC 2 D126 B1-13 K100 s and SDC 4 D126 B1-13 K100 s.
- The sharpening performance, the type of bonding, the brand of diamond grains and their coverage all have a significant impact on the productivity of diamond wheels when sharpening TC tools. These indicators characterize the quantitative side of the process.
- Knowledge of the quality side of the process is also required, i.e., what phenomena occur in diamond grains and bond when interacting with the surface layer of the polished hard alloy. What is the reason for the higher or lower consumption of diamond, the higher or lower the sharpening resistance, etc.?
- Joint analysis of the quantitative and qualitative sides of the process will allow the optimization of the sharpening process of tungsten carbide tools.

REFERENCES

1. Gochev Zh. (2008), Investigation on the grinding quality of planing knives made of high-speed steel (HSS) type M2 and specific consumption of cubic boron nitride (CBN), The 6th International Scientific Conference: proceedings of papers, „Chip and Chipless Woodworking Processes“: proceedings of papers, Technical University-Zvolen, 11-13.IX. Šturovo, Slovakia, pp. 89-97, ISBN 978-80-228-1913-8.
2. Gochev Zh., P. Vitchev, G. Vukov (2019), Determination of performance indicators and quality of TCT knives when sharpened with PCD grinding wheels, 4-th International scientific conference „Wood Technology & Product Design“: proceedings of papers, S.S Cyril and Methodius University, Skopje, Faculty of Design and Technologies of Furniture and Interior, Republic of North Macedonia, 4-7 September 2019, University congress centre, Ohrid, pp. 119-126, ISBN 978-608-4723-03-5.
3. Gochev Zh., P. Vitchev, G. Vukov (2019), Determination of Performance Index and Effective Power for Sharpening of TC Planer Knives with PCD Abrasive Wheels, 30th International Conference on Wood Science and Technology – ICWST 2019, Impementation of Wood Science in Woodworking Sector and 70th anniversary of Drvna industrija Journal, proceeding of papers, 12-13 December, Zagreb, pp. 53-60, ISBN 978-953-292-062-8.
4. Korotovskikh V. (2012), Determination of diamond wheels working efficiency in order to optimize their composition, Bulletin of Kurgan State University, Technical Science Series, Issue 7 № 2 (24), pp. 122-124, ISSN 2222-3347 (in Russian).

5. Korotovskikh V. (2017), Efficiency of hard-face tool grinding with diamond circles on organic bonds, Bulletin of Kurgan State University, Technical Science Series, Issue 12 № 2 (45), pp. 71-73, ISSN 2222-3347 (in Russian).
6. Kurdyukov V. (2014), Fundamentals of abrasive machining, Основы абразивной обработки, Textbook, Kurgan State University, pp. 195, ISBN 978-5-4217-0254-2 (in Russian).
7. Ostrovskii V. (1981), Theoretical foundations of the grinding process, Leningrad University Press, Leningrad, p. 142 (in Russian).
8. Rowe W. B. (2009), Principles of Modern Grinding Technology, Linacre House, Jordan Hill, Oxford OX2 8DP, UK, p. 480, ISBN 978-0-323-24271-4.
9. Zaharenko I. (1981), Fundamentals of diamond sharpening of tungsten carbide tools, Naukova, dumka, Kiev, p. 299 (in Russian).
10. <https://www.zmm-sm.com/zmmsm/english/wood.htm>
11. <http://carbide.ultra-met.com/viewitems/iso-grades/iso-grade-classifications-tungsten-carbide>

Acknowledgement: This paper is supported by the Scientific Research Sector at the University of Forestry – Sofia, Bulgaria, under contract № НИС-Б-1012/27.03.2019.



HIGH-TEMPERATURE DRYING OF SPRUCE REACTION WOOD

Ivan Klement – Miroslav Uhrín – Tatiana Vilkovská – Peter Vilkovský

Abstract

Reaction wood is a type of wood, which is primarily a gravitropic response to an exterior forces that moves a tree from an optimal, usually upright, position (for example: strong wind, heavy snow, landslide...) (TIMELL 1986). Since reaction (compression) wood has got different physical, mechanical and chemical properties it is a source of problems in the woodworking industry. Because of thicker cell walls, narrower lumens and lesser amount of bordered pits, it can also be a source of complications in the drying process. The aim of this paper was to analyse the differences in drying behaviour between reaction and opposite spruce wood, under the high-temperature drying process. Reaction wood samples and corresponding samples from the opposite side of the log were dried at the temperature of $t = 120\text{ }^{\circ}\text{C}$. The desired final moisture content was 10 %. The differences in drying rate, moisture content and oven-dry density were analysed. The differences in temperature distribution across the thickness of the samples were monitored as well. Our results revealed some differences between reaction wood and opposite wood: especially higher density of reaction wood but also lower drying rate of reaction wood in the free water removal domain and the differences in the temperature distribution as well.

Key words: reaction wood, compression wood, high temperature drying, spruce, drying rate

INTRODUCTION

Spruce (*Picea abies* L. Karst) is the most economically important wood species in the Slovakia, even though its amount decreased by 4,3 % since 2000. Its area in the Slovak forests was 22,5 % in 2019 (Zelená správa 2019). Spruce wood is irreplaceable raw material in the construction industry. It is used for production of load-bearing parts of structures, such as trusses, beams or formwork, etc. The common natural defect of spruce wood is reaction (compression) wood. Strong wind, asymmetrical crown, heavy snow and growth on unstable steep slope are factors that contribute to the reaction wood formation (SCHWEINGRUBER 1993, TIMELL 1986, DOUDA 1948).

Reaction wood of gymnosperms is called compression wood. Compression wood is darker in color than normal wood. The cross section of the tracheids is round shaped, what results in intercellular spaces creation. They are also shorter than tracheids of normal wood. The cell walls are thicker. This, together with a higher proportion of lignin in the cell walls, causes the wood to have a higher density, be less permeable and have a higher compressive strength. STRAŽE and GORIŠEK (2006) reported the density of compression spruce wood $540\text{ kg} \times \text{m}^{-3}$. Similarly, KLEMENT and HURÁKOVÁ (2015) reported the value of 527 and

$560 \text{ kg} \times \text{m}^{-3}$. The angle of the microfibrils in the S2 layer of the cell wall is bigger, which reduces the tensile strength and modulus of elasticity. The larger angle of the microfibrils also causes the compression wood to have higher longitudinal shrinkage but lower transverse shrinkage. This explains the warping of lumber containing both compression and normal wood (BARNETT *et al.* 2014).

The main properties of normal and reaction (compression) wood of spruce (*Picea abies* L. Karst) are already well known. However, the drying behavior of compression wood is still quite unknown. DAVIS *et al.* (2002) found a limited drying rate of *Pinus radiata* compression wood compared to normal wood in the range of moisture content 100 – 40 %. The author attributes the lower drying rate to a larger proportion of latewood, narrower lumens and a lack of bordered pits on the radial walls of the longitudinal tracheids. Nevertheless, the drying time may be similar due to the lower initial moisture content of the compression wood. STRAŽE and GORIŠEK (2006) also reported a lower drying rate of spruce compression wood in the initial drying phase, but an insignificant difference in the phase of bound water removal.

The aim of this paper was to analyze the differences in high-temperature drying of reaction and opposite spruce wood. The partial goals of the paper were to analyze the differences in oven-dry density, initial moisture content, moisture gradients and temperature distribution.

MATERIAL AND METHODS

Material

Spruce (*Picea abies* L. Karst) log with clearly visible content of reaction wood on the cross section was chosen for experimental measurements (Fig. 1 left). The diameter of the log was 38 cm on the narrow end. The total length was 4 m.

Sample preparation

Based on the distribution of the reaction wood on the log cross section, two boards were cut out from the sapwood according to sawing pattern (Fig. 1 right) – one board from the reaction wood zone (CW) and the second one from the opposite side of the log (OW). Four drying samples were subsequently cut out from these boards (CW1, CW2 and OW1, OW2). Also, samples for measuring of the chosen properties (density, moisture content and moisture gradient) were cut out (Fig. 2 left). The dimensions of the drying samples were as follows: $100 \times 30 \times 300 \text{ mm}$ (thickness \times width \times length).

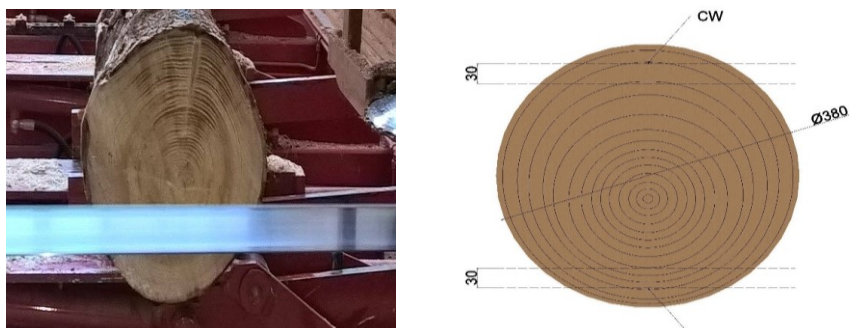


Figure 1 Spruce log with clearly visible zone of reaction wood on the cross section (left) and sawing pattern (right)

Drying mode

The process of drying was conducted using a laboratory kiln Memmert HCP 108 (Mettler GmbH + Co. KG, Schwabach, Germany) (Fig. 2 right). High temperature drying mode was used. During the first stage of drying (from the beginning until the samples reached approximately 30 % moisture content), the temperature of the dry bulb (t_d) was set to 90 °C and the relative humidity was set to $\varphi = 94$ %. After reaching of this moisture content the temperature was set to 120 °C and the humidity of the ambient air was no longer regulated. The desired moisture content of the samples was 10 %. The weight of samples CW1 and OW1 was weighed every 24 hours in order to determine their actual moisture content using the gravimetric method.

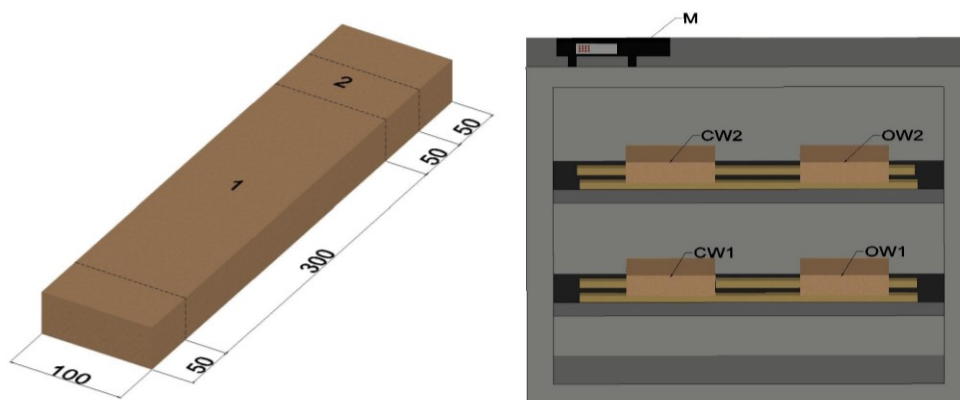


Figure 2 Method of samples preparation (left) (1 – drying sample, 2 – density, moisture content and moisture gradient sample) and placing of samples in drying chamber (right) (CW – compression wood, OW – opposite wood, M – temperature measurement)

Density

The density of wood at 0 % moisture content was measured according to STN EN 49 0108.

Moisture content

The initial and final moisture content of wood was measured using the gravimetric method according to STN EN 49 0103.

Moisture gradient

Moisture gradient was measured before and after the drying process. The samples were cut into three layers according to Fig. 3. The moisture content of layers was measured using gravimetric method according to STN EN 49 0103. Subsequently, the moisture gradient was calculated using Eq. (1)

$$\Delta MC = w_m - \frac{\Sigma w_s}{2} (\%) \quad (1)$$

where w_m is moisture content of the middle layer and w_s is moisture content of surface layer.



Figure 3 Moisture gradient sample (w_m – moisture content of middle layer, w_s – moisture content of surface layer)

Temperature distribution

Type T (Cu-CuNi) thermocouples were used for CW2 and OW2 samples temperature distribution measurement. Thermocouples were placed under the surface and in the middle of sample thickness according to fig. 4. The Comet MS6R device (Comet system, Rožnov pod Radhoštěm, Czechia) was used for temperature measurement and recording. Temperature measurement and recording was performed automatically every 60 seconds.

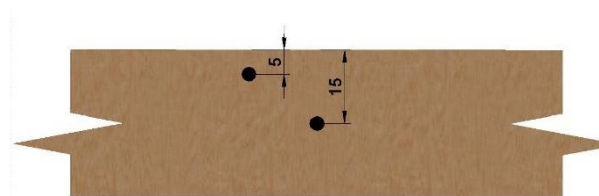


Figure 4 Position of thermocouples in the drying sample

RESULTS AND DISCUSSION

The measured values of density, moisture content and overall drying time are summarized in Table 1. The values of oven-dry density confirm the statements of above-cited authors. The average density of the reaction wood was $562,2 \text{ kg} \times \text{m}^{-3}$, while it was only $479,2 \text{ kg} \times \text{m}^{-3}$ for the opposite wood. The density is approximately 15 % higher due to the thicker cell walls and the higher proportion of latewood in the reaction wood samples.

Sample	Moisture content (%)		Drying time t (h)	Average density ρ_0 ($\text{kg} \times \text{m}^{-3}$)
	initial w_i (%)	final w_f (%)		
Reaction wood	89,78	9,6	150,5	562,2
	88,89	9,71		
Opposite wood	87,59	9,59	149	479,2
	86,76	9,38		

Table 1 Moisture content, density and drying time of samples

When looking at the initial moisture content, only a slight (negligible) difference between the reaction and opposite wood is visible. Thus, the lower initial moisture content of the reaction wood was not confirmed in our case, despite the opinion that the reaction wood reaches a lower value of the initial moisture content.

The values of moisture gradients representing the difference between moisture content of middle layer and surface layers are summarized in Table 2. From the measured data it is possible to see the initial variability of moisture content between the individual layers. In our case, the negative effect of the reaction wood on the size of the moisture gradient could not be proven. The negative moisture gradient that was measured before the drying process was caused by freezing of the samples and subsequent condensation of water on the surfaces of the samples after defreezing.

Table 2 Moisture gradient

Sample	Moisture content (%)			\bar{w}_s	Δw
	w_s	w_m	w_s		
before drying					
Reaction wood	79,96	80,97	83,44	81,7	-0,73
	91,61	86,16	84,55	88,08	-1,92
Opposite wood	88,25	84,51	77,92	83,09	1,42
	93,8	95,66	97,77	95,78	-0,13
after drying					
Reaction wood	3,66	4,41	4,6	4,13	0,28
	3,48	5,15	4,02	3,75	1,4
Opposite wood	4,49	3,22	4,5	4,49	-1,27
	4,81	4,67	3,95	4,38	0,29

Drying curves of both wood modifications are presented in Figure 5. It is clear that during the first 24 hours of drying, the reaction wood dried more slowly than the opposite wood. Opposite wood achieved greater moisture losses from during the first 72 hours of drying. After exceeding this limit, however, the greater moisture losses were achieved by the reaction wood. This is especially visible in the phase below 30 % moisture content, i.e. in the phase of bound water removing. Eventually, the reaction wood reached the required final moisture content of 10 % at about the same time as the opposite wood. TARMIAN *et al.* (2009) and STRAŽE and GORIŠEK (2006) also reported lower drying rate of reaction wood above fibre saturation point. The different behaviour of reaction and normal wood in the drying process is given by specific anatomical features influencing the moisture pathways through which water escapes from the wood. Bordered pits on the radial walls of longitudinal tracheids, the most effective moisture pathways in gymnosperms, are unusually small in reaction wood. In addition, a smaller percentage of them occur in the tracheids of the reaction wood. As a result, small and rare bordered pits appear in principle to be responsible for the limited flow of water through the reaction wood. The above-mentioned authors state that when removing bound water, the reaction wood dries at a comparable rate as opposite wood. This is basically confirmed by our results.

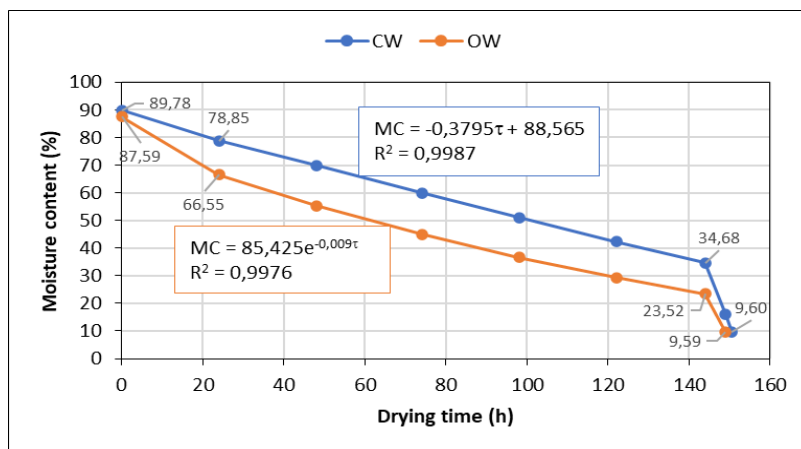


Figure 5 Drying curves

The results from the measurement of the temperature distribution in the reaction and opposite wood are presented in Figure 6. From the beginning of drying to fibre saturation point (FSP), the surface layer of the reaction wood reached a slightly higher temperature, but the middle layer temperature was slightly higher in the opposite wood. The wood temperature curves approximately copied the dry bulb temperature curve. In the hygroscopic range (from FSP to 10 % moisture content), after increasing the temperature of the dry bulb from 90 °C to 120 °C, the temperature increase was more rapid in the reaction wood. This fact can be explained by the higher moisture content of the reaction wood when changing the temperature parameters. At this point, the moisture content of the reaction wood was 34.68 %, while the moisture content of the opposite wood was only 23.52 %. At this phase, the reaction wood reached a higher temperature of the middle and surface layer and it remained higher until the end of the drying process. The temperature of the samples at this phase was significantly lower than the temperature of the dry bulb.

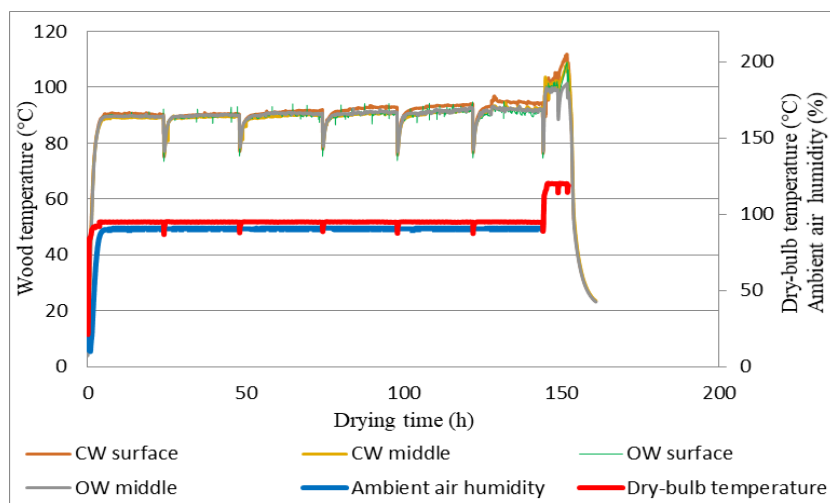


Figure 6 Temperature of wood, dry-bulb temperature and ambient air humidity.

CONCLUSIONS

The following conclusions can be drawn from our measurements:

- The average oven-dry density of the reaction wood was 15 % higher than the density of the opposite wood. This may be due to thicker cell walls and a higher proportion of higher density latewood in the reaction wood samples.
- No differences in initial moisture content were found. The reaction wood reached approximately the same moisture content as the opposite wood.
- The negative effect of the reaction wood on the resulting values of moisture gradients after the drying process has not been proven.
- Differences in the drying rate were visible especially at the beginning of the drying process, when the opposite wood dried faster. As the moisture content approached the area of bound water, the differences in drying rate decreased and the reaction wood finally reached the desired moisture content at about the same time as the opposite wood.
- The temperature curves of the reaction and opposite wood approximately copied the temperature curve of the dry bulb. Samples with the reaction wood had a slightly higher surface layer temperature, while the middle layer temperature was higher for the opposite wood. After changing the temperature of the dry bulb from 90 °C to 120 °C, the increase in the temperature of the surface and middle layer was faster in the reaction wood. The temperatures of the opposite and reaction wood samples at this phase did not reach the temperature of the dry bulb.

ACKNOWLEDGEMENTS

This work was supported by the Slovak Research and Development Agency under the contract no. SK-PL-18-0052.

REFERENCES CITED

- BARNETT, J., SARANPÄÄ, P., GRIL, J. 2014. The Biology of Reaction Wood. Berlin Heidelberg: Springer-Verlag, p. 7. ISBN 978-3-642-10813-6.
- DAVIS, C. P., CARRINGTON, C. G., SUN, Z. F. 2002. The influence of compression wood on the drying curves of *Pinus radiata* in dehumifier conditions. In Drying Technology, 2002, 20(4): 2005 – 2026.
- DOUDA, V., 1948. Studie o významu reakčného dreva. Praha, Sborník ČZA: 48.
- KLEMENT, I., HURÁKOVÁ, T. 2015. Vplyv sušenia na vlastnosti a kvalitu smrekového reziva s obsahom reakčného dreva. Acta Facultatis Xylogologiae Zvolen: vedecký časopis Drevárskej fakulty. 2015. zv. Roč. 57, č. 1, s. 75--82. ISSN 1336-3824.

SCHWEINGRUBER, F. H. 1993. Jahrringe und Umwelt – Dendroökologie. Bimensdorf, Eidgenössische Forschungsanstalt für Wald, Schnee und Landschaft, p. 474. ISBN 5-8752-011-9.

STRAŽE, A., GORIŠEK, Z. 2006. Drying characteristics of compression wood in Norway spruce (*Picea abies* Karst.). In Wood structure and properties. Zvolen: Arbora Publishers, pp. 399–403

TARMIAN, A., REMOND, R., FAEZIPOUR, M., KARIMI, A., PERRE', P. 2009 Reaction wood drying kinetics: tension wood in *Fagus sylvatica* and compression wood in *Picea abies*. Wood Sci. Technol. 43:113–130

TIMELL, T. E. 1986. Compression Wood in Gymnosperms, Volume 1. Bibliography, Historical Background, Determination, Structure, Chemistry, Topochemistry, Physical Properties, Origin and Formation of Compression Wood. Berlin, Springer Verlag, p. 705. ISBN 978-3-540-15715-1

ZELENÁ SPRÁVA. 2019. Zelená správa [online]. Bratislava: Ministerstvo pôdohospodárstva Slovenskej republiky. 2019, p. 66. [cit. 01-05-2020]. dostupné na internete < <https://www.mpsr.sk/zelena-sprava-2019/123---14927/>>. ISBN 978 - 80 - 8093 - 286 - 2



THE EFFECT OF DRYING INTENSITY ON THE COLOR CHANGES OF PINE WOOD (*PINUS SYLVESTRIS L.*)

Aleksandra Konopka – Jacek Baranski – Kazimierz A. Orlowski –
– Daniel Chuchala

Abstract

*The effect of the selection of drying process parameters on the color change of Scots pine wood (*Pinus Sylvestris L.*) is presented. In this work the experimental studies have been performed. The research focused on the influence of drying intensity on the changes of color after drying process. Intensity of drying process was determined on the basis of the average drying gradient. To determine the color of wood before and after drying process the series of experiments have been performed, using color reader device. The wood samples were dried according to three different drying modes, namely: mild, normal and intense. Experiments were conducted in the laboratory dryer. The measurement of wood samples was made using international standards: ISO 11664-2 and ISO 11664-4 of total color change after drying. As a result of the performed statistical tests, there were observed statistically significant color changes of the wood surface for intensive drying mode.*

Key words: *drying process, pine wood, color changes, process intensity*

INTRODUCTION

Wood color is one of the main criteria of assessing its quality and it affects how wood product is perceived by clients. According to ABRAHÃO (2005) homogeneity of wood color is relevant in assessing quality, since, it determines final appearance of wood product. Objective color measurement is performed instrumentally in such a way that it corresponds to visual assessment, using spectrophotometers or color readers devices and is defined in numerical form based on a standardized colorimetric calculation developed by the International Commission on Illumination (CIE - Comission Internationale de l'Eclairage) (KAZIMIERSKA, 2014). In the treatment processes, wood was mechanically processed, dried or subjected to thermal modification, which significantly changes its natural color and chemical composition (GONZALEZ DE CADEMARTORI *et al.* 2013, BARCÍK *et al.* 2015). Significant changes in the structure of wood appear after exceeding 180 °C, while at the temperature of 250 °C the carbonization process begins (KACÍKOVÁ *et al.* 2011).

Instrumental methods for determining colorimetric parameters of color and color difference are subject to ISO standards. Standards contain basic definitions, requirements for colorimetric systems, basics of colorimetric calculus, information for the correct

implementation of instrumental color measurement. In the study, the color change of dried wood was assessed using the three-axis system (Figure 1), measuring: brightness (L^*) and chromaticity coordinates (a^* , b^*), in accordance with ISO 11664-2 and ISO 11664-4. The CIELAB system recommended by CIE consists of two axes with two parameters a^* and b^* , which are at right angle to each other and define the color tone. Third axis is brightness L^* and it is perpendicular to the a^* - b^* plane.

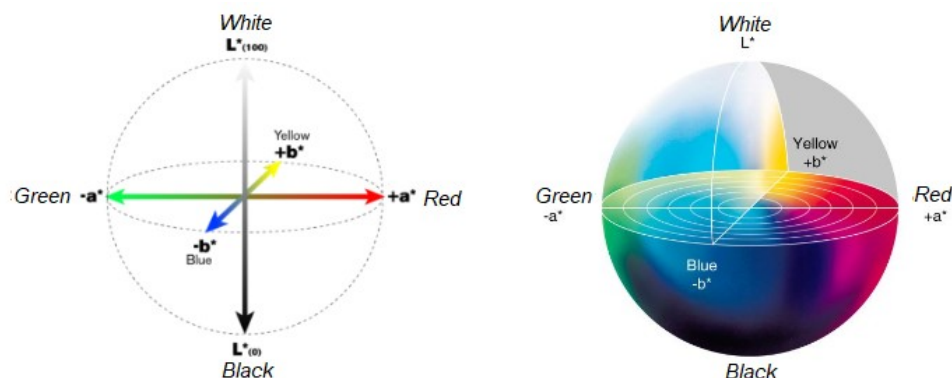


Figure 1. Diagram of a three-axis color change measurement system (SEHLSTED-PERSSON, 2003)

Colorimetric measurement is useful in wood quality control process and in assessing the color of final products of high-temperature drying (KLEMENT *et al.* 2015). The mechanism of color changes is a complicated process and depends on many differentiating and degrading factors (MCCURDY *et al.* 2005, KUDRA *et al.* 2003, McDONALD *et al.* 2010). GLIJER *et al.* 2005 determined the intensity of the drying process based on the drying gradient, which is defined as follows:

$$a = \frac{MC}{EMC} [-] \quad (1)$$

where: MC – wood moisture content [%], EMC – equilibrium moisture content, for the given temperature and relative humidity of drying medium [%].

The aim of the experimental research was to determine the color change of pine wood after drying process using three modes with different levels of the process intensity.

MATERIAL AND METHODS

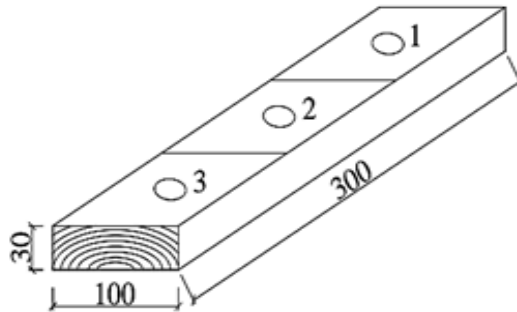
The drying process of pine wood on laboratory scale was carried out in the HCP108 dryer manufactured by Memmert GmbH + Co.KG from Büchenbach, Germany. Three drying modes were used in the work, the parameters of which are summarized in Table 1.

Table 1. Drying medium parameters for modes: mild, normal and intense

Drying mode	MC [%]	t_s [°C]	EMC [%]	Δt [°C]	α [%/°C]	RH [%]
mild	> 24 ^(FSP)	50 ±1	11.3	6.3	1.46	70 ±2
	23.9 - 8	60 ±1	9.1	9.0		62 ±2
normal	> 24 ^(FSP)	70 ±1	9.0	9.0	1.77	65 ±2
	23.9 - 8	80 ±1	7.5	11.7		60 ±2
intense	> 40	90 ±1	14.1	2.8	2.56	90 ±2
	39.9 - 24 ^(FSP)	90 ±1	10.0	7.3		75 ±2
	23.9 - 8	120 ±1	4.0	20.0		3 ±2

Legend: FSP – Fiber Saturation Point, MC – moisture content, t_s – temperature of drying medium, EMC – equilibrium moisture content, Δt – psychrometric difference, α – drying gradient, RH – relative humidity

In order to perform a statistical analysis, for each drying mode, 30 pine wood samples (*Pinus sylvestris* L.) with a tangential cross-section were selected. In the Figure 2 was shown schematically the locations of boards to measure the color change of pine wood after drying. Each of 10 boards dried in the process for each intensity mode had three color measurement points before and after drying respectively.

**Figure 2.** The points position of color measurement on samples

The color space of the dried material was determined using Konica Minolta Color Reader type CR10 device. It describes the output coordinates L^* , a^* , b^* by the color change in the color space (Figure 1) using the Equation 2. The color changes were obtained as comparison of measured values of the parameters respectively L^* , a^* , b^* before and after drying (CIVIDINI *et al.* 2007).

$$\Delta E = \sqrt{(L_2^* - L_1^*)^2 + (a_2^* - a_1^*)^2 + (b_2^* - b_1^*)^2} [-] \quad (2)$$

where L_1^* , a_1^* , b_1^* are the values of color spectra before drying process, and L_2^* , a_2^* , b_2^* are the values of color spectra after drying process.

Parameters L^* , a^* , and b^* are coordinates of colorimetric space. The color change criteria are presented below:

- $\Delta E < 0.2$: invisible color change
 $2 > \Delta E > 0.2$: slight change of color
 $3 > \Delta E > 2$: color change visible in high filter
 $6 > \Delta E > 3$: color changes visible with the average quality of the filter
 $12 > \Delta E > 6$: high color change
 $\Delta E > 12$: different color

Bar graphs were prepared and Duncan's test was performed to compare all possible pairs of arithmetic means. If the probability value is greater than the assumed significance level $p > \alpha$, there is no reason to reject the so-called the null hypothesis which states that the observed effect is due to chance. The analysis assumed a significance level of $\alpha = 0.05$ and the STATISTICA 13 (StatSoft, Inc., Tulsa OK Oklahoma, US) program was used to determine the probability.

RESULTS AND DISCUSSION

The measurement data presented in Table 2 contain a summary of the results of the total color change of the tested samples after drying with the use of three drying modes.

Table 2. Color change measurement results for: mild, normal and intense drying processes

Drying mode	Statistic values	L_1^* [-]	a_1^* [-]	b_1^* [-]	L_2^* [-]	a_2^* [-]	b_2^* [-]	ΔE^* [%]
mild	average	70.6	9.1	29.9	74.6	6.7	26.5	6.4
	standard deviation	2.6	1.5	3.3	2.5	1.5	1.7	2.0
normal	average	77.0	6.7	25.6	74.3	8.0	29.2	4.8
	standard deviation	0.5	0.8	1.7	1.3	0.7	1.4	1.1
intense	average	74.2	6.6	24.9	65.2	12.0	33.3	13.9
	standard deviation	1.3	0.5	1.5	3.2	2.3	5.1	5.6

Table 3. Duncan's test for the complete color change of pine wood depending on the drying program used

		Mild	Normal	Intense
		ΔE_1 [-]	ΔE_2 [-]	ΔE_3 [-]
Mild	ΔE_1 [-]	-	0.083619	0.000114
Normal	ΔE_2 [-]	0.083619	-	0.000053
Intense	ΔE_3 [-]	0.000114	0.000053	-

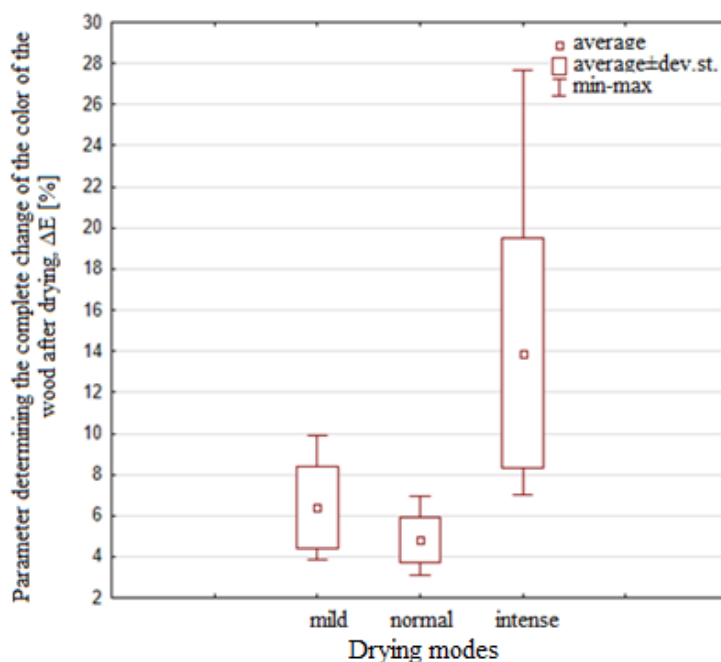


Figure 4. Wood color changes after drying processes with the use of three modes

By analyzing the obtained results (Table 2, Figure 4), it was found that the color change of pine wood after drying, determined by the value of ΔE , increases when the process takes place at temperatures above 100 °C. The change in the color of pine wood turned out to be the smallest for normal drying (the average value of the ΔE parameter was 4.81 %, with a standard deviation of 1.1 %). The greatest color change was achieved during intensive drying (the mean value of the ΔE parameter was 13.9 %, with a standard deviation of 5.6 %).

Duncan's test (Table 3) confirmed a strong statistical difference in the total change in the color of wood after drying between the intensive program and the other drying programs ($p < \alpha$). The drying program at a temperature t_s above 100 °C requires increased relative air humidity RH in the initial stage of the process and its strong reduction when the temperature of the drying agent exceeds 100 °C. This can increase the value of the ΔE parameter, which explains a greater color change. The tendency to stronger discoloration of the wood was also observed by ESTEVES *et al.* (2008), GONZALEZ DE CADEMARTORI *et al.* (2013), UNSAL *et al.* (2003), who underwent thermal modification of eucalyptus and pine wood, as well as the rectification process - MOURA *et al.* (2011).

CONCLUSION

The conducted empirical investigations of pine wood kiln drying revealed that:

- the change of pine wood color depend on the drying mode only for the intensive drying mode, when temperature of the process exceed 100°C;
- according to Duncan's test drying modes mild and normal do not affect the surface color of pine wood.

ACKNOWLEDGEMENTS

This work was supported by the Slovak Research and Development Agency under the contract no. SK-PL-18-0052 and **Polish National Agency for Academic Exchange** NAWA, Poland, Grant no PPN/BIL/2018/100162 are kindly acknowledged.

REFERENCES

- ABRAHÃO, C. P., 2005: Estimation for some properties of the wood of *Eucalyptus urophylla* by spectrometry, Viçosa, Brazil: PhD Thesis, Federal University of Viçosa, pp. 182.
- BARCÍK, Š., GAŠPARÍK, M., RAZUMOV, E. Y., 2015: Effect of temperature on the color changes of wood during thermal modification. *Cellulose Chemistry and Technology*. 49 (9-10), pp. 789-798.
- CIVIDINI, R., TRAVAN, L., ALLEGRETTI, O., 2007: White beech: a tricky problem in the drying process. Québec City, Canada, 24–26 September.
- ESTEVES, B., VELEZ MARQUES, A., DOMINGOS, I., PEREIRA, H., 2008: Heat induced colour changes of pine (*Pinus pinaster*) and eucalyptus (*Eucalyptus globulus*) wood. *Wood Science and Technology*. 42 (5), pp. 369-384.
- ISO 11664-2: 2007 Colorimetry - Part 2: CIE standard illuminants. *International Organization for Standardization*, Geneva, Switzerland.
- ISO 11664-4: 2008 Colorimetry - Part 4: CIE 1976 L*a*b* Colour space. *International Organization for Standardization*, Geneva, Switzerland.
- GLIJER, L., 2005: Suszenie i parowanie drewna, Warszawa: Wieś Jutra.
- GONZALEZ DE CADEMARTORI, P. H., SCHNEID, E., GATTO, D. A., STANGERLIN, D. M., BELTRAME, R., 2013: Thermal modification of *Eucalyptus grandis* wood: Variation of colorimetric parameters. *Maderas. Ciencia y tecnología*. 15 (1), pp. 57-64.
- KACÍKOVÁ, D., KACÍK F., 2011: Chemical and Mechanical Changes during Thermal Treatment of Wood. *Technical University in Zvolen (Slovakia)*, pp. 71.
- KAZIMIERSKA, M., 2014: Obiektywna ocena barwy wyrobów użytkowych. *Technologia i Jakość Wyrobów*. 59, pp. 44-47.
- KLEMENT, I., HURÁKOVÁ, T., 2015: High temperature drying of beech wood with content of red heartwood. Selected Processes at the Wood Processing, Hokovce (Slovakia).
- KUDRA, V. S., VITTER, R. M., GAIDA, Y. I., 2003: Effect of false heart on the quality of beech wood. *Lesnoe Khozyaistvo*. 5, pp. 23-24.
- MCCURDY, M. C., PANG, S., KEYEY, R. B., 2005: Measurement of colour development in *Pinus radiata* sapwood boards during drying at various schedules. *Maderas. Ciencia y Tecnología*. 7 (2), pp. 79-85.
- MCDONALD, A. G., FERNANDEZ, M., KREBER, B., LAYTNER, F., 2010: The chemical nature of kiln brown stain in *Radiata* pine. *Holzforschung*. 54, pp. 12-22.
- MOURA, L. F., BRITO, J. O., 2011: Effect of thermal rectification on colorimetric properties of *Eucalyptus grandis* and *Pinus caribaea* var. *hondurensis* woods. *Scientia Forestalis*. 39 (89), pp. 69-76.
- SEHLSTED-PERSSON, M., 2003: Color responses to heat treatment of extractives and sap from pine and spruce. The 8th International IUFRO wood drying conference pp. 461, ISBN 973-635-198.
- UNSAI, O., KORKUT, S., ATIK, C., 2003: The effect of heat treatments on some properties and colour in *Eucalyptus camaldulensis* Dehn. Wood. *Maderas. Ciencia y Tecnología*. 5 (2), pp. 145-152.



MODIFIKÁCIA VYBRANÝCH DRUHOV DREVA ÚČINKOM NÍZKOTEPLOTNEJ PLAZMY

Igor Novák¹ – Ján Sedliačik² – Ivan Chodák¹ – Angela Kleinová¹ –
Ján Matyašovský³ – Peter Jurkovič³

Abstrakt

Plazmová úprava zvyšuje povrchovú energiu dreva naviazaním polárnych funkčných skupín. Povrch dreva sa takto stáva hydrofilnejším a dosahuje lepšiu adhéziu k adhezívam a náterom na báze vodných disperzií. Merania kontaktného uhla vody na povrchu dreva modifikovaného rádio-frekvenčnou (RF) plazmou potvrdili jeho výrazné zníženie, čím sa vytvorili vhodné podmienky jeho ďalšieho spracovania lepením alebo povrchovou úpravou.

Kľúčové slová: *modifikácia dreva, nízkotepelná plazma, hydrofilnosť a hydrofóbnosť dreva, lepenie a povrchová úprava dreva.*

ÚVOD

Vhodnou metódou na zvýšenie hydrofilnosti je modifikácia dreva účinkom nízkotepelnej plazmy. V dôsledku plazmovej úpravy sa povrchová energia dreva zvyšuje naviazaním polárnych funkčných skupín na upravený povrch dreva, ktorý sa stáva hydrofilnejším (Kamdem a kol. 2000). Vysokofrekvenčná výbojová plazma pri zníženom tlaku predstavuje „zelenú“ ekologicky akceptovateľnú metódu úpravy povrchu dreva. Pre potreby priemyselného využitia musia rôzne typy dreva disponovať širokou škálou rôznych povrchových charakteristík vrátane polarít, schopnosti farbenia, odolnosti proti poškrabaniu, adhéznym vlastnostiam na mieru a antibakteriálnej odolnosti (Wolkenhauer a kol. 2009; Acda a kol. 2012, Dzurenda a kol. 2020). Zvýšenie hydrofilnosti dreva je nevyhnutnou podmienkou na dosiahnutie vyššej adhézie k polárnym adhezívam a náterom na báze vodných disperzií (Moghadamzadeh a kol. 2011; Novák a kol. 2012; Odrášková a kol. 2008; Reinprecht a Šomšák 2015).

Existujú dva dôvody použitia nízkotepelnej plazmy na povrchovú modifikáciu dreva (Odrášková a kol. 2008), ktorá v prostredí vzduchu významne zvyšuje jeho hydrofilnosť, pričom vznikajú rôzne polárne skupiny (hydroxylové, karboxylové, karbonylové). Makromolekuly celulózy a hemicelulóz v dreve pôsobením plazmy sieťujú, čo má za následok zvýšenie odolnosti proti poškrabaniu a k zlepšeniu bariérových vlastností dreva. Druhým dôvodom použitia plazmy je zvýšenie adhézie v adhéznom spoji medzi polymérom adhezívom a drevným substrátom v dôsledku rastu hydrofilnosti dreva, čo je veľmi dôležité pre priemyselné aplikácie. Zvýšením hydrofilnosti, resp. zmáčateľnosti dreva modifikovaného plazmou sa zlepšuje kontakt adhezíva s povrchom dreva v

¹ Ústav polymérov SAV, Dúbravská cesta 9 845 41 Bratislava

² Technická univerzita vo Zvolene, T.G. Masaryka 24, 960 01 Zvolen

³ VIPO a.s., Generála Svobodu 1069/4, 958 01 Partizánske

molekulovom meradle, pričom ide o rozhodujúci faktor na dosiahnutie vysokej adhézie na rozhraní adhezívum – drevo (Kúdela a kol. 2017).

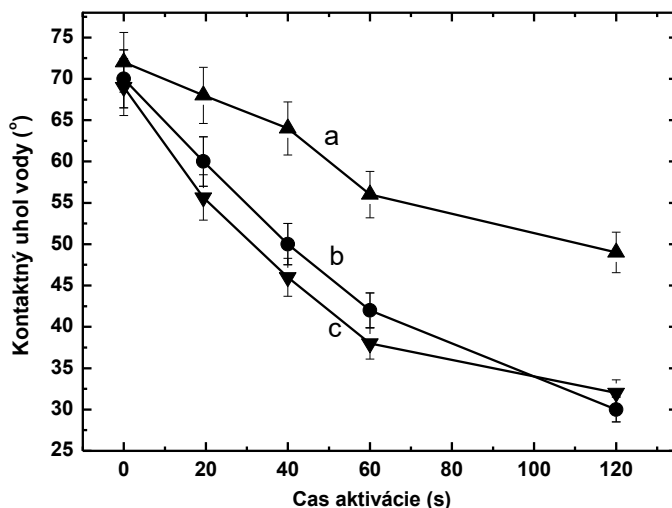
EXPERIMENTÁLNA ČASŤ

Vzorky drevín buk (*Fagus Sylvatica*), breza (*Betula Alba*) a javor (*Acer Pseudoplatanus*) s rozmermi 50×15×5 mm (Drevárska fakulta TU vo Zvolene) s obsahom vlhkosti 8 % boli modifikované účinkom RF plazmy pri tlaku 100 Pa vo vzduchu. Modifikácia dreva kapacitne viazanou RF plazmou sa uskutočňovala v plazmovom generátore pracujúcom pri zníženom tlaku 100 Pa, napätie plazmového RF generátora bolo 2 kV, frekvencia 13,56 MHz, intenzita prúdu bola max. 0,6 mA a maximálny výkon zdroja RF plazmy dosahoval 1200 W. Vzorky dreva boli modifikované RF plazmou pri výkone 350 W.

Voľná povrchová energia dreva sa merala stanovením kontaktných uhlov (θ) s redestilovanou vodou ako testovacou kvapalinou (Odrášková et al. 2008). Kvapky testovacej kvapaliny ($V = 20 \mu\text{l}$) sa umiestnili na povrch dreva s mikropipetou (Biohit, Fínsko) a závislosť $\theta = f(t)$ sa extrapolovala na $t = 0$. Uhly vody sa merali na zariadení SEE (Surface Energy Evaluation) (Advex, Česká republika). Merania FTIR sa uskutočňovali na spektrometri FTIR NICOLET 8700 (Thermo Scientific, UK).

VÝSLEDKY A DISKUSIA

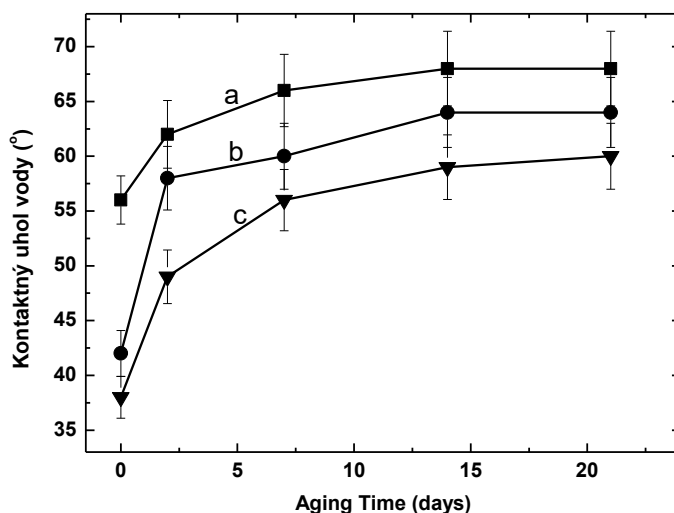
Na obr. 1 je znázornená závislosť kontaktných uhlov vody na povrchu rôznych druhov dreva (breza, buk, javor) od času aktivácie RF plazmou.



Obr. 1 Kontaktné uhly vody na povrchu dreva v závislosti od času aktivácie RF plazmou:
a – breza, b – buk, c – javor

Kontaktné uhly vody na povrchu dreva v závislosti od času aktivácie RF plazmou vykazujú pokles súvisiaci s rastom hydrofilnosti povrchov dreva pri zvyšovaní času modifikácie RF plazmou. Podľa obr. 1 bol pokles kontaktných uhlov vody a nárast hydrofilnosti vzoriek

dreva najvyšší v prípade javora upraveného RF plazmou, nižší pokles bol pozorovaný pre RF plazmou modifikované bukové drevo a najnižší prírastok bol zaznamenaný pre brezové drevo. Hydrofilnosť RF plazmou upraveného dreva klesala po 60 s modifikácie RF plazmou vo vzduchu v postupnosti javor > buk > breza.



Obr. 2 Starnutie RF plazmou upraveného dreva v závislosti od času, ktorý uplynul od modifikácie (t = 60 s): a – breza, b – buk, c – javor

Obr. 2 znázorňuje starnutie RF plazmou upraveného dreva v závislosti od času, ktorý uplynul od modifikácie plazmou. Kontaktný uhol vody na povrchu skúmaných troch druhov dreva (breza, buk, javor) rastie intenzívnejšie počas prvých dvoch dní od modifikácie RF plazmou a potom sa jeho hodnota stabilizuje. Najvyšší prírastok počas prvých dvoch dní od modifikácie RF plazmou bol pozorovaný pre bukové drevo, nižší bol zistený pre javorové a brezové drevo.

V tabuľkách 1, 2 a 3 sú uvedené hodnoty prírastkov polarity skúmaných troch druhov dreva v závislosti od modifikácie RF plazmou vo vzduchu. Koncentrácia skupín COOH, C–O a C=O po úprave dreva účinkom RF plazmy vo vzduchu významne vzrástla a vzrástli aj hodnoty koncentrácie –OH skupín vyjadrené integrovanými píkmi P(3400 cm⁻¹, OH stretch) a podielmi P(OH)/P(CH₂) v dreve. Polarita dreva je vyjadrená podielmi P(OH)/P(CH₂) získanými z výsledkov meraní FTIR RF plazmou upraveného dreva. V tabuľkách 1 až 3 sú uvedené integrované píky P(2895 cm⁻¹, CH₂ stretch) a P(3400 cm⁻¹, OH stretch) zistené z meraní FTIR pre bukové, brezové a javorové drevo modifikované RF plazmou vo vzduchu.

Tabuľka 1

BUK	P(2895 cm ⁻¹ , CH ₂ stretch)	P(3400 cm ⁻¹ , OH stretch)	P(OH)/P(CH ₂)
Nemodifikovaný	0.496	4.203	8.474
20 s plazma	0.364	5.086	13.973
40 s plazma	0.306	6.311	20.624
60 s plazma	0.284	6.528	22.986

Tabuľka 2

BREZA	P(2895 cm ⁻¹ , CH ₂ stretch)	P(3400 cm ⁻¹ , OH stretch)	P(OH)/P(CH ₂)
Nemodifikovaná	0.670	4.440	6.627
20 s plazma	0.614	6.223	10.135
40 s plazma	0.542	7.962	14.690
60 s plazma	0.495	9.223	18.632

Tabuľka 3

JAVOR	P(2895 cm ⁻¹ , CH ₂ stretch)	P(3400 cm ⁻¹ , OH stretch)	P(OH)/P(CH ₂)
Nemodifikovaný	0.763	4.538	5.948
20 s plazma	0.538	6.141	11.914
40 s plazma	0.483	6.784	14.046
60 s plazma	0.430	7.293	16.960

ZÁVER

Kontaktný uhol vody na povrchu dreva sa po modifikácii RF plazmou vo vzduchu výrazne znížil pre brezové, bukové aj javorové drevo (kontaktný uhol bukového dreva sa znížil zo 70° na 30°). Kontaktný uhol vody dreva modifikovaného RF plazmou vykazoval pri starnutí intenzívny pokles najmä počas prvých 2 dní. Koncentrácia skupín OH, COOH, C–O a C=O po úprave dreva účinkom RF plazmy vo vzduchu významne vzrástla ako potvrdili FTIR merania, pričom sa zistilo zvýšenie polarity najmä dôsledku vzrastu koncentrácie –OH skupín. Povrch dreva modifikovaného RF plazmou by mal byť na základe uvedeného zistenia do 2 dní upravený ďalšími technologickými postupmi, napr. lepením.

POĎAKOVANIE

Tento výskum bol podporený Agentúrou na podporu výskumu a vývoja projektami APPV-14-0566, APVV-16-0177, APVV-18-0378 a Vedeckou grantovou agentúrou MŠVVaŠ SR a SAV VEGA, Grant No. 1/0570/17.

POUŽITÁ LITERATÚRA

- ACDA M.N., DEVERA E.E., CABANGON R.J., RAMOS H.J. 2012. Effects of plasma modification on adhesion properties of wood. In *International Journal of Adhesion and Adhesives* 32, 2017, p. 70-75.
- DZURENDA, L., GEFFERT, A., GEFFERTOVA, J., DUDIÁK, M. 2020. Evaluation of the Process Thermal Treatment of Maple Wood Saturated Water Steam in Terms of Change of pH and Color of Wood. In *BioResources* 15(2), 2020, p. 2550-2559.
- KAMDEM D.P., PIZZI A., TRIBOULOT M.C. 2000. Heat-treated timber: potentially toxic byproducts presence and extent of wood cell wall degradation. In *Holz als Roh- und Werkstoff* 58, 2000, p. 253-257.
- KÚDELA J., ŠTRBOVÁ M., JAŠ F. 2017. Influence of accelerated ageing on morphology and wetting of wood surface treated with a modified water-based coating system. In *Acta Facultatis Xylogiae Zvolen*, 59(1), 2017, p. 27-39.

MOGHADAMZADEH H., RAHIMI H., ASADOLLAHZADEH M., HEMMATI A.R. 2011. Surface treatment of wood polymer composites for adhesive bonding. In *International Journal of Adhesion and Adhesives* 31, 2011, p. 816-821.

NOVÁK I., POPELKA A., KRUPA I., CHODÁK I., JANIGOVÁ I., NEDELČEV T., ŠPÍRKOVÁ M., KLEINOVÁ A. 2012. High-density polyethylene functionalized by cold plasma and silanes. In *Vacuum* 86, 2012, p. 2089-2094.

ODRÁŠKOVÁ M., RÁHEE J., ZAHORANOVÁ A., TIŇO R., ČERNÁK M. 2008. Plasma activation of wood surface by diffuse coplanar surface barrier discharge. In *Plasma Chemistry and Plasma Processing* 28, 2008, p. 203-211.

WOLKENHAUER A., AVRAMIDIS G., HAUSWALD E., MILITZ H., VIÖL W. 2000. Sanding vs. plasma treatment of aged wood: A comparison with respect to surface energy. In *International Journal of Adhesion and Adhesives* 29, 2000, p. 18-22.



QUALITY OF FINISH ON LIGHTWEIGHT PLYWOOD

Gabriela Slabejová – Mária Šmidriaková

Abstract

Quality of finish on lightweight plywood. The article deals with quality of finish on lightweight plywood made from beech veneers with spaces of air. The finish was formed of water-based coating materials. The properties of the finish (gloss value, film hardness, impact resistance and resistance to cold liquids) were evaluated according to the standards. The coatings were formed of water-based coating materials suitable for children's furniture: PAMLAK (with density of 1050 kg/m³), HOBBYLAK, and KIVA (with density of 1000 kg/m³). Quality of water-based coating materials was different. The gloss of the transparent surface finish was affected by direction of wood fibers in the substrate. HOBBYLAK reached the highest surface hardness; and at the impact resistance testing, the smallest intrusion was formed on this surface. The resistance of the finishes to some liquids was significantly different.

Key words: *beech veneer, lightweight plywood, water-based coating material, gloss value, impact resistance, resistance to cold liquids*

INTRODUCTION

Wood is an anisotropic material of relatively inhomogeneous structure, formed by macromolecular substances (cellulose, hemicelluloses, lignin and extractives). Wood is characterized by sufficient strength, flexibility, good heat insulating, and specific acoustic performance (KAČÍK *et al.*, 2010).

Wood has many positive characteristics, but also some deficiencies, e.g. insufficient dimensional stability. To achieve better dimensional stability and improve mechanical properties of wood, the composite materials are produced. The composite materials are materials of large-scale dimensions, characterized by steadiness of mechanical properties, and greater resistance to the environment (KING and HRÁZSKÝ, 2005). The traditional composite layered materials are plywood and laminated timber. Currently, in practice, the composite materials having a layer of wood and a layer of wood with spaces of air (e.g. lightweight plywood) are used. Various modified veneers can be used to make plywood. Veneers modified by pressing were researched by BEKHTA *et al.* (2016). Various modifications of wood were dealt by FEKIAČ *et al.* (2020), FEKIAČ, GÁBORÍK (2018), FEKIAČ *et al.* (2015), ŠHULGA (2015), ZEMÍAR *et al.* (2014), LANGOVÁ and JOŠČÁK (2014), and SLABEJOVÁ and ŠMIDRIAKOVÁ (2014). Just like the surface of solid wood, the surface of lightweight plywood must be finished.

The aim of this study was to determine the quality of coatings on the surface of lightweight plywood. The gloss value of the surface finishes, film hardness of the coatings, impact resistance, and resistance of coatings to cold liquids were assessed.

MATERIALS AND METHODS

In experiments, beech wood (*Fagus sylvatica* L.) veneer was used for production of a lightweight plywood. The surface of the lightweight plywood was subsequently finished by coating materials.

The dimensions of beech lightweight plywood were 300 mm × 300 mm × 14 mm, wood moisture content of 8 ± 2 %. Before testing, the test specimens were conditioned at room temperature of 23 ± 2 °C and relative humidity of 60 ± 5 % for 28 days. Then the surface of the test pieces was finished by water-based coating materials applied by brush. Selected coating materials were:

- HOBBYLAK (density ca. 1000 kg/cm³, non-volatile components min. 37 % mass, consistency F4 / 23 °C min. 45 s, pH: 7-8).
- PAMLAK (density ca.1050 kg/m³, non-volatile components min. 30 % mass, consistency F4 / 23 °C min. 25 s).
- KIVA (density ca.1000 kg/cm³, non-volatile components min. 32 % mass).

All the chosen coating materials had to meet the following:

- water-based acrylic paint for wood,
- suitable for children's furniture and toys,
- applied by brush, roller or spray.

After curing, the paint coatings had the thickness summarised in Tab. 1. Paint coatings' thickness was measured using non-destructive method with the PosiTector 200.

Tab. 1 Thickness of cured paint coatings

Surface Finish	Coating thickness on substrate [µm]		
	HOBBYLAK	KIVA	PAMLAK
Beech veneer	34.8	42.8	40.6

Gloss value

Gloss value of the surface finishes was measured at geometries of 20°, 60° and 85° according to the STN EN ISO 2813 (2016) using the BYK-Gardner gloss meter. The evaluation was done according to Tab. 2.

Tab. 1 Gloss at 60 degrees

Gloss value	Verbal description	Gloss units
5	Matt	Less than 10
4	Semi Matt	10 – 40
3	Semi Gloss	41 – 70
2	Gloss	71 – 85
1	High Gloss	More than 85

Film hardness

The film hardness was determined by the Pencil test according to the standard STN EN ISO 15184 (2012). The results of the test were evaluated according the pencil that scratched the surface (Tab. 3). The test started with the softest pencil – number 1.

Tab. 3 Degrees of film hardness

Pencil number	1	2	3	4	5	6	7	8	9	10	11	12	13
Pencil hardness	3B	2B	B	HB	F	H	3H	4H	5H	6H	7H	8H	9H

Impact resistance

The impact resistance of the surface finishes was determined according to the standard STN EN ISO 6272-2 (2011). The intrusion (diameter of the intrusion) was measured and the surface finish was evaluated subjectively according to Tab. 4.

Tab. 4 Impact resistance: degree and evaluation

Degree	Visual evaluation
1	No visible changes
2	No cracks on the surface and the intrusion was only slightly visible
3	Visible light cracks on the surface, typically one to two circular cracks around the intrusion
4	Visible large cracks at the intrusion
5	Visible cracks were also off-site of intrusion, peeling of the coating

Resistance to cold liquids

Surface resistance to cold liquids was determined according to the standard STN EN 12720+A1 (2014) on all test specimens. Table 5 shows the selected cold liquids.

Tab. 5 Cold liquids used

Cold Liquid	Characteristic
Acetic acid	10 % (m/m) aqueous solution
Citric acid	10 % (m/m) aqueous solution
Ethanol (p.a.)	96 % (V/V)
Sodium chloride	
Olive oil	
Ink	
Condensed milk	10 % fat content
Coffee	Dissolve 4 g of instant coffee, medium roasted, freeze-dried, in 100 ml boiling water

After 2 hour exposure to a cold liquid, the surfaces was cleaned by gently wiping with absorbent cloth, soaked first in a cleaning solution and then in water. Finally, the surfaces were carefully dried with a dry cloth.

Tab. 6 Surface resistance to cold liquids: degree and evaluation

Degree	Description of Quality
5	No visible changes (no damage)
4	Slight change in gloss – visible only in reflection of light source
3	Slight traces of damage (gloss) – visible from different directions
2	Strong traces of damage usually without changing the structure of varnish
1	Strong damage with change in varnish structure

Damage to the surface, i.e. discoloration, changes in gloss and color and other defects were evaluated in an observation box with direct light and graded according to Tab. 6. The total resistance to cold liquids was evaluated as the average value of resistance to used eight cold liquids.

RESULTS AND DISCUSSION

Gloss value

Tab. 7 shows that on all surface finishes, higher gloss was measured in the direction longitudinal with wood fibers than in the transverse direction. PAMLAK and HOBBYLAK were semi-matt in the longitudinal direction and matt in the transverse direction. The measurements confirmed the conclusions by SLABEJOVÁ *et al.* (2016), BEKHTA *et al.* (2017) that the gloss of the surface finish is non-negligibly impacted by direction of wood fibers. The KIVA surface finish achieved a matte gloss in both the longitudinal and transverse directions.

Tab. 7 Gloss value of the surface finishes

Wood Fibers	Geometry	PAMLAK	HOBBYLAK	KIVA
∥	20°	14.33	13.7	12.87
∥	60°	13.47	14.87	9.27
∥	85°	12.63	16.93	11.53
⊥	20°	5.13	7.1	5.73
⊥	60°	8.47	7.5	4.57
⊥	85°	3.47	8.33	4.05

Film hardness

The degrees of surface hardness are summarized in Tab. 8. KIVA coating applied on beech veneer reached the film hardness of 8, HOBBYLAK the film hardness of 9, and PAMLAK veneer reached the film hardness of 7.

Tab. 8 shows that the surface finishes did not meet the requirement for surface hardness for the work surfaces of furniture (film hardness of 10). The evaluated surface finishes could be applied to the surfaces of lightweight boards used in furniture for other surfaces. The priority for the chosen surface finishes was health safety (suitability for children's furniture) not high surface hardness.

Tab. 8 Film hardness by pencil test

Coating Material	PAMLAK	HOBBYLAK	KIVA
Film Hardness	7	9	8
Pencil hardness	3H	5H	4H

Impact resistance

As shown in Tab. 9, the impact resistance (degree of surface damage) of all three tested coating materials were the same. Differences were in size of the intrusion. The smallest intrusion was measured for HOBBYLAK paint coating.

Comparing the results of surface hardness and impact resistance of the tested surface finishes showed that HOBBYLAK reached the highest surface hardness; and at the impact resistance testing, the smallest intrusion was formed on this surface. HAZIR and KOC (2019) pointed out that harder surfaces can be more brittle. But in the case of the tested surface finishes such assumption has not been confirmed. At the impact resistance testing, at drop heights of 100, 200 and also 400 mm, the cracks appeared at the intrusions.

Tab. 9 Diameter of intrusion and impact resistance on lightweight plywood

Surface Finish	PAMLAK		HOBBYLAK		KIVA	
Drop height [mm]	Diameter of Intrusion (mm)	Impact resistance	Diameter of Intrusion (mm)	Impact resistance	Diameter of Intrusion (mm)	Impact resistance
10	-	1	-	1	-	1
25	2	2	-	2	3	2
50	3	2	2	2	4	2
100	4	3	3	3	5	3
200	5	3	5	3	6	3
400	7	3	6	3	8	3

Resistance to cold liquids

Tab. 10 shows that PAMLAK and HOBBYLAK had the lowest resistance to ethanol, while KIVA achieved the excellent resistance to this liquid. All three surface finishes were less resistant (grade 3) to ink and condensed milk. PAMLAK achieved resistance of grade 4 to Acetic acid and coffee.

Tab. 10 Surface resistance to cold liquids

Cold Liquid	PAMLAK	HOBBYLAK	KIVA
Acetic acid	4	5	5
Citric acid	5	5	5
Ethanol (p.a.)	1	1	5
Sodium chloride	5	5	5
Olive oil	5	5	5
Ink	3	3	3
Condensed milk	3	3	3
Coffee	4	5	5

CONCLUSIONS

Based on the results, we can make the following conclusions:

- The gloss of the transparent surface finish is affected by direction of wood fibers in the substrate. Gloss value of the surface finish measured in the direction parallel with wood fibers can be different from the gloss measured in the direction across the fibers.
- Surface hardness of the coating film determined by static stressing gives partial information on the impact resistance of the surface finish, but it does not inform about fragility of the coating film.
- Resistance of surface finishes to cold liquids is not a priority feature for surface finishes intended for children's furniture; and therefore the resistance to some liquids can be significantly different.

Acknowledgements: This work was supported by the Scientific Grant Agency of the Ministry of Education SR Grant VEGA No. 1/0556/19.

REFERENCES

- BEKHTA, P., KRYSOPIAK, T., PROSZYK, S., LIS, B. 2017. Surface gloss of lacquered medium density fibreboard panels veneered with thermally compressed birch wood. *Progress in Organic Coatings* 117:10-19
DOI: 10.1016/j.porgcoat.2017.12.020
- BEKHTA, P., MAMOŇOVÁ, M., SEDLIAČIK, J., NOVÁK, I. 2016. Anatomical study of short-term thermo-mechanically densified alder wood veneer with low moisture content. *European Journal of Wood and Wood Products*. 1–10.
- FEKIAČ, J., GÁBORÍK, J., ŠMIDRIAKOVÁ, M. 2020. 3D-formability of perforated materials based on veneer. *Acta Facultatis Xylogiae*. 62(1): 55-65. ISSN 1336-3824.
- FEKIAČ, J., GÁBORÍK, J. 2018. Influence of veneer perforation on 2D formability of two-layer material. In *Annals of Warsaw University of Life Sciences*. 53-59. ISSN 1898-5912.
- FEKIAČ, J., ZEMJAR, J., GAFF, M., GÁBORÍK, J., GAŠPARIK, M., MARUŠÁK, R. 2015. 3D-moldability of veneers plasticized with water and ammonia. In *BioResources*. 10(1):866-876. ISSN 1930-2126.
- KAČÍK, F., KUBOVSKÝ, I., JAMNICKÝ, I., SIVÁK, J. 2010. Zmeny sacharidov pri ožarovaní javorového dreva CO₂ laserom. *Acta Facultatis Xylogiae*. 52(1): 33–40. ISSN 1336-3824.
- KRÁL, P., HRÁZKY, J. 2005. Kompozitní materiály na bázi dřeva. 2. Část: Mendelova Zemědělská a Lesnická univerzita v Brně. 154 p. ISBN 80-7157-878-9.
- LANGOVÁ, N., JOŠČÁK, P. 2014. Effect of mechanical modification of wood veneers on their planar formability. *Annals of Warsaw University of Life Sciences. Forestry and Wood Technology*. (87): 142–147. ISSN 1898-5912.
- SHULGA, G., NEIBERTE, B., VEROVKINS, A., JAUNSLAVIETIS, J., SHAKELS, V., VITOLINA, S., SEDLIAČIK, J. 2015. Eco-friendly constituents for making wood-polymer composites. *International Symposium on Selected Processes at the Wood Processing*. ISSN:1013-9826.
- SLABEJOVÁ, G., ŠMIDRIAKOVÁ, M., FEKIAČ, J. 2016. Gloss of transparent coating on beech wood surface. *Acta Facultatis Xylogiae*. 58(2), 37–44. ISSN 1336-3824.
- SLABEJOVÁ, G., ŠMIDRIAKOVÁ, M. 2014. Influence of modification of veneers on 3D - forming. *Annals of Warsaw University of Life Sciences. Forestry and Wood Technology*. (85): 226–229. ISSN 1898-5912.
- SLABEJOVÁ, G., ŠMIDRIAKOVÁ, M. 2013. Bending strength of layered material based on wood and foamed PVC. *Annals of Warsaw University of Life Sciences. Forestry and Wood Technology*. (84): 180–185. ISSN 1898-5912.
- STN EN ISO 2813 (2016) Paints and varnishes. Determination of gloss value at 20 degrees, 60 degrees and 85 degrees. Slovak Office of Standards, Metrology and Testing, Bratislava, Slovakia.
- STN EN 12720+A1 (2014) Furniture - Assessment of surface resistance to cold liquids. Slovak Office of Standards, Metrology and Testing, Bratislava, Slovakia.
- STN EN ISO 15184 (2012). Paints and varnishes. Determination of film hardness by pencil test. Slovak Office of Standards, Metrology and Testing, Bratislava, Slovakia.
- STN EN ISO 6272-2 (2011). Paints and varnishes - Rapid-deformation (impact resistance) tests - Part 2: Falling-weight test, small-area indenter. Slovak Office of Standards, Metrology and Testing, Bratislava, Slovakia.
- ZEMJAR, J., FEKIAČ, J., GÁBORÍK, J. 2014. Strengthening of veneers for 3D-forming. *Annals of Warsaw University of Life Sciences. Forestry and Wood Technology*. (88): 297–303. ISSN 1898-5912.



COLOUR OF THERMALLY MODIFIED WOOD FINISHED WITH TRANSPARENT COATINGS

Gabriela Slabejová – Mária Šmidriaková

Abstract

Colour of Thermally Modified Wood Finished with Transparent Coatings. The article evaluates the differences in the colour of maple wood after surface finishing. Native wood and thermally modified wood were surface finished with transparent coating materials. Two modes of heat treatment were performed. For the surface finishing, three types of coating material were used: water-based, synthetic polyurethane, and oil-wax coating material. The greatest difference in colour was noticed on native and also on thermally modified wood after the synthetic polyurethane was applied; and the smallest difference in colour after the oil-wax surface finishing. The polyurethane surface finish caused bigger difference in colour on thermally modified wood than on native wood. This difference was significant. The difference in wood colour caused by oil-wax surface finish was insignificant; bigger difference in colour was noticed on native wood than on thermally modified wood.

Key words: *color, maple wood, native, thermally modified wood, transparent coating*

INTRODUCTION

Thermally modified wood (TMW) is considered as an available, dimension stable and durable material. TMW products are commonly used as nonstructural material for various indoor and above-ground outdoor applications, e.g. flooring, cladding or decking. The surface of the TMW needs to be finished with transparent coating materials to preserve the color and protect the surface. Surface finishing is necessary to protect an attractive appearance and the color of thermally modified wood (VIDHOLDOVÁ *et al.* 2019).

Color is one of the aesthetic properties that can be identified subjectively with the naked eye, or measured objectively using a spectrophotometer. Transparent coating materials can change the colour of wood visibly. Transparent coating is designed to enhance the light stability of wood surface and not to cover the wood texture. Change in colour of wood surface after a transparent coating material was applied is an interaction of the colour of coating film with the colour of wood surface.

Various transparent finishes cause different colour on wood surface. The impact of transparent finish on emphasizing the aesthetic properties of wood textures was dealt by REINPRECHT and VIDHOLDOVÁ (2011). Colour stability of wood exposed to thermal treatment were evaluated by LEE *et al.* (2018); SANDBERG *et al.* (2017); PONCSAK *et al.*

(2011); KUČEROVÁ *et al.* (2019). DZURENDA and DUDIÁK (2020) determined the effect of the temperature of saturated water steam on the colour of wood of *Acer pseudoplatanus* L.

In the experiment, total colour difference ΔE^* of wood surfaces on native wood and TMW after coating with three transparent coating materials were monitored.

MATERIALS AND METHODS

Material

In the experiments, maple wood (*Acer pseudoplatanus* L.) was used. The test specimens were made from tangential and radial boards:

- native wood (wood without any thermal modification),
- wood thermally modified:
 - ✓ Mode I at $105\text{ °C} \pm 2.5\text{ °C}$ for 6 hours (TMW 105).
 - ✓ Mode III at $135\text{ °C} \pm 2.5\text{ °C}$ for 6 hours (TMW 135).

Wood was thermally modified with saturated water steam in the pressure autoclave APDZ 240 (Himmasch AD, Haskovo, Bulgaria) in cooperation with Sundermann s.r.o. Banská Štiavnica. The conditions of thermal treatment to achieve colour modification are described in DZURENDA and DUDIÁK (2020). The dimensions of the specimens made from thermally modified wood were $1000 \times 100 \times 40$ mm. The surface of test specimens was grinded with sandpapers with grid numbers of 60 and 80.

Surface finishing process

The following surface finishes for interior use were made:

- Water-based surface finish: Transparent two components water-based polyurethane top coat *Natural Touch-05 + 15% CA507* (catalyst for water-based coat). *Natural Touch* can be spray-applied as a single coat. It offers high levels of chemical resistance and resistance to yellowing, as well as good scratch resistance.
- Synthetic polyurethane surface finish: Transparent polyurethane top coat *OP 383-01 + 50% C376A* (catalyst). It offers high levels of chemical resistance and resistance to yellowing.
- Oil-wax surface finish: Water-based coat *Balakryl* with natural waxes and oils. It is designed for protective and decorative coatings of wooden floors, furniture, stairs, etc.

Colour analyse

Colours of the TMW surfaces were analysed according to the CIE $L^*a^*b^*$ colour system using the colour Reader CR-10 (Konica Minolta, Japan). This device works with a D65 light source by simulating the daylight; its sensor head is 8 mm in a diameter. Colour of wood before and after surface finishing was measured. The colour coordinates L^* (darkness: black (0) – white (100), a^* (– green, + red), and b^* (– blue, + yellow) of each sample were measured in ten places. Measurements were performed on all samples conditioned in room at the temperature of $20 \pm 2\text{ °C}$ and a relative air humidity of $60 \pm 5\%$ for 24 hours. The objective colour response assessment before (index 1) and after surface finishes (index 2) was expressed through the total colour difference ΔE^* calculated according to the following equations:

$$\Delta E^* = \sqrt{\Delta L^{*2} + \Delta a^{*2} + \Delta b^{*2}} \quad (1)$$

where: $\Delta L^* = L^*_2 - L^*_1$; $\Delta a^* = a^*_2 - a^*_1$; $\Delta b^* = b^*_2 - b^*_1$

L^*_1, a^*_1, b^*_1 coordinate values represent the colour of wood before surface finishing,

L^*_2, a^*_2, b^*_2 coordinate values represent the colour of wood after surface finishing.

The magnitude of ΔE^* can be classified according to the grading rules reported in Table 1.

Table 1 Colorimetric evaluation (CIVIDINI *et al.* 2007)

$0,2 > \Delta E$	Not visible difference
$0,2 < \Delta E < 2$	Small difference
$2 < \Delta E < 3$	Colour difference visible with high quality screen
$3 < \Delta E < 6$	Colour difference visible with medium quality screen
$6 < \Delta E < 12$	High colour difference
$\Delta E > 12$	Different colours

The change in wood colour, besides changes in the chromatic coordinates in the *CIE L*a*b** colour space, was assessed also following the changes in the lightness ΔL^* , chroma ΔC^* and hue angle h° in the *CIE L*C*h°* colour space using cylindrical coordinates. Chroma C^* is an integration of the values of the coordinates of red colour a^* and yellow colour b^* projected onto the chromatic plane of cylindrical colour space. Hue angle h° is expressed in positive degrees starting at the positive a^* axis and progressing in a counter clockwise direction and is described in DZURENDA and DUDIÁK (2020).

RESULTS AND DISCUSSION

In Table 2 there are listed the coordinates L^* , a^* , b^* , C^* and h° for the surface of native wood and thermally modified wood before and after surface finishing.

The water-based surface finish resulted in: decreased coordinate L^* , increased coordinates a^* , b^* , C^* , and slightly increased hue angle h° .

The synthetic polyurethane surface finish resulted in: decreased coordinate L^* , increased coordinates a^* , b^* , C^* and slightly increased hue angle h° .

The oil-wax surface finish resulted in various changes of coordinates: The coordinate L^* was only slightly decreased. The coordinate a^* was decreased on native wood and TMW 135; and increased on TMW 105. The coordinate b^* was increased on native wood and TMW 105; and decreased on TMW 135. The coordinate Chroma C^* was increased on native wood and TMW 105; and decreased on TMW 135. The hue angle h° was increased. The changes in coordinates were very small.

The total colour differences ΔE^* on surfaces of native wood and TMW after surface finishing are shown in Fig. 1. The largest total colour difference was noticed when the synthetic polyurethane surface finish was applied. The total colour difference on native wood $\Delta E^* = 4.98$ was graded as “Colour difference visible with medium quality screen”. The total colour difference on TMW 105 ($\Delta E^* = 7.37$) and on TMW 135 ($\Delta E^* = 6.80$) were graded as “High colour difference” if evaluated according to CIVIDINI *et al.* (2007).

Table 2 The chromatic coordinates in the $CIE L^*a^*b^*$ colour space and the $CIE L^*C^*h^\circ$ colour space for the surface finishes

Thermal modification wood	Before surface finish					Water-based surface finish				
	L^*	a^*	b^*	C^*	h°	L^*	a^*	b^*	C^*	h°
Native	84.01	6.98	16.59	17.98	67.16	81.61	7.72	17.85	19.4	66.66
TMW 105	80.88	7.99	17.74	19.46	65.73	78.56	8.97	19.74	21.66	65.56
TMW 135	64.82	11.66	19.91	23.08	59.63	60.7	13.16	22.15	25.75	59.27
	Before surface finish					Synthetic polyurethane surface finish				
	L^*	a^*	b^*	C^*	h°	L^*	a^*	b^*	C^*	h°
Native	82.57	6.69	17.54	18.8	69.08	79.8	8.03	21.46	22.94	69.5
TMW 105	79.95	8.21	17.93	19.72	65.36	75.94	10.76	23.56	25.9	65.59
TMW 135	67.53	11.09	20.9	23.66	62.09	62.45	13.55	24.7	28.17	61.23
	Before surface finish					Oil wax surface finish				
	L^*	a^*	b^*	C^*	h°	L^*	a^*	b^*	C^*	h°
Native	86.15	6.32	15.98	17.13	68.42	85.05	6.24	16.24	17.87	69.55
TMW 105	78.98	8.77	19.52	21.38	65.81	78.21	8.86	19.74	21.63	65.86
TMW 135	65.96	11.4	19.89	22.93	60.18	65.45	10.76	19.82	22.56	61.47

The water-based surface finish caused less colour differences than the synthetic polyurethane surface finish. The total colour difference on native wood $\Delta E^* = 2.81$ was graded as "Colour difference visible with high quality screen". The total colour difference was increasing with increasing temperature of heat treatment. The total colour difference on TMW 105 ($\Delta E^* = 3.22$) and on TMW 135 ($\Delta E^* = 4.92$) were graded as "Colour difference visible with medium quality screen" if evaluated according to CIVIDINI *et al.* (2007).

The oil-wax surface finish caused less colour differences than the water-based surface finish and also than the synthetic polyurethane surface finish. The total colour difference on native wood ($\Delta E^* = 1.13$), on TMW 105 ($\Delta E^* = 0.81$), and also on TMW 135 ($\Delta E^* = 0.82$) can be graded as "Small difference" (according to CIVIDINI *et al.* 2007).

According to DZURENDA and DUDIÁK (2020) the values of total colour difference for maple wood ΔE^* caused by the processes of thermal treatment with saturated water steam at the temperature ranging from 105 °C to 135 °C were $\Delta E^* = 6.5 \div 21.5$. Our experiment showed that not only the thermal treatment changes the colour of wood, but also a transparent surface finish can change the colour of wood surface. The colour differences were significant and depended on the type of surface finish. The scanned surfaces are shown in Fig. 2.

On thermally modified wood, the synthetic polyurethane surface finish caused the "High colour difference". The water-based surface finish caused the "Colour difference visible with medium quality screen". The oil-wax surface finish caused only the "Small difference".

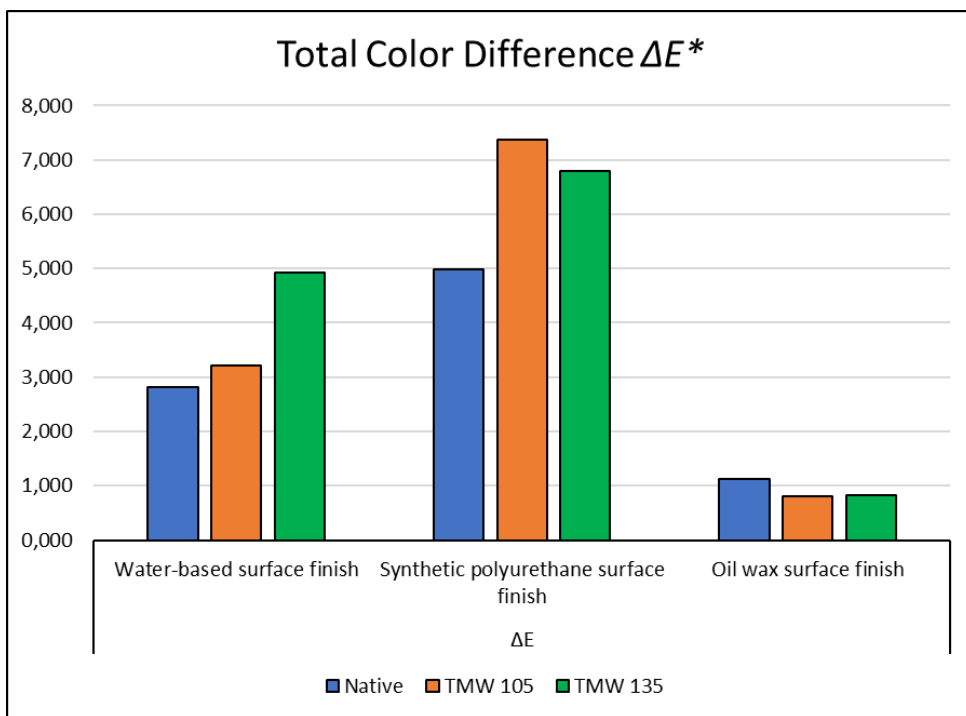


Fig. 1 Total colour difference ΔE^* for surface finishes on native wood and thermally modified wood


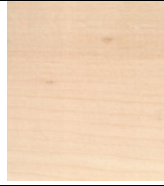
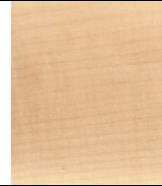
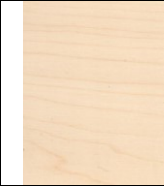
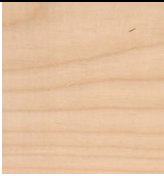
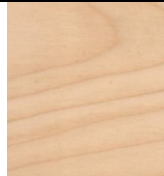

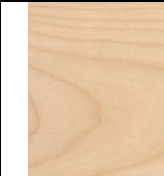

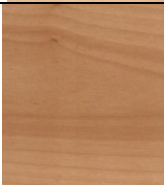
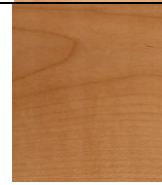

		Control	Water-based surface finish	Synthetic polyurethane surface finish	Oil-wax surface finish
Maple	Native				
	TMW 105				
	TMW 135				

Fig. 2 Scanned wood surfaces.

CONCLUSIONS

From the results of colour of the tested surface finishes, the following conclusions can be drawn:

- The synthetic polyurethane surface finish caused bigger colour differences than the water-based and oil-wax surface finishes.
- The synthetic polyurethane surface finish caused bigger colour difference on TMW than on native wood. The total colour differences on TMW were graded as “High colour difference”.
- The oil-wax surface finish caused the smallest colour differences. The total colour differences caused by the oil-wax surface finish on native wood and also on TMW were graded as “Small difference”.
- The transparent surface finishes have an impact on colour of wood surface; and the level of colour difference depends mainly on type of coating material.

REFERENCES

- CIVIDINI, R., TRAVAN, L., ALLEGRETTI, O. 2007. White beech: A tricky problem in drying process. In International Scientific Conference on Hardwood Processing, Quebec City, Canada.
- DZURENDA, L., DUDIÁK, M. 2020. The Effect of the Temperature of Saturated Water Steam on the Colour Change of Wood *Acer Pseudoplatanus* L. *Acta Facultatis Xylogologiae Zvolen*, 62(1): 19–28, 2020
- KUČEROVÁ V.; LAGAŇA R.; HÝROŠOVÁ T. 2019. Changes in chemical and optical properties of silver fir (*Abies alba* L.) wood due to thermal treatment. *J Wood Sci*, 65: 21. <https://doi.org/10.1186/s10086-019-1800-x>
- LEE S.H.; ASHAARI Z.; LUM W.C.; HALIP J.A.; ANG A.F.; TAN L.P.; CHIN K.L.; TAHIR P.M. 2018. Thermal treatment of wood using vegetable oils: A review. *Constr Build Mater*, 181, 408–419. <https://doi.org/10.1016/j.conbuildmat.2018.06.058>
- PONCSAK S.; KOCEAFE D.; YOUNSI R. 2011. Improvement of the heat treatment of Jack pine (*Pinus banksiana*) using ThermoWood technology. *Eur J Wood Wood Prod*, 69, 281–286. <https://doi.org/10.1007/s00107-010-0426-x>
- REINPRECHT L.; VIDHOLDOVÁ Z. 2011. *Thermowood*. Šmíra – Print, s.r.o.: Ostrava, Czech Republic; 89 p.
- SANDBERG D.; KUTNAR A.; MANTANIS G. 2017. Wood modification technologies-a review. *IForest*, 10, 895–908. <https://doi.org/10.3832/ifor2380-010>
- VIDHOLDOVÁ Z.; SANDAK A.; SANDAK, J. 2019. Assessment of the chemical change in heat treated pine wood by Near infrared spectroscopy *Acta Fac Xylogologiae Zvolen*, 61, 31–42. <https://doi.org/10.17423/afx.2019.61.1.03>

Acknowledgements: This work was supported by the Scientific Grant Agency of the Ministry of Education SR Grant APVV-17-0456.



THE EFFECT OF DRYING TEMPERATURES ON SIZE OF LONGITUDINAL CONTRACTION DIFFERENT WOOD SPECIES (*FAGUS SYLVATICA* L. AND *PICEA ABIES* L.)

Tatiana Vilkovská – Ivan Klement – Peter Vilkovský – Miroslav Uhrín

Abstract

European beech (*Fagus sylvatica* L.) and Spruce (*Picea abies* L.) are an important tree species with a rather large distribution in western and central Europe. The reaction wood (tension and compression wood) has different anatomical and also chemical characteristics from normal (opposite) wood. The zone of compression spruce wood is easily visible by the naked eye and therefore there is no problem with its identification. On the other hand, identification of tension wood is much difficult. One of many factors, to evaluate content of the tension beech wood in lumber is longitudinal warping, the woolly appearance of surface, eccentric pith and shiny appearance of reaction beech wood in wood rings calling them “white rings were observed in the transverse plane. The length dimension of the samples was measured before and during in different time of drying process to determine longitudinal contraction. Based on results longitudinal contraction was remarkable in reaction wood, where it was several times higher (FSP was found as boundary point in all measurements), what could be expected considering the physical properties of reaction beech wood. Measurements confirmed that drying time and temperature has noticeable effect on longitudinal contraction.

Key words: spruce, beech, longitudinal contraction, reaction wood, compression wood, tension wood

INTRODUCTION

European beech (*Fagus sylvatica* L.) and Spruce (*Picea abies* L.) are an important tree species with a rather large distribution in western and central Europe (Čunderlík *et al.* 2017). The reaction wood (tension and compression wood) has different anatomical and also chemical characteristics from normal (opposite) wood. Kúdela and Čunderlík (2012) stated 14% up to 21% ratio of reaction beech wood in beech raw material. Tarmian *et al.* (2009) investigated wood of *Picea abies* containing a high proportion of well-developed reaction wood. Tarmian *et al.* (2009) put forward that reaction wood had a much lower drying rate than normal wood. Due to reaction beech wood occurrence, the consequences are shown in form of deformations, increased portion of waste, and decreased quality of final products (Vilkovská *et al.* 2016). Kúdela and Čunderlík (2012), Yamamoto *et al.* (2005) studied an influence of reaction wood on material. Authors stated that increased portion of cellulose in reaction wood, where by weaker bonding between G-layer and S2 layer bigger swelling of other layers occurs and therefore, another sorption sites are created,

as the main reason of its possible higher moisture content (MC). As also shown by Čunderlík *et al.* (1995) their measurements prove that highest longitudinal contraction occurred at temperatures above 100°C. Lower values of longitudinal contraction were observed at lower temperatures. Longitudinal contraction is a very serious problem in production of solid wood panels assembled of beech lamellae joined alternatively breadth wise and longwise into large-sized blocks (Kúdela *et al.* 2014). The aim of this paper is to identify sizes of longitudinal contraction between tension and opposite wood with use different drying modes.

MATERIAL AND METHODS

Beech wood (*Fagus sylvatica* L.) and Spruce wood (*Picea abies* L.) were used for the experimental measurements. Samples were chosen logs with a diameter of 48 cm and length of 150 cm. Logs were selected from forests belonging to University Forest Enterprise of the Technical University in Zvolen, Slovakia. The zone of compression spruce wood is easily visible by the naked eye and therefore there is no problem with its identification. On the other hand, identification of tension wood is much difficult. One of many factors, to evaluate content of the tension beech wood in lumber is longitudinal warping, the woolly appearance of surface, eccentric pith and shiny appearance of reaction beech wood in wood rings calling them “white rings were observed in the transverse plane. All mentioned methods were used for detection. In addition, for detailed observation we provided detection of reaction beech wood. Based on the identification of the reaction zone using the above methods, were prepared groups of samples containing the reaction beech (BK) and spruce (SM) wood (R₁ and R₂) and the group containing the opposite wood (O₁ a O₂) of beech and spruce. The sample had final dimensions of thickness 30 mm, width 100 mm and length 300 mm. The experiment was carried out in a Memmert HCP 108 laboratory dryer. The drying mode was divided into two phases restricted by the presence of free water and bound water in the dried wood. Temperature were used 60, 80 and 120°C. (Tab. 1)

Tab. 1 Parameters of drying mode

Drying mode	Above FSP			Under FSP		
	Temperature of surrounding air (°C)	Δt (°C)	φ (%)	Temperature of surrounding air (°C)	Δt (°C)	φ (%)
1	60	2	91	60	12	52
2	80	2	93	80	12	65
3	120	2	94	120	-	-

The length dimension of the samples was measured before and during in different time of drying process to determine longitudinal contraction. The measurement was carried out every 24 hours using a sliding scale, always at the same location on the cross section of the samples. Subsequently, longitudinal contraction, were evaluated using Eq. 3 based on the quoted work Čunderlík *et al.* (1995):

$$\alpha_{l_i} = \frac{l_{\text{before}} - l_{\text{after}}}{l_{\text{before}}} \cdot 100 \quad (\%) \quad (1)$$

where: l_{before} - length of sample before drying process (mm), l_{after} - length of sample in different time of drying process (mm).

RESULTS AND DISCUSSION

Longitudinal contraction was analysed every 24 hours of drying process, recorded data are presented in Tab. 2. Highlighted are values of samples reached a moisture content of about 28 % (FSP), also changing the drying parameters. Graphical representation of the longitudinal contraction reaction and opposite samples with use different drying modes 60, 80, 120 are shown in Fig. 1 - 3.

Tab. 2 Longitudinal contraction beech and spruce wood with different drying times and drying modes

Drying mode	Spruce (SM)			Beech (BK)		
	Drying time (h)	Longitudinal contraction (%)		Drying time (h)	Longitudinal contraction (%)	
		Reaction	Opposite		Reaction	Opposite
60	0	0.00	0.00	0	0.00	0.00
	24	0.06	0.03	7	0.18	0.02
	48	0.07	0.04	31	0.29	0.04
	72	0.08	0.04	52	0.64	0.12
	96	0.10	0.08	76	0.81	0.14
	121	0.13	0.11	100	0.91	0.15
	145	0.38	0.15	124	0.96	0.25
	169	0.42	0.18	148	0.98	0.30
			172	1.40	0.33	
80	0	0.00	0.00	0	0.00	0.00
	18	0.27	0.00	12	0.21	0.00
	43	0.26	0.00	28	0.44	0.00
	67	0.28	0.04	52	0.69	0.01
	91	0.62	0.05	76	0.80	0.02
	115	0.62	0.07	100	0.85	0.02
	122	0.67	0.07	120	0.90	0.02
120	0	0.00	0.00	0	0.00	0.00
	24	0.15	0.13	8	0.87	0.08
	48	0.15	0.13	28	1.11	0.08
	74	0.17	0.13	54	1.35	0.11
	98	0.17	0.14	76	1.40	0.11
	122	0.18	0.14	100	1.56	0.11
	144	0.18	0.14	124	1.67	0.14
	149	0.22	0.16	148	1.98	0.14
	152	0.36	0.18	165	2.26	0.14

Remarkable changes in longitudinal contraction occurred in reaction beech wood samples. Opposite samples longitudinal contraction had almost 0%. In case of used drying mode for beech wood at 60, the contraction of opposite wood is 0.33 %. The spruce wood had this value longitudinal contraction almost about one-half decreased.

The temperature 60 °C were caused increased longitudinal contraction of spruce wood about 0.2 % and beech wood about 1 %. The temperature 80 °C has increased longitudinal contraction of beech wood about 0,9 % spruce wood about 0.6%. The biggest longitudinal contraction increased were discovered for beech wood and temperature 120 °C (about 2%).

Our results were confirmed by articles Kúdela and Čunderlík (2012), Yamamoto *et al.* (2005) and Čunderlík *et al.* (1995) where authors discovered that highest longitudinal contraction occur at temperatures about 100 °C. Spruce wood reached value only 0,2 %. Given measurement can be affected by the fact that reaction beech wood could be found in the opposite wood in small amount.

Drying time can also be the cause increased or decreased of longitudinal contraction what confirmed our results presented in Tab. 2. Lower values of longitudinal contraction were observed at shorter drying time.

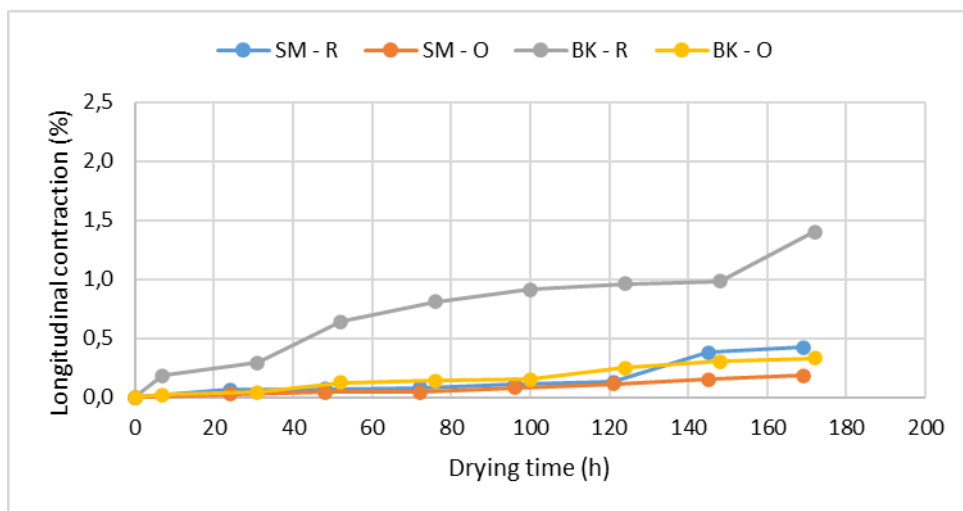


Fig. 1 Longitudinal contraction in temperature 60 °C

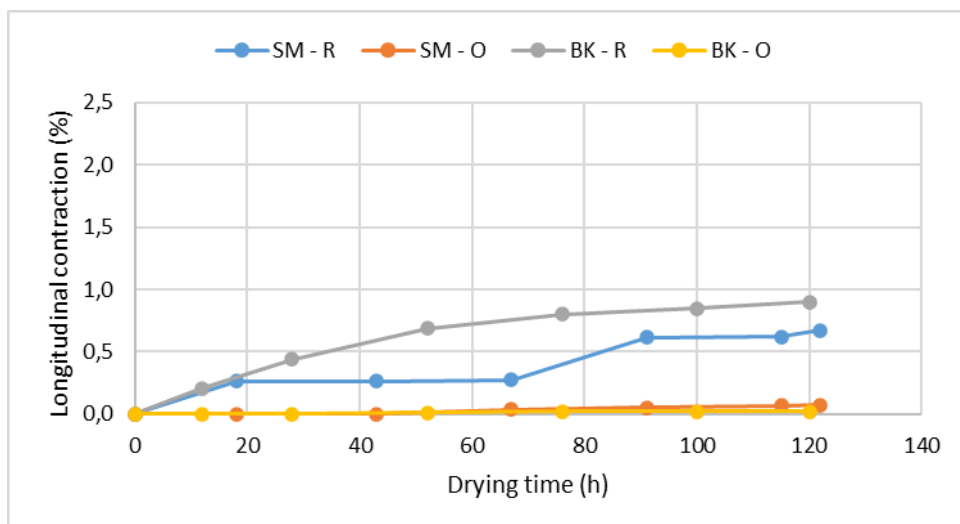


Fig. 2 Longitudinal contraction in temperature 80 °C

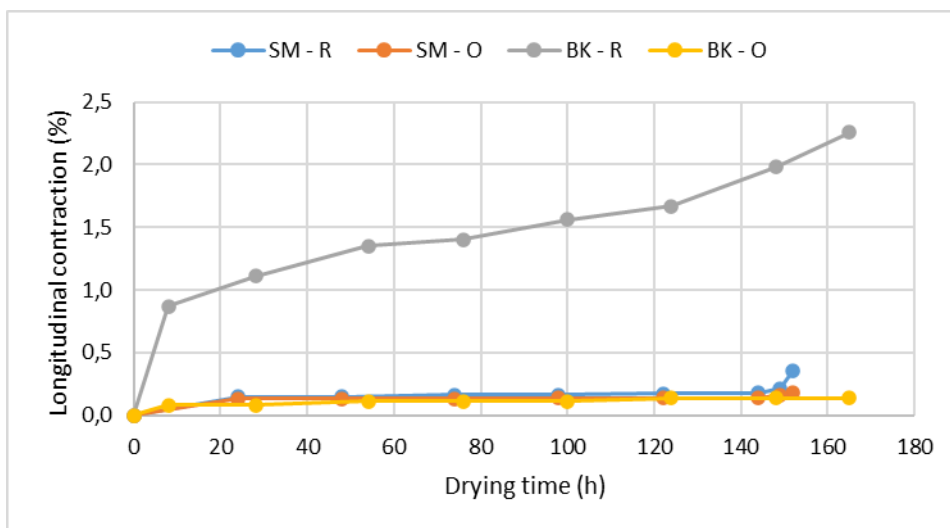


Fig. 3 Longitudinal contraction in temperature 120 °C

Many authors analysed definition of longitudinal contraction and its evaluation (Kúdela and Čunderlík 2012; Mellerowicz et al. 2008; Kopen (1989,1991); Jourez 2001). The above mentioned authors deal with problematic of increased contraction of reaction beech wood, where they examined the differences at FSP values of reaction and normal beech wood. Shrinkage and swelling of reaction beech wood is more pronounced in longitudinal direction, what causes higher values of longitudinal warping.

The analyses confirmed that the main cause of samples deformation with reaction beech wood content is 6 times higher longitudinal shrinkage of reaction beech wood compared to normal (opposite) wood and microscopic structure as well.

CONCLUSIONS

- Longitudinal contraction was remarkable in reaction wood, where it was several times higher (*FSP was found as boundary point in all measurements*), what could be expected considering the physical properties of reaction beech wood
- Measurements confirmed that drying time and temperature has noticeable effect on longitudinal contraction.
- Bigger longitudinal contraction was measured for beech wood in temperature 60 °C (about 1 %) and 120 °C (about 2 %).
- In temperature 60°C and 120 °C had almost identical drying time.
- Bigger longitudinal contraction 0.6% was measured for spruce wood in temperature 80 °C.
- Drying time was for beech wood and spruce wood in temperature 80 °C shortened about 40 hours in comparison with other temperature (60 °C and 120 °C)
- The result provide that longitudinal contraction are distinct showed for reaction wood of beech wood. This fact is very important keep in mind for drying of beech wood.

- The longitudinal contraction spruce wood was remarkably lower with compare of beech wood
- The Quantity and quality of reaction wood remarkable affected to size of longitudinal contraction in a both types of wood.

ACKNOWLEDGEMENTS

This work was supported by the Slovak Research and Development Agency under the contract no. SK-PL-18-0052

REFERENCES

- ČUNDERLÍK, I., KÚDELA, J., BLUSKOVA, G., 1995: Relaxation of stresses in streamed beech tension wood. *Lesotechnicesko Obrazovanie v Bulgarii*. Sofia, 199-205.
- ČUNDERLÍK, I., VILKOVSKÝ, P., RAČKO, V., 2017: Shear strength and analysis of shear area on wood/bark interface on beech wood (*Fagus sylvatica* L.). *Wood research*. Roč. 5, 691-699. ISSN 1336-4561
- JOUREZ, B., RIBOUX, A., LECLERCQ, A., 2001: Anatomical characteristics of tension wood and opposite wood in young inclined stems of poplar (*Populus euramericana* CV. "Ghoy"). *IAWA Journal*. Roč. 22, 133-157
- KOPEN, S., TORRATI, T., KANERVA, P., 1991: Modelling longitudinal elastic and shrinkage properties of wood, *Wood Science Technology* No. 25, 25-32, ISSN: 0043-7719
- KOPEN, S., TORRATI, T., KANERVA, P., 1989: Modelling longitudinal elastic and shrinkage properties of wood., *Wood Science Technology* No. 23, 55-63, ISSN: 0043-7719
- KÚDELA, J., ČUNDERLÍK, I., 2012: Bukové drevo štruktúra, vlastnosti, použitie, *Technická univerzita vo Zvolene*, 152 p. ISBN 978-80-228-2318-0.
- KÚDELA, J., GRYC, V., TÓTH, V., 2014: Deformation of beech wood – the sources and their identification before beech logs processing, *Annals of Warsaw University of Life sciences*, No. 87,121-125.
- MELLEROWICZ, E.,J, IMMERZEEL, P., HAYASHI, T., 2008: The molecular muscle of trees. *Annals Bot.*, 102, 659-665
- TARMIAN, A., PERRÉ, P. 2009: Air permeability in longitudinal and radial directions of compression wood of *Picea abies* L. and tension wood of *Fagus sylvatica* L. In *Holzforschung.*, 63(3), s. 352-356
- VILKOVSKÁ, T., KLEMENT, I, KONOPKA, A., BARAŇSKI, J., 2016: High temperature drying of beech with content of tension wood. In *Chip and chipless woodworking processes 2016: 10th international science conference*, September 8-10, Technical University in Zvolen. Zvolen: 2016, 333-339, ISSN 1339-8350.
- YAMAMOTO, H., ABE, K., ARAKAWA, Y., OKUYAMA, T., GRIL, J., 2005: Role of the gelatinous layer (G-layer) on the origin of the physical properties of the reaction beech wood of *Acer sieboldianum*. *Wood Science*, Roč. 51, 222-233



FORCED SPATIAL VIBRATIONS OF A WOOD SHAPER, CAUSED BY THE CUTTING FORCES ON THE WORN CUTTING TOOL

Georgi Vukov – Valentin Slavov – Pavlin Vitchev – Zhivko Gochev

Abstract

This study presents the results of conducted investigations of the forced spatial vibrations of a wood shaper, caused by the cutting forces on the worn cutting tool. The paper is based on a specific mechanical - mathematical model, developed by the authors, which allows studying of vibrations of this type of machinery. In this model the wood shaper is regarded as a system of three rigid bodies, which are connected by elastic and damping elements with each other and with the motionless floor. This study renders an account the mass, inertia, elastic and damping properties and geometric parameters of the machine. It considers forces on the cutting tool from its interaction with the processed material - cutting force, tangential and radial components. A system of matrix differential equations is compiled and analytical solutions are presented. The results of the numerical investigations are presented. They are obtained through modern software and by using parameters of a particular machine. Machine data is used in a typical operating mode with a certain degree of wearing of the cutting tool.

Key words: *forced spatial vibrations, cutting tool, woodworking shaper*

INTRODUCTION

Wear and damage of the cutting tools of woodworking shapers change the characteristics of the forces of their interaction with the processing material. This affects performance of the machines and impairs the accuracy and quality of their production (Gochev and Vukov 2017, Obreshkov 1996, Rousek et al. 2010). Uneven wear or damage of the tool and accumulation of superposition in separate parts of the instrument have main influence. Exactly the unbalance of the cutting tool most strongly affects the cutting force and creates additional variable loads during the operation of the wood shapers. These loads are transmitted to the spindle and by its two bearing units reach the other elements and the machine's body. Specific studies for investigating the effect of the uneven wear and the damage of the cutting tool on the cutting forces and the machine's work are required (Beljo-Lučić and Goglia 2001, Keturakis and Juodeikiene 2007). The machine can be seen as a mechanical vibrating system with known characteristics in this studies (Amirouche 2006; Veits 1971; Slavov and Vukov 2019).

The forced spatial vibrations of a woodworking shaper caused by the cutting forces from uneven wear and damage of the cutting tool, leading to its unbalance, are investigated in the proposed study. This study is a continuation of previous studies of the authors (Gochev and Vukov 2017, Vukov et al. 2018, 2019).

MATERIALS AND METHODS

A mechanic - mathematical model of woodworking shapers with lower spindle is built for studying its forced spatial vibrations. The model is shown in Figure 1.

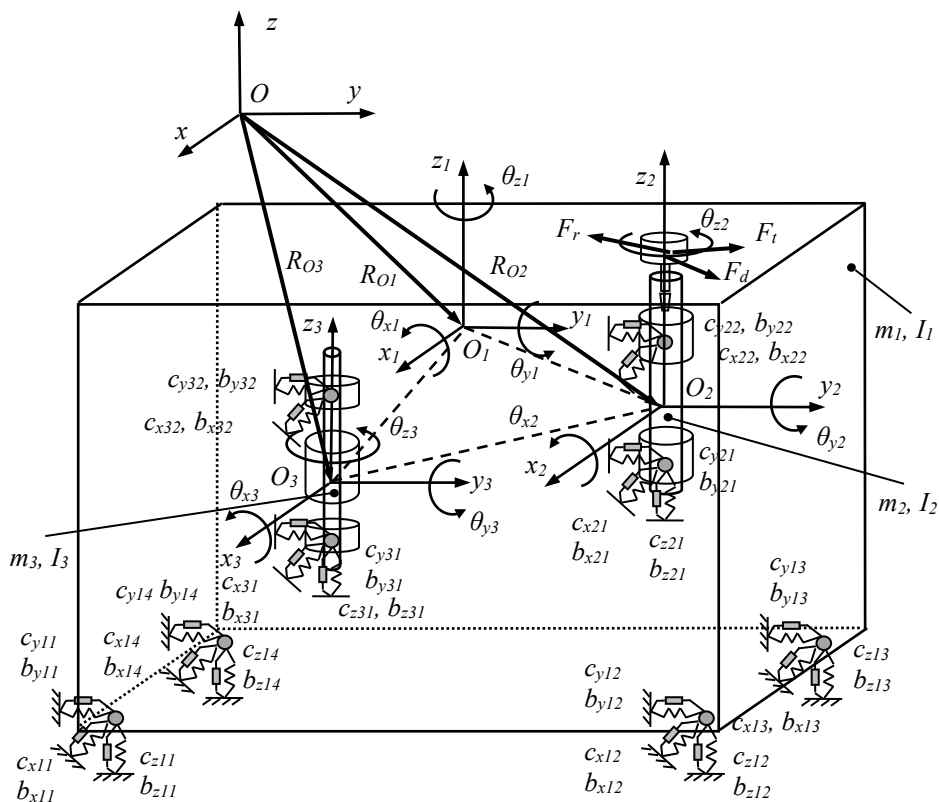


Figure 1. Mechanic-mathematical model of the wood shaper

The following symbols are used:

m_1, m_2, m_3 – mass of the shaper's body, the spindle and the rotor of the driving electric motor;

I_1, I_2, I_3 – inertia moment tensors of the woodworking shaper's body, the spindle and the rotor of the driving electric motor;

$c_{x1i}, c_{y1i}, c_{z1i}, i = 1, 2, 3, 4$ – elastic coefficients of the vibroisolators between the machine's body and the floor;

$b_{x1i}, b_{y1i}, b_{z1i}, i = 1, 2, 3, 4$ – damping coefficients of the vibroisolators between the machine's body and the floor;

$c_{x2i}, c_{y2i}, c_{z2i}, i = 1, 2$ – elastic coefficients between the body of the machine and the spindle;
 $b_{x2i}, b_{y2i}, b_{z2i}, i = 1, 2$ – damping coefficients between the body of the machine and the spindle;

$c_{x3i}, c_{y3i}, c_{z3i}, i = 1, 2$ – elastic coefficients between the body of the machine and the rotor of the driving electric motor;

$b_{x3i}, b_{y3i}, b_{z3i}, i = 1, 2$ – damping coefficients between the body of the machine and the rotor of the driving electric motor.

The three bodies of the mechanical system perform spatial vibrations - three small translations and three small rotations relative to the axes of the rectangular local coordinate systems that are fixedly connected to the bodies. It is assumed that the axes of the local coordinate systems are parallel to the axes of the reference coordinate system. The position of the mechanical system in space is defined by the vector of the generalized coordinates, which is

$$\mathbf{q} = [x_1 \ y_1 \ z_1 \ \theta_{x_1} \ \theta_{y_1} \ \theta_{z_1} \ x_2 \ y_2 \ z_2 \ \theta_{x_2} \ \theta_{y_2} \ \theta_{z_2} \ x_3 \ y_3 \ z_3 \ \theta_{x_3} \ \theta_{y_3} \ \theta_{z_3}]^T. \quad (1)$$

The mechanical system has 18 degrees of freedom. The sequence of building of its mechanic-mathematical model is presented in previous works of the authors (Vukov et al. 2019). In this work, the model is further developed for the study of forced vibrations, caused by the cutting forces on the worn cutting tool.

The differential equations of the forced spatial vibrations are derived by using the Lagrange's method

$$\frac{d}{dt} \left(\frac{\partial E_K}{\partial \dot{q}} \right) - \left(\frac{\partial E_K}{\partial q} \right) + \frac{\partial F_b}{\partial \dot{q}} + \frac{\partial E_P}{\partial q} = \mathbf{Q} \quad (2)$$

where E_K and E_P are respectively the kinetic and the potential energy of the systems, and F_b is the dissipation energy or dissipative function. \mathbf{Q} is the vector of generalized forces.

The obtained system of differential equations, which describes the forced spatial vibrations of the mechanical system, is

$$\mathbf{M}_{18 \times 18} \cdot \ddot{\mathbf{q}}_{18 \times 1} + \mathbf{B}_{18 \times 18} \cdot \dot{\mathbf{q}}_{18 \times 1} + \mathbf{C}_{18 \times 18} \cdot \mathbf{q}_{18 \times 1} = \mathbf{Q}_{18 \times 1} \quad (3)$$

The matrix in these equations which characterizes the mass-inertial properties of the mechanical system is \mathbf{M} . \mathbf{B} is the matrix that characterizes the damping properties of this system and \mathbf{C} – the elastic properties

The kinetic energy of the mechanical system is

$$E_K = \sum_{i=1}^3 E_{K_i}, \quad (4)$$

$$\text{where } E_{K_i} = \frac{1}{2} \cdot (\mathbf{m}_{RR}^i \cdot \mathbf{V}_{Ci}^0 \cdot \mathbf{V}_{Ci}^0 + \mathbf{\Omega}_i^{iT} \cdot \mathbf{I}_{\Theta\Theta}^i \cdot \mathbf{\Omega}_i^i), \quad \mathbf{m}_{RR}^i = \int_{V_i} \rho_i \cdot \mathbf{I} \cdot dV_i = m_i \cdot \mathbf{I} \cdot$$

The elements of the matrix \mathbf{M} of mass-inertial properties are defined by the expression

$$m_{i,j} = \frac{\partial^2 E_K}{\partial \dot{q}_i \cdot \partial \dot{q}_j} \quad (5)$$

Potential energy is defined by

$$E_P = E_{PK}(q)_m + E_{PG}(q)_i \quad (6)$$

$$\text{where } E_{PK}(q)_m = \sum_{k=1}^8 \frac{1}{2} \cdot \mathbf{q}^T \cdot \mathbf{C}(q) \cdot \mathbf{q}, \quad E_{PG}(q)_i = \sum_{i=1}^3 -m_i \cdot \mathbf{g}^T \cdot \mathbf{R}_{Ci}^0,$$

$\mathbf{C}(q)$ is a matrix of elastic properties;

$\mathbf{g} = [0 \ 0 \ g \ 0]^T$ – vector of gravitational acceleration,

k is the number of the elastic element between two bodies of the mechanical system.

The elements of the matrix \mathbf{C} of elastic properties are determined by the expression

$$c_{m,n} = \frac{\partial^2 E_{PK}(q)_j}{\partial q_n \cdot \partial q_m} \quad (7)$$

Dissipative function is calculated by the formula:

$$F_b = \sum \frac{1}{2} \cdot b_k \cdot (\delta \dot{\mathbf{r}}_k)^2 \quad (8)$$

where $\dot{\delta \mathbf{r}}_k$ is the deformation velocity of the elastic elements.

The elements of matrix \mathbf{B} are obtained by replacing the elements of matrix $\mathbf{C} - c_{ij}$ with b_{ij} .

The vector of the generalized external forces has the form

$$\mathbf{Q} = \left[0 \ 0 \ 0 \ 0 \ 0 \ 0 \ 0 \ \mathbf{Q}_{F(3 \times 1)}^T \ \mathbf{Q}_{Q(3 \times 1)}^T \ 0 \ 0 \ 0 \ 0 \ 0 \ 0 \right]^T, \quad (9)$$

where $\mathbf{Q}_F = \mathbf{Q}_{Fd} + \mathbf{Q}_{Fc}$; $\mathbf{Q}_Q = \mathbf{Q}_{Qd} + \mathbf{Q}_{Qc}$.

$$\mathbf{Q}_{Fd} = \begin{bmatrix} F_x \\ F_y \\ 0 \end{bmatrix}, \quad (10)$$

where $F_x = F_d \cdot \cos(\omega t)$; $F_y = F_d \cdot \sin(\omega t)$

$$\mathbf{Q}_{Qd}(F_d) = \mathbf{U}_1^{00T} \cdot (\tilde{\mathbf{r}}_{P2}^{0T} \cdot \mathbf{Q}_{Fd}) \quad (11)$$

Where

$$\mathbf{U}_1^{00T} = \begin{bmatrix} 1 & 0 & \theta_{y1} \\ 0 & 1 & -\theta_{x1} \\ 0 & \theta_{x1} & 1 \end{bmatrix}^T; \quad \tilde{\mathbf{r}}_{P2}^{0T} = \begin{bmatrix} 0 & l_{P2z}^0 & -l_{P2y}^0 \\ -l_{P2z}^0 & 0 & l_{P2x}^0 \\ l_{P2y}^0 & -l_{P2x}^0 & 0 \end{bmatrix};$$

$$\mathbf{r}_{P2}^0 = \begin{bmatrix} l_{Px2}^0 \\ l_{Py2}^0 \\ l_{Pz2}^0 \end{bmatrix} = \begin{bmatrix} l_{x1}^0 + l_{x2}^1 + l_{Px2}^1 \\ l_{y1}^0 + l_{y2}^1 + l_{Py2}^1 \\ l_{z1}^0 + l_{z2}^1 + l_{Pz2}^1 \end{bmatrix}; \quad \mathbf{r}_{P2} = \begin{bmatrix} l_{Px2} \\ l_{Py2} \\ l_{Pz2} \end{bmatrix}.$$

Cutting force is a distributed force acting on the cutting edge of the tool. This force is replaced by its resultant force, whose application point S is in the middle of the cutting edge. Resultant force's two components - tangential and radial – are used in practice. Each of these forces also creates a moment relative to the starting coordinate system. Thus the generalized force includes the generated forces and moments from the cutting forces.

The generalized forces of the components of the cutting force are

$$\mathbf{Q}_{Fc} = \begin{bmatrix} \frac{F_t}{2} + \frac{F_r}{2} \cdot \cos(6 \cdot \omega \cdot t) + \frac{F_r}{2} + \frac{F_r}{2} \cdot \cos(6 \cdot \omega \cdot t) \\ \frac{F_t}{2} + \frac{F_r}{2} \cdot \sin(6 \cdot \omega \cdot t) + \frac{F_r}{2} + \frac{F_r}{2} \cdot \sin(6 \cdot \omega \cdot t) \\ 0 \end{bmatrix}, \quad (12)$$

where: F_t – tangential component of the cutting force;

F_r – radial component of the cutting force.

The generalized moments of the components of the cutting force are

$$\mathbf{Q}_{Qc}(F_c) = \mathbf{U}_1^{00T} \cdot (\tilde{\mathbf{r}}_{S2}^{0T} \cdot \mathbf{Q}_{Fc}), \quad (13)$$

where: $\mathbf{M}(F_c) = \tilde{\mathbf{r}}_{S2}^{0T} \cdot \mathbf{Q}_{Fc}$;

$$\mathbf{U}_1^{00T} = \begin{bmatrix} 1 & 0 & \theta_{y1} \\ 0 & 1 & -\theta_{x1} \\ 0 & \theta_{x1} & 1 \end{bmatrix}^T; \quad \tilde{\mathbf{r}}_{S2}^{0T} = \begin{bmatrix} 0 & l_{S2z}^0 & -l_{S2y}^0 \\ -l_{S2z}^0 & 0 & l_{S2x}^0 \\ l_{S2y}^0 & -l_{S2x}^0 & 0 \end{bmatrix};$$

$$\mathbf{r}_{S2}^0 = \begin{bmatrix} l_{Sx2}^0 \\ l_{Sy2}^0 \\ l_{Sz2}^0 \end{bmatrix} = \begin{bmatrix} l_{x1}^0 + l_{x2}^1 + l_{Sx2}^1 \\ l_{y1}^0 + l_{y2}^1 + l_{Sy2}^1 \\ l_{z1}^0 + l_{z2}^1 + l_{Sz2}^1 \end{bmatrix}; \quad \mathbf{r}_{S2} = \begin{bmatrix} l_{Sx2} \\ l_{Sy2} \\ l_{Sz2} \end{bmatrix}$$

Obtaining the common solutions of the system (3) is related to the determination of the initial conditions of movement $q(0)$ и $\dot{q}(0)$.

The general solutions of the system of differential equations in matrix form, with initial conditions $t = 0, q(0) = q_0, \dot{q}(0) = \dot{q}_0$, are

$$\begin{aligned}
 q(t) = & \sum_{r=1}^{18} \frac{2}{g_r^2 + h_r^2} [G_r \cdot M \cdot \dot{q}(0) + (-\alpha_r \cdot G_r \cdot M + \beta_r \cdot H_r \cdot M + G_r \cdot B) \cdot q(0)] \cdot e^{-\alpha_r t} \cdot \cos \beta_r t + \\
 & + \sum_{r=1}^{18} \frac{2}{g_r^2 + h_r^2} [H_r \cdot M \cdot \dot{q}(0) + (-\alpha_r \cdot H_r \cdot M - \beta_r \cdot G_r \cdot M + H_r \cdot B) \cdot q(0)] \cdot e^{-\alpha_r t} \cdot \sin \beta_r t + \\
 & + \text{Re} \left\{ \sum_{k=0}^n \sum_{r=1}^{18} \frac{2}{g_r^2 + h_r^2} \cdot \frac{\alpha_r \cdot G_r + \beta_r \cdot H_r + i \cdot k \cdot \Omega \cdot G_r}{\omega_r^2 - k^2 \cdot \Omega^2 + i \cdot 2 \cdot k \cdot \sigma_r \cdot \omega_r \cdot \Omega} \cdot Q \cdot e^{ik\Omega t} \right\}
 \end{aligned} \tag{14}$$

where

$$\begin{aligned}
 g_r = & -2 \cdot \alpha_r \cdot (V_r^T \cdot M \cdot V_r - W_r^T \cdot M \cdot W_r) - 4 \cdot \beta_r \cdot V_r^T \cdot M \cdot W_r + V_r^T \cdot B \cdot V_r - W_r^T \cdot B \cdot W_r; \\
 h_r = & 2 \cdot \beta_r \cdot (V_r^T \cdot M \cdot V_r - W_r^T \cdot M \cdot W_r) - 4 \cdot \alpha_r \cdot V_r^T \cdot M \cdot W_r + 2 \cdot V_r^T \cdot B \cdot W_r; \\
 G_r = & g_r \cdot L_r + h_r \cdot R_r; \quad L_r = V_r \cdot V_r^T - W_r \cdot W_r^T; \\
 H_r = & h_r \cdot L_r - g_r \cdot R_r; \quad R_r = V_r \cdot W_r^T + W_r \cdot V_r^T.
 \end{aligned} \tag{15}$$

The whole machine and the three bodies are modelled with software Solid Works. These models are shown respectively in Figure 2, Figure 3, Figure 4 and Figure 5. Figure 2 shows the local coordinate systems and the reference coordinate system that coincides with the coordinate system of the body 1 and in which all the vectors are projected.

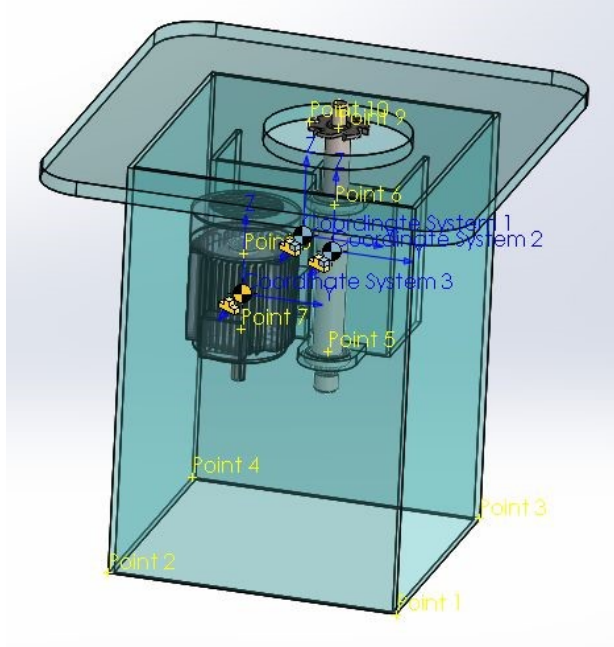


Figure 2. Model of the whole machine

It is assumed that the axes of the local coordinate systems are parallel to the axes of the reference coordinate system. The elastic-damping elements are marked with points 1 to 8. The application point of the disturbing force F_d , which coincides with the mass center of

the tool, is marked by point 9 (P). The application point of the cutting force F_c is marked by point 10 (S). It is in the middle of the cutting edge of the tool.

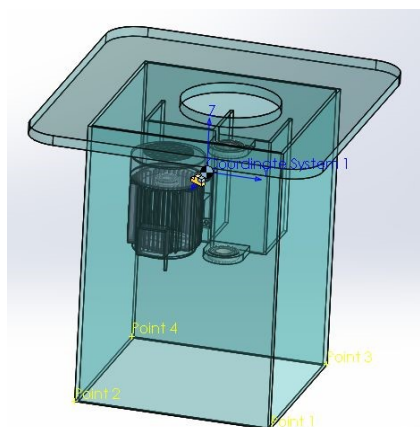


Figure 3. Model of body1

Figure 4. Model of body2

Figure 5. Model of body3

Table 1. Technical characteristics of the machine

Body №	Mass, kg	Mass inertia moments, kg.m ²				Coordinates of the mass centers, m				
	m	J _{xx}	J _{yy}	J _{zz}	J _{xy}	J _{yz}	J _{xz}	l _{Cx}	l _{Cy}	l _{Cz}
1	391,52	49,2672	52,000	47,9480	0,0395	0,4405	0,2525	0	0	0
2	11,123	0,2937	0,2937	0,0052	0	0	0	0,009	0,066	-0,020
3	14,378	0,0516	0,0516	0,0206	0	0	0	0,019	-0,115	-0,134
Coordinates of the supporting points of the elastic and damping elements										
In the coordinate system of the body 1						In the coordinate system of the body 2				
τ.	l _{xi} , m	l _{yi} , m	l _{zi} , m							
1	0,309	0,316	-0,654	5	0	0	-0,214			
2	0,309	-0,284	-0,654	6	0	0	0,096			
3	-0,291	0,316	-0,654	9	-0,005	0,005	0,258			
4	-0,291	-0,284	-0,654	10	0,0065	0,0631	0,2624			
In the coordinate system of the body 3						In the coordinate system of the body 1				
τ.	l _{xi} , m	l _{yi} , m	l _{zi} , m	τ.	l _{xi} , m	l _{yi} , m	l _{zi} , m			
7	0	0	-0,076	5	0,009	0,066	-0,234			
8	0	0	0,084	6	0,009	0,066	0,076			
				7	0,019	-0,015	-0,210			
				8	0,019	-0,015	-0,050			
Damping coefficients										
Between Bodies		b _{xi} (N.s)/m	b _{yi} (N.s)/m	b _{zi} (N.s)/m						
0 и 1		980	670	470						
1 и 2		980	670	470						
1 и 3		980	670	470						

Elasticity coefficients			
Between Bodies	c_{xi} , N/m	c_{yi} , N/m	c_{zi} , N/m
0 и 1	1000000	1000000	1500000
1 и 2	2250000	2250000	2250000
1 и 3	2250000	2250000	2250000
Angular speed: $100 \text{ s}^{-1} = 15,9 \text{ Hz}$.			
Disturbing forces: $F_d = 19,62 \text{ N}$; $F_d = 29,44 \text{ N}$; $F_d = 39,24 \text{ N}$			
Feed, m/min	Disturbing forces: F_c , N		
	Tangential F_t	Radiol F_r	
2	3,5	1,9	
6	8,1	4,9	
10	11,9	7,1	

RESULTS AND DISCUSSION

The vibrations on all 18 generalized coordinates of this mechanical system are obtained as a result of the provided investigations. Due to the limited volume of the article, only a few of them are illustrated here. The linear vibrations on the three coordinates of the machine’s body, the rotor of the electric motor and the spindle are presented. The results are given at angular speed 100 s^{-1} , feed 10 m/min and disturbing force $39,24 \text{ N}$. The amplitudes of the considered coordinates are

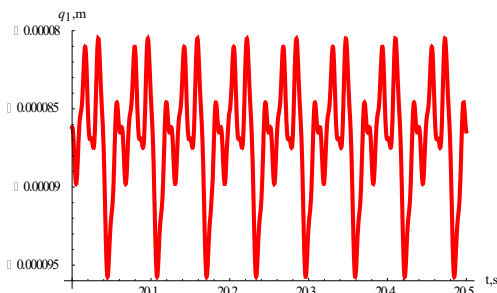


Figure 6. – Graph of $q_1(x_1)$

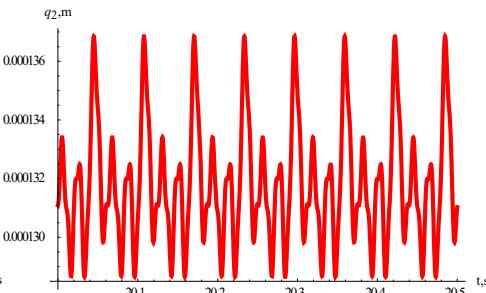


Figure 7. – Graph of $q_2(y_1)$

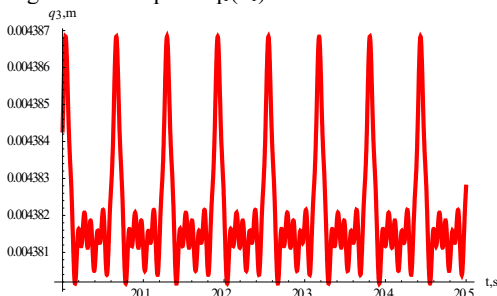


Figure 8. – Graph of $q_3(z_1)$

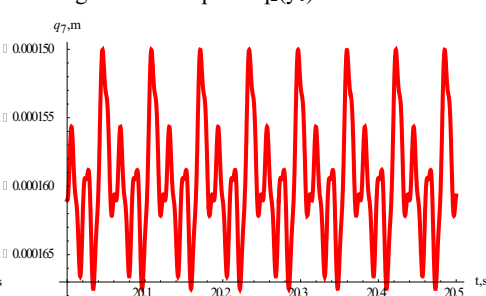
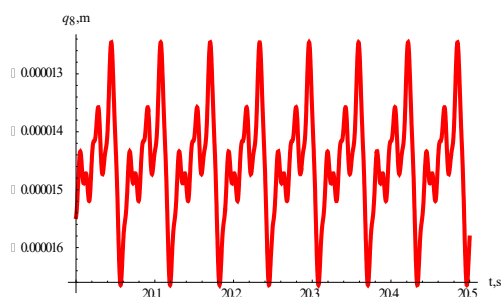
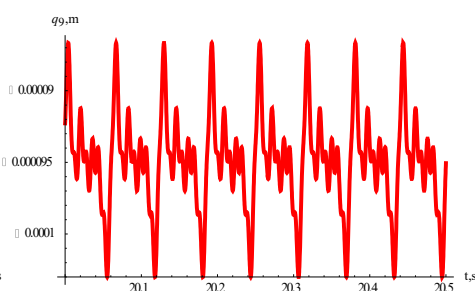
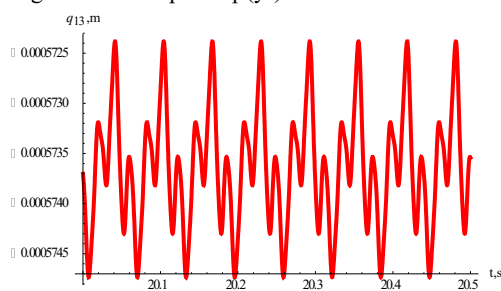
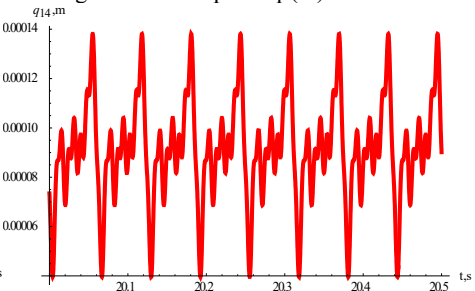
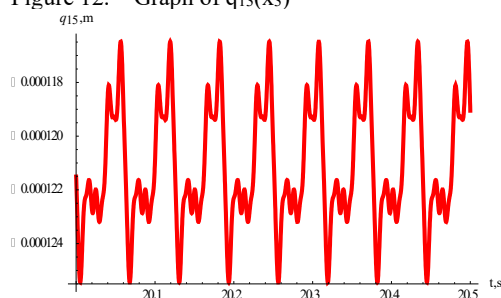


Figure 9. – Graph of $q_7(x_2)$

Figure 10. – Graph of $q_8(y_2)$ Figure 11. – Graph of $q_9(z_2)$ Figure 12. – Graph of $q_{13}(x_3)$ Figure 13. – Graph of $q_{14}(y_3)$ Figure 14. – Graph of $q_{15}(z_3)$

The analysis of the results shows that the cutting force of the woodworking shapers generates spatial vibrations not only on the spindle (body 2) but also on the entire machine. The amplitude of these vibrations increases substantially with the increase in the feed rate. The amplitude on coordinates y_2 and y_3 increases more pronounced. The specific values depend on the machine's parameters and its operating conditions. This confirms the need for precise preparation of the cutting tool, which is especially important for high speed woodworking machines. The amplitudes of the forced vibrations increase slightly as the unbalanced force rises. The cutting forces more influence on the amplitudes of the forced vibrations.

CONCLUSION

The paper presents a study of the forced spatial vibrations of a woodworking shaper caused by the cutting forces on the worn cutting tool. Some numerical calculations are carried out with a developed machine's model and modern computer programs. The calculations use the parameters of a woodworking machine used in the practice. The vibrations of the

mechanical system on all generalized coordinates are obtained as a result of these investigations. The results are analyzed and conclusions are drawn for the vibrations amplitudes by the individual coordinates. The study clarifies the impact of wear of the cutting tool in two aspects. The inevitable unbalance of the tool as a result of wear by itself has little effect on the vibration of the machine and its components. However, the cutting force of the worn tool generates considerable spatial vibration. They are obtained on the spindle, but then spread over the entire machine. The amplitude of these vibrations increases substantially with the increase in the feed rate and depends on the characteristics of the process material. These findings confirm the need for precise preparation of the cutting tool and careful monitoring of its state.

Acknowledgements: This paper is supported by the Scientific Research Sector at the University of Forestry – Sofia, Bulgaria, under contract № НИС-Б-1012/27.03.2019.

REFERENCES

1. Amirouche F. (2006): *Fundamentals of Multibody Dynamics – Theory and Applications*. Birkhäuser, Boston, 345 p.
2. Beljo-Lučić R, Goglia V. (2001): *Some possibilities for reducing circular saw idling noise*. Journal of Wood Science, 47(5): pp. 389–393,
3. Gochev Zh., Vukov G. (2017): *Influence of the Wearing of the Saw Unit Elements of the Wood Shaper on the System Vibration*. Acta Facultatis Xylogologiae Zvolen, 59(2): pp. 147–153.
4. Keturakis, G.; Juodeikiene, I. (2007): *Investigation of Milled Wood Surface Roughness*. Materials science 13(1): pp. 47–51.
5. Obreshkov P (1996), *Woodworking machines* (in Bulgarian). Technics. Sofia.
6. Rousek, M.; Kopecký, Z.; Svatoš, M. (2010): *Problems of the quality of wood machining by milling stressing the effect of parameters of machining on the kind of wood*. Annals of Warsaw University of Life Sciences – SGGW 72 No 72: pp. 233–242.
7. Slavov V., Vukov G. (2019): *Modelling and researching of forced spatial vibrations of axial fans*. MATEC Web of Conferences V.287, a.№ 03006.
8. Veits V., Kochura A., Martinenko A. (1971): *Dynamical investigations of drive machines*. Moscow: 328 p.
9. Vukov G., Zh. Gochev, V. Slavov, P. Vitchev, V. Atanasov (2017), *Numerical Investigations of the Forced Spatial Vibrations of Wood Shaper and its Spindle, Caused by Unbalance of the Cutting Tool*, PRO LIGNO, Transilvania University Press Brasov, Romania, Vol. 13, №4, pp. 154÷161.
10. Vukov G., Atanasov V., Slavov V., Gochev Zh. (2018): *Investigation of Spatial Vibrations of a Wood Milling Shaper and its Spindle, Caused by Cutting Force*, Proceedings of the 5th International Conference on Processing Technologies for the Forest and Bio-based Products Industries (PTF BPI 2018) Freising/Munich: pp. 144÷152.
11. Vukov G., V. Slavov, P. Vichev, Zh. Gochev (2019), *Investigations of the Free Space Vibrations of a Woodworking Shaper, Considered as a Mechanical System with Three Main Bodies*, Proceedings 4th International Scientific Conference "WOOD TECHNOLOGY & PRODUCT DESIGN", Ohrid, Republic of Macedonia, pp. 127–135.